

Search for Bioactive Compounds from Plant Sources as Inhibitors of the Wnt Signal Pathway

A dissertation presented

by

ROLLY GARNACE FUENTES

in partial fulfillment of the requirements
for the degree of

DOCTOR OF PHILOSOPHY
(Pharmaceutical Sciences)

**GRADUATE SCHOOL OF PHARMACEUTICAL SCIENCES
CHIBA UNIVERSITY**

September 2014

DISSERTATION COMMITTEE

This dissertation entitled “Search for Bioactive Compounds from Plant Sources as Inhibitors of the Wnt Signal Pathway” was evaluated by the following committee authorized by the Graduate School of Pharmaceutical Sciences, Chiba University, and is accepted as a requirement for the degree of Doctor of Philosophy (Pharmaceutical Sciences).

Chairman: Professor Hiromitsu TAKAYAMA, PhD
Graduate School of Pharmaceutical Sciences

Members: Professor Atsushi NISHIDA, PhD
Graduate School of Pharmaceutical Sciences

Professor Motoyuki ITOH, PhD
Graduate School of Pharmaceutical Sciences

PREFACE

This dissertation was conducted under the supervision of Prof. Dr. Masami ISHIBASHI of the Natural Products Chemistry Laboratory. The main theme of the research project is on the discovery of potent Wnt signal inhibitors from natural resources. Some of the plants used in the isolation were identified as potent source of compounds with biological activity based on the screening study conducted by the past members of the laboratory. Moreover, the assay systems used in this research followed the established or constructed assay system of the laboratory. Chapters 3-6 present most of the works on the Wnt signal inhibition including activity assay, isolation and structural elucidation of the potent compounds, and plausible mechanism. A version of Chapter 3 has been published [Fuentes, R. G.; Toume, K.; Arai, M. A.; Koyano, T.; Kowithayakorn, T.; Ishibashi, M. *Heterocycles* **2014**, 88, 1501-1509]. In Chapter 7, the possible role of one Wnt inhibitor, scopadulciol, in overcoming TRAIL resistance is discussed. Chapters 9-12 present the work on the induction of Ngn2 promoter activity using an assay system constructed by the laboratory. This research project was conducted in the early part of my PhD work.

ACKNOWLEDGEMENT

First and foremost, I would like to express my sincere and deepest gratitude to my supervisor, Prof. Dr. Masami ISHIBASHI, for his excellent guidance and unwavering support during my doctoral research. His immense knowledge, motivation, and passion for natural products research has been a source of inspiration to me.

I am also very grateful to Assoc. Prof. Dr. Midori A. ARAI for her valuable advice and suggestions, and help on my research.

I would also like to express my sincere thanks to Asst. Prof. Dr. Kazufumi TOUME for the support, encouragements, patience, and valuable discussions during the conduct of my research.

I would also like to express my heartfelt thanks to the members of the Dissertation Committee Prof. Dr. Hiromitsu TAKAYAMA, Prof. Dr. Atsushi NISHIDA, and Prof. Dr. Motoyuki ITOH for their valuable comments and suggestions.

I am also thankful to the present and past members of the Natural Products Laboratory for the help and friendship. To Dr. Hyun Yeong Park for the assistance in the Wnt study; Mr. Tadashi Habu for helping me with the TRAIL study; Mr. Kazune Koryudzu and Mr. Yuichi Maekawa for the help in the Ngn2 project; To Mr. Tatsuro Yoneyama and Mr. Kentarou Tsukahara for the valuable discussions in many laboratory techniques. I would also like to thank the staff of the Graduate School of Pharmaceutical Sciences, and International Student Division for their administrative help.

I would like to acknowledge the Japanese Government through the Ministry of Education, Culture, Sports, Science and Technology for the financial support (Monbukagusho Scholarship) which enabled me to pursue my PhD studies in Chiba University, Japan.

Also, I am thankful to the University of the Philippines Visayas Tacloban College for allowing me to have my study leave to pursue my doctoral studies.

I would also like to express my thanks to the international students of Chiba University who helped me in many ways during my stay in Japan. To Dr. Guzel Bikbova, Dr. Nattie Tatiya and Mr. Tahn Min Quang for the genuine friendship and enormous help. Likewise, I am thankful to all my friends and colleagues in U.P. Tacloban, especially to Asst. Prof. John Paul Yusiong and Ms. Lynie Pajota for the help, support and encouragements.

I would like to express my heartfelt thanks to my mama, jimboy and bamba for the love and encouragements and, for always supporting me in my academic endeavors. I dedicate this work to my late father, and brother Titan who were always proud of me.

To GOD, the almighty, the source of everything, all praises and glory are yours.

Rolly G. Fuentes

TABLE OF CONTENTS

	PAGE
PREFACE	v
ACKNOWLEDGMENT	vii
LIST OF FIGURES	xiii
LIST OF TABLES	xix
LIST OF APPENDICES	xxi
ABSTRACT	xxiii
1. Introduction	1
1.1. Background of the study	1
1.2. The Wnt Signalling Pathway	2
1.2.1. Alternative pathway for the degradation of β -catenin	4
1.3. Wnt Signal and Diseases	5
1.4. Wnt inhibitors and their mechanism of action	6
1.5. Screening of potential Wnt inhibitors: Cell-based luciferase Assay system	8
1.6. Cytotoxicity assay using FMCA	11
1.7. Aim of study	11
References	13
2. Methods	17
2.1. General Experimental Procedure	17
2.2. Cell culture	17
2.3. Reporter gene assay and transfection	18
2.4. Cell viability assay	19
2.5. TRAIL-resistance overcoming activity assay	19
2.6. Western blot analysis	20
2.7. Cell cycle analysis by flow cytometry	21
2.8. Apoptosis study by flow cytometric analysis	21
References	22
3. Diarylheptanoids from <i>Curcuma comosa</i> with Wnt/β-catenin signal inhibitory activity	23
3.1. Plant description	23
3.2. Isolation of the constituents	24
3.3. Characterization of the isolated compounds	26
3.4. β -Catenin/TCF transcriptional inhibitory activity	34
References	36

4. Cytotoxicity of scopadulciol from <i>Scoparia dulcis</i>	
Against Wnt-dependent cancer cells	39
4.1. Plant description	39
4.2. Isolation of the constituents	40
4.3. Characterization of the isolated compounds	41
4.4. β -Catenin/TCF transcriptional inhibitory activity and cytotoxic activities of compound 11	45
References	49
5. Trichillins from <i>Azadirachta excelsa</i> inhibit	
Wnt/β-catenin transcriptional activity	51
5.1. Plant description	51
5.2. Isolation of the constituents	52
5.3. Characterization of the isolated compounds	54
5.4. TCF/ β -catenin transcriptional inhibitory activity of the isolated compounds	61
5.5. Cytotoxic activity of compounds 17-19	63
5.6. Effect of 18 on the β -catenin and c-myc level in HCT116	64
References	66
6. Scopadulciol (11) induces β-catenin degradation in	
AGS human gastric adenocarcinoma cells	67
6.1. Rationale	67
6.2. Scopadulciol induces degradation of β -catenin in AGS	67
6.3. Degradation of β -catenin by 11 is mediated by proteasome activity	69
6.4. p53 is involved in the degradation of β -catenin by scopadulciol (11)	70
6.5. Scopadulciol (11) inhibits TCF/ β -catenin transcriptional activity and downregulates the expression of β -catenin target proteins in AGS	71
6.6. Scopadulciol (11) exerted p53-dependent cytotoxicity in AGS	73
References	74
7. Scopadulciol (11) sensitizes AGS to TRAIL-induced apoptosis	77
7.1. Background of the study	77
7.2. Scopadulciol (11) has TRAIL-resistance overcoming activity	78
7.3. Scopadulciol (11) affected the level of the apoptosis-related proteins	81
7.4. Combination of TRAIL and scopadulciol (11) enhanced degradation of β -catenin in AGS	82
References	84
8. Summary and Conclusion	85

PROJECT 2: Search for Natural Compounds That Enhance Ngn2 Promoter Activity	89
9. Regulation of neurogenesis by the basic helix-loop-helix (bHLH) transcription factors	91
9.1. Overview	91
9.2. The basic helix-loop-helix transcription factors	92
9.3. Reported compounds that induce neuronal differentiation	95
References	96
10. Ngn2 Promoter Assay Protocol	99
10.1. Cell-based luciferase assay system	99
10.2. Methods	99
10.2.1. Ngn2 reporter assay	99
10.2.2 Neuronal differentiation assay	100
References	102
11. Phenolic compounds from <i>Oroxylum indicum</i> that Activate Ngn2 promoter activity	103
11.1. Plant description	103
11.2. Isolation of the constituents	104
11.3. Characterization of the isolated compounds	106
11.4. Ngn2 promoter activity of compounds 23-28	110
11.5. Neuronal differentiation activity of 23	110
References	114
12. Ngn2 promoter activity of longistylin C isolated From <i>Cajanus cajan</i>	117
11.1. Plant description	117
11.2. Isolation of the constituents	118
11.3. Characterization of the isolated compounds	118
11.4. Ngn2 promoter activity of longistylin C (30)	121
References	122
13. Summary and Conclusion	123
APPENDICES	125

LIST OF FIGURES

<u>FIGURE</u> <u>NO.</u>		<u>PAGE</u>
1.1	The Wnt/ β -catenin Pathway. LRP: lipoprotein receptor-related protein; β -cat: β -catenin; Dsh: deshevelled; GSK3 β : glycogen synthase kinase 3 β ; CK1 α : casein kinase 1 α ; APC: adenomatous polyposis coli; β -TrCP: β -transducin repeat containing protein; TLE: transducin-like enhancer of split; TCF: T-cell factor.	3
1.2	β -Catenin regulation via the Siah mechanism. Siah-1: seven in absentia homolog 1; SIP: Siah interacting protein; Skp1: S-phase kinase-associated protein 1.	4
1.3	Wnt signal inhibition of some reported compounds via the (a) conventional pathway and (b) via an alternative pathway, Siah-1 mechanism.	7
1.4	Some Wnt inhibitors reported by our group.	9
1.5	a. Cell-based luciferase assay system using TOP and FOP assays. b. Oxidative conversion of luciferin to oxyluciferin catalyzed by the enzyme luciferase.	10
1.6	Enzymatic hydrolysis of fluorescein diacetate to fluorescein.	11
3.1	Bar graphs showing the dose-dependent TOP activity of KKP261 MeOH extract. The line graph represents cell viability All data are presented as the mean \pm s.d. (n=3).	23
3.2	Isolation chart of <i>C. comosa</i> .	25
3.3	Selected key HMBC of 2 .	28
3.4	Acetonide derivative (2a) of compound 2 and its HMQC.	29
3.5	TOP and FOP activity of compounds 1 , 6 , 7 and 8 . TOP was measured using HEK293 cells stably transfected with SuperTOPflash reporter gene (STF/293) while the FOP activity was measured using HEK293 cells transiently transfected with SuperFOPflash reporter gene. Line graph represents the viability of STF/293 cells. Data were representative from one experiment of at least two independent experiments (mean \pm s.d). All data are presented as the mean \pm s.d. (n=3).	34
4.1.	Bar graphs showing the dose-dependent TOP activity of KKB302 MeOH extract. The line graph represents cell viability. All data are presented as the mean \pm s.d. (n=3).	39
4.2	Isolation chart of <i>S. dulcis</i> .	41

4.3	Column shows the TOP and FOP activity of 11 . TOP activity was measured using HEK293 cells stably transfected with SuperTOPflash reporter gene (STF/293) while the FOP activity was measured using HEK293 cells transiently transfected with SuperFOPflash reporter gene. Line graph represents the viability of STF/293 cells. Quercetin was used as the positive control for TOP assay. Data were representative from one experiment of at least two independent experiments (mean \pm s.d).	45
4.4	Effect of 11 on the viability of cancer cells AGS, RKO, SW480, HCT116, DLD1 and non-cancer cell HEK293. Cells were treated with 11 of different concentrations (125, 250 and 500 nM) for 24, 48 and 72 h. Viability was determined using FMCA and was calculated relative to 0 day.	46
4.5	Effect of 11 on the cell cycle of RKO cells (upper panel) and AGS cells (lower panel). Cells were exposed to 11 (150 and 300 nM) for 24 h, stained with propidium iodide and analyses using FACS.	48
4.6	The involvement of caspase in the antiproliferative activity of 1 was determined by treating AGS cells with 1 in the absence or presence of z-VAD-fmk (50 μ M), a pan-caspase inhibitor. Viability in both experiments was determined using FMCA assay and was normalized to 0 day.	48
5.1	Bar graphs showing the dose-dependent TOP activity of KKB302 MeOH extract. The line graph represents cell viability All data are presented as the mean \pm s.d. (n=3).	51
5.2	Isolation chart of <i>A. excelsa</i> .	53
5.3	Column shows the TOP and FOP activity of 17-20 . TOP was measured using HEK293 cells stably transfected with SuperTOPflash reporter gene (STF/293) while the FOP activity was measured using HEK293 cells transiently transfected with SuperFOPflash reporter gene. Line graph represents the viability of STF/293 cells. Data were representative from one experiment of at least two independent experiments (mean \pm s.d).	61
5.4	Effect of 17-19 on the viability of cancer cells AGS, RKO, SW480, HCT116, DLD1 and non-cancer cell HEK293. Cells were treated with the compounds of different concentrations (100, 200 and 400 nM) for 48 h. Viability was determined using FMCA.	63

5.5	Western blot analysis of β -catenin and c-myc in HCT116 cells treated with 18 for 24 h. Cytoplasmic and nuclear lysates from HCT116 cells were obtained and subjected to Western blot analysis with anti- β -catenin and anti-c-myc antibodies. β -actin serves as protein control for full and cytoplasmic fractions while histone H1 for the nuclear fraction.	65
6.1	Effect of 11 on the level and localization of β -catenin in AGS after treatment with different concentrations of 11 (100, 200, 400 nM) for 24 h. Whole cell, cytoplasmic and nuclear lysates from AGS cells were obtained and subjected to Western blot analysis with anti- β -catenin antibody. β -actin serves as protein control for full and cytoplasmic fractions while histone H1 for the nuclear fraction.	68
6.2	Western blot analysis on the level of (a) GSK3 β and CK1 α , and (b) phosphorylated β -catenin in AGS cells after treatment with different concentrations of 11 (100, 200, 400 nM) for 24 h.	68
6.3	Effect of (a) MG132 and (b) epoxomicin on β -catenin level in AGS cells treated with 11 . Cells were pre-treated with either MG132 (10 μ M) or epoxomixin (10 μ M) for 1 h and treated with 11 (400 nM) for 24 h.	69
6.4	Effect of (a) z-VAD-fmk and (b) calpastatin pretreatment on β -catenin level in AGS cells treated with 11 . Cells were pre-treated with either z-VAD-fmk (50 μ M) or calpastatin (10 μ M) for 1 h and treated with 11 (400 nM) for 24 h.	70
6.5	Level of β -catenin in AGS treated with 11 (200 nM) for 24 h in the absence or presence of pifithrin- α (20 μ M), p53 transcriptional activity inhibitor	71
6.6	TOP and FOP activity of 11 in AGS cells. AGS cells were co-transfected with either SuperTOPflash or SuperFOPflash reporter gene and pRL-CMV plasmids for 24 h. After transfection, cells were incubated with 1 . Luciferase activities were measured after 24 h post-transfection.	72
6.7	Western blot analysis using full lysate on the level of TCF/ β -catenin target proteins in AGS cells after treatment with different concentrations (100, 200, 400 nM) of 1 for 24 h. Whole cell lysate were obtained and subjected to Western blot analysis.	73
6.8	Effect pifithrin- α (20 μ M) on the viability of AGS treated with 11 (100 nM) for 48 h. Viability of AGS was measured using FMCA.	73
7.1	Intrinsic and extrinsic TRAIL (tumor necrosis-related apoptosis inducing ligand) signaling pathway.	78

7.2	Compound 11 showed TRAIL-overcoming resistance activity in AGS cells. Cells were exposed to the different treatments as described for 24 h and assayed for viability using FMCA. Lut = Luteolin serves as control for the TRAIL-overcoming resistance activity assay.	79
7.3	FACS analysis on the induction of apoptosis in AGS cells by TRAIL+ 11 combined treatment. Cells were exposed to the different conditions as described for 12 h. Cells were collected and stained with annexin V and propidium iodide. The population of viable, apoptotic and dead cells were quantified by FACS analysis.	80
7.4	Effect of combined treatment of TRAIL and 11 against non-cancer cell HEK293. Cells were exposed to the different treatments as described for 24 h. Viability was determined using FMCA assay and was normalized to control (0 nM).	80
7.5	(a) Western blot analysis of p53, DR4, DR5 and Bcl2 in AGS treated with different concentration of 11 . Cells were treated with 11 at different concentrations (50, 200, 200 nM) for 24 hr and analyzed by Western blot.) Effect of z-VAD-fmk (50 μ M) on the viability of AGS cells treated with combined TRAIL and 11 . Cells were pretreated with z-VAD-fmk (50 μ M) for 1 h, then treated as described for 24 h. Viability was calculated relative to the control (no inhibitor and TRAIL) treatment. Data are representative from one experiment of at least two independent experiments (mean \pm s.d.).	81
7.6	(a) Western blot analysis of β -catenin in AGS cells treated with 11 (200 nM) + TRAIL (100 ng/mL) for 12 h. (b) Effect of z-VAD-fmk pretreatment on β -catenin level in AGS treated with 11 and TRAIL. Cells were pre-treated with z-VAD- fmk (50 μ M) for 1 h and treated with 1 (200 nM) + TRAIL (100 ng/mL).	83
9.1	Differentiation of neural stem cells to neuron, astrocyte, and oligodendrocyte.	91
9.2	Role of bHLH factors in neurogenesis.	92
9.3	Regulatory pathways controlled by the activator and repressor bHLH. Figure adapted from Kageyama <i>et al.</i> (2005).	94
9.4	Reported compounds that induce neurogenesis and their respective effective concentrations.	95
10.1	Ngn2 reporter plasmid.	99
11.1	Ngn2 promoter activity of <i>O. indicum</i> hexane, EtOAc, BuOH and aqueous fractions.	103

11.2	Isolation scheme of <i>O. indicum</i>	105
11.3	Concentration-dependent Ngn2 promoter activity of compounds 23-29 .	111
11.4	Time-dependent Ngn2 promoter activity of compounds 23-29 .	112
11.5	Neuronal differentiation activity of 23 using MEB5 cells. TUJ1 (Green): Neurons; GFAP (Red): Astrocyte; TO-PRO (Blue): Nucleus.	113
11.6	Histogram of neurite length of MEB5 treated with 23 for 4 d.	113
12.1	Ngn2 promoter activity of the 1 series.	117
12.2	Isolation scheme of <i>C. cajan</i> .	119
12.3	Dose-dependent Ngn2 promoter activity of 30 .	121

LIST OF TABLES

<u>TABLE</u> <u>NO.</u>		<u>PAGE</u>
1.1	List of diseases associated with aberrant activation of the Wnt signal.	5
1.2	Some gastrointestinal cancer cells with active Wnt signalling pathway.	6
3.1	¹ H (600 MHz) and ¹³ C (150 MHz) spectral data for compounds 1 and 2 .	27
3.2	¹ H (600 MHz) and ¹³ C (150 MHz) spectral data for compounds 3, 4 and 5 .	31
3.3	¹ H (600 MHz) and ¹³ C (150 MHz) spectral data for compounds 6, 7 and 8 .	32
3.4	NMR spectroscopic data of compounds 9 and 10 (in CDCl ₃).	33
4.1	NMR spectroscopic data of compounds 11 and 12 (in CDCl ₃).	43
4.2	NMR spectroscopic data of compounds 13 and 14 (in CDCl ₃).	44
4.3	IC ₅₀ values for the cytotoxic activity of 11 .	47
5.1	NMR spectroscopic data of compound 15 and 16 (in CDCl ₃).	55
5.2	NMR spectroscopic data of compounds 17 and 18 (in CDCl ₃).	58
5.3	NMR spectroscopic data of compounds 19 and 20 (in CDCl ₃).	59
5.4	NMR spectroscopic data of compounds 21 and 22 (in CDCl ₃).	60
5.5	Structure-activity relations of compounds 15-22 .	62
5.6	IC ₅₀ for the cytotoxic activity of compounds 17-19 .	64
11.1	NMR spectroscopic data of compounds 23, 24 and 25 (DMSO- <i>d</i> ₆ , 400 MHz).	107
11.2	NMR spectroscopic data of compounds 26, 27 , and 28 (DMSO- <i>d</i> ₆).	108
11.3	NMR spectroscopic data of compound 29 (in CD ₃ OD, 600 MHz).	109
12.1	NMR spectroscopic data of compound 30 (in CDCl ₃).	120
12.2	NMR spectroscopic data of compound 31 (in CDCl ₃).	120

LIST OF APPENDICES

<u>APPENDIX</u>		<u>PAGE</u>
<u>NO.</u>		
I	Screening of the KKB Plant Extracts (TOP Assay)	127
II	List of KKB Plant Extracts (TOP Assay)	129
III	Screening of the KKP Plant Extracts (TOP Assay)	130
IV	List of KKP Plant Extracts (TOP Assay)	131
V	Screening of the KKB Plant Extracts (Ngn2 Promoter Assay)	132
VI	List of KKB Plant Extracts (Ngn2 Promoter Assay)	134
VII	Screening of the KKP Plant Extracts (Ngn2 Promoter Assay)	136
VIII	List of KKP Plant Extracts (Ngn2 Promoter Assay)	137
IX	Characteristics of the new compounds	139

ABSTRACT

The Wnt signal plays a crucial role in many biological processes. Deregulation of the pathway has been implicated in the occurrence of human diseases particularly in cancer and tumorigenesis. As we continue our efforts to search for Wnt signal inhibitors, we have identified three plant extracts KKP261 *Curcuma comosa*, KB302 *Azadirachta excelsa* and KKB304 *Scoparia dulcis* to possess Wnt signal inhibitory activity. Activity-guided multi-step separation of the extracts led to the isolation of ten compounds (**1-10**) from *C. comosa*, four (**11-14**) from *S. dulcis* and eight (**15-22**) from *A. excelsa*. Compounds **1**, **2** and **15** are new compounds. Six compounds (**1**, **8**, **17-20**) were identified potent Wnt inhibitors using the STF/293 reporter (TOP) assay. Compound **18** showed cytotoxic activity against AGS and HCT116 cancer cell line. It did not affect the level and localization of β -catenin, but downregulated the c-myc level. Compound **11**, though was not identified as a positive compound using STF/293, it showed cytotoxicity against AGS which has an active Wnt signal. It exhibited Wnt inhibition in AGS by p53- and proteasome-mediated β -catenin degradation and inhibition of nuclear β -catenin accumulation. Furthermore, **11** sensitizes AGS to TRAIL-induced apoptosis.

CHAPTER 1

Introduction

1.1. Background of the study

In the last 30 years, natural products are still considered as important sources of leads for the development of drugs for the treatment of human diseases.¹ One of the natural resources utilized since the ancient times are the plants. Since the early civilizations, as we all know, plants were already used for medicinal purposes. It is reported that there is approximately 300,000 species of higher plants, and this figure tells that the plant kingdom offers huge areas for exploration of compounds with pharmaceutical application.²

With the advent of new technologies and research techniques, scientists are able to fully understand the biochemistry of many human diseases. One of these important discoveries is the Wnt signal pathway. From its discovery in the 1980s, important findings had been reported on its association with human diseases particularly cancer.³ Even though there are several advances and developments to cure cancer, to win the fight against cancer remains a challenge. According to the GLOBOCAN Project of the International Agency for Research on Cancer (IARC), cancer is one of the leading causes of death in the world.⁴ From the same report, the top five most frequent cancers are lung, breast, colorectal, prostate and stomach cancers. In Japan, stomach, colon and rectum are among the leading cancer sites among Japanese in 2008.⁵ About 70-80% of colorectal cancer has an active Wnt signal. Thus, targeting the Wnt pathway provides a promising therapeutic strategy for the management of these diseases.

With the vast compounds available from natural resources such as plants, they are considered as potential sources of Wnt inhibitors. Several compounds had been reported to affect the Wnt signal and showed cytotoxicity against some colorectal cancer, and possibly, could be leads for drug development.⁶ Though our laboratory has already reported some Wnt inhibitors derived from plants, it is still significant to continue exploring other compounds that could be potent Wnt inhibitors.

1.2 The Wnt Signalling Pathway

The Wnt/ β -catenin pathway is a conserved signalling cascade that regulates the cellular development and fate determination.⁷ **In the absence of the Wnt protein**, β -catenin binds to the destruction complex which is composed of axin, adenomatous polyposis coli (APC), glycogen synthase kinase-3 β (GSK3 β), and casein kinase-1 α (CKI α) (Figure 1.1). In the destruction complex, β -catenin is sequentially phosphorylated by CKI α and GSK-3 β .⁸ CKI α primes the β -catenin by phosphorylating it at S45, then GSK-3 β phosphorylates at S33, S37 and T41. β -Transducin repeat-containing protein (β -TrCP) recognizes the phosphorylated β -catenin, and facilitates the ubiquitination process which is then rapidly degraded by the proteasome.⁹ Removal of β -catenin from the destruction complex is accomplished by the direct proteasomal degradation. **In the presence of the Wnt protein**, the Wnt protein binds to frizzled and low-density-lipoprotein related protein (LRP5/6). The destruction complex translocate to the membrane, and axin associates with the phosphorylated LRP.¹⁰ Inactivation of the destruction complex is said to be accomplished by the following mechanisms:

- a. Upon Wnt-receptor ligand interaction, binding of the destruction complex results in the dissociation of β -TrCP.¹¹ Without the β -TrCP, phosphorylated β -catenin is

no longer ubiquitinated and degraded. The destruction complex is inactivated due to saturation of phosphorylated β -catenin which makes GSK3 β inactive by feedback inhibition. This also results to the inability of newly synthesized β -catenin to bind in the destruction complex.

- b. Another mechanism also showed that in the presence of the Wnt protein, dishevelled (Dsh), by an unknown mechanism, is hyperphosphorylated which then inhibits the GSK3 β activity.

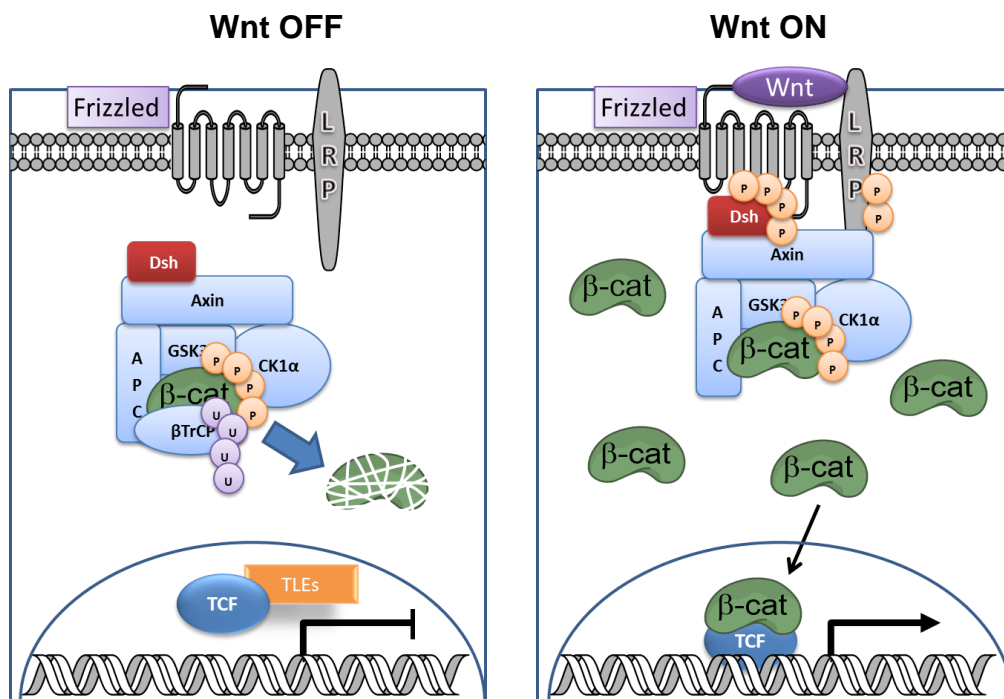


Figure 1.1. The Wnt/ β -catenin Pathway. LRP: lipoprotein receptor-related protein; β -cat: β -catenin; Dsh: deshevelled; GSK3 β : glycogen synthase kinase 3 β ; CK1 α : casein kinase 1 α ; APC: adenomatous polyposis coli; β -TrCP: β -transducin repeat containing protein; TLE: transducin-like enhancer of split; TCF: T-cell factor

When the destruction complex is inactivated, cytosolic β -catenin accumulates and increases its stability which will lead to its nuclear translocation. Then, β -catenin complexes with and activates T-cell factor/lymphoid enhancing factor (TCF/LEF) for the transcription of target genes such as *c-myc*, *cyclin D1*, and *survivin*.^{12, 13, 14}

1.2.1. Alternative pathway for the degradation of β -catenin

β -Catenin is also reported to be degraded independent of GSK3 β phosphorylation and β -TrCP. It was found that β -catenin can be degraded by the action of Siah-1 which has been shown to induce cell cycle arrest, tumor suppression, and apoptosis. Siah-1 expression is reported to be p53-inducible in response to DNA damage.^{15,16} In this mechanism, Siah-1 makes a complex with SIP (Siah interacting protein) and Skp1 (S-phase kinase associated protein 1), and interacts with APC. Ebi binds β -catenin and recruits it to the Siah-1-SIP-Skp1 complex for polyubiquitination and proteasomal degradation (Figure 1.2).¹⁶

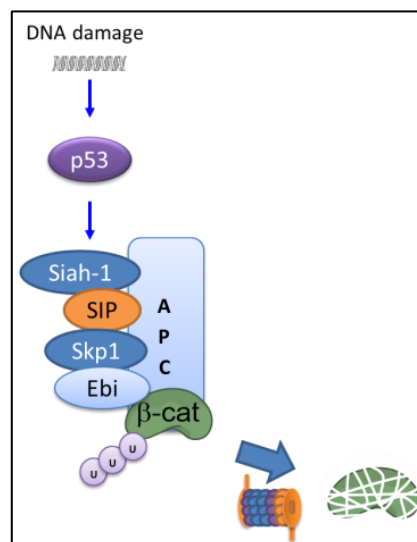


Figure 1.2. β -Catenin regulation via the Siah mechanism. Siah-1: seven in absentia homolog 1; SIP: Siah interacting protein; Skp1: S-phase kinase-associated protein 1.

1.3. Wnt Signal and Diseases

Aberrant activation of the Wnt signal pathway is implicated in the development of various diseases and abnormalities. Most cancer cells, particularly colon and melanoma cancer cells, harbor mutations which upregulate the Wnt signaling pathway.^{6, 7} In fact, about 70-80% of the colorectal cancer cells have an active Wnt signal.¹⁷ These cells contain mutations in APC, axin or in β -catenin itself which leads to β -catenin stabilization and upregulation of the TCF-transcription activity. Furthermore, deregulated activation of the Wnt pathway is not restricted only to cancer development. It has also been linked to the incidence of type II diabetes, and contributes to abnormalities including high bone mass and oligodontia.¹⁸ Table 1.1 shows some diseases associated with the aberrant activation of the Wnt pathway.

Table 1.1 List of diseases associated with aberrant activation of the Wnt signal.¹⁸

Wnt pathway abnormalities	Disease
Increased expression of the Wnt ligands	Colon cancer, breast cancer, melanoma, gastric cancer, Barrett's esophagus, rheumatoid arthritis, schizophrenia
Mutations or reduced expression in APC (decrease of activity)	Colon cancer, Barrett's esophagus
Mutations in β -catenin (increase in activity)	Colon cancer, gastric cancer, hepatocellular cancer
Mutation in Axin (decrease in activity)	Colon cancer, oligodontia
Increase in activity of LRP5	High bone density
Increased expression of TCF4	Type II diabetes

Most of the gastrointestinal cancer cells have an active Wnt signal because they harbour mutations in either APC or β -catenin.¹⁹ Table 1.2 shows the different mutations found in some gastrointestinal cancer cells. These mutations lead to the accumulation of the β -catenin in the cytoplasm due to the inability of the destruction complex to phosphorylate β -catenin, or impairment of the β -TrCP/ubiquitin-mediated degradation.²⁰

Table 1.2. Some gastrointestinal cancer cells with active Wnt signalling pathway.^{19, 20}

Cancer cell Line	Mutation	
<i>Colon cancer</i>		
SW480	<ul style="list-style-type: none"> • APC truncation C-terminus residue 1338 • Wild type β-catenin 	β -Catenin phosphorylation present but degradation is slow.
DLD1	<ul style="list-style-type: none"> • APC truncation • C-terminus residue 1427 • Wild type β-catenin 	β -Catenin phosphorylation present but degradation is slow.
HCT116	<ul style="list-style-type: none"> • Wild type APC • One allele wild-type β-catenin • One allele mutated β-catenin (S45 deletion) 	Lesser S45 phosphorylation
<i>Gastric</i>		
AGS	<ul style="list-style-type: none"> • Wild type APC • β-catenin mutation (G34E) 	Reduce ubiquitin-proteasome degradation of β -catenin

1.4. Wnt inhibitors and their mechanism of action

Several natural compounds, as well as synthetic compounds, have been reported to inhibit the Wnt signal (Figure 1.3). Quercetin, a flavonoid, exhibits inhibitory activity of the Wnt signal in SW480 by decreasing the level of nuclear β -catenin and TCF proteins.²¹ Synthetic compounds XAV939 and IWR-1 were shown to increase the stability of axin. XAV939 was reported to inhibit the activity of tankyrase which promotes ubiquitination of axin.²² Pyrvinium pamoate was first reported to inhibit the Wnt signal through the activation of CK1 α .²³ However, a recent study had presented another probable action mechanism of pyrvinium pamoate.²⁴ Their study showed that pyrvinium pamoate is not a *bona fide* activator of CK1 α but promotes Akt/PKB downregulation and GSK3 activation. Other compounds inhibit the Wnt signal by alternative pathways. These alternative mechanisms are important as they involve degradation of mutant β -catenin that cannot be phosphorylated by GSK3 β . Hexachloropene and isoreserpine showed degradation of β -catenin via the Siah-1-upregulation in HCT116.^{25, 26} Degradation of β -catenin via the Siah-1 mechanism is

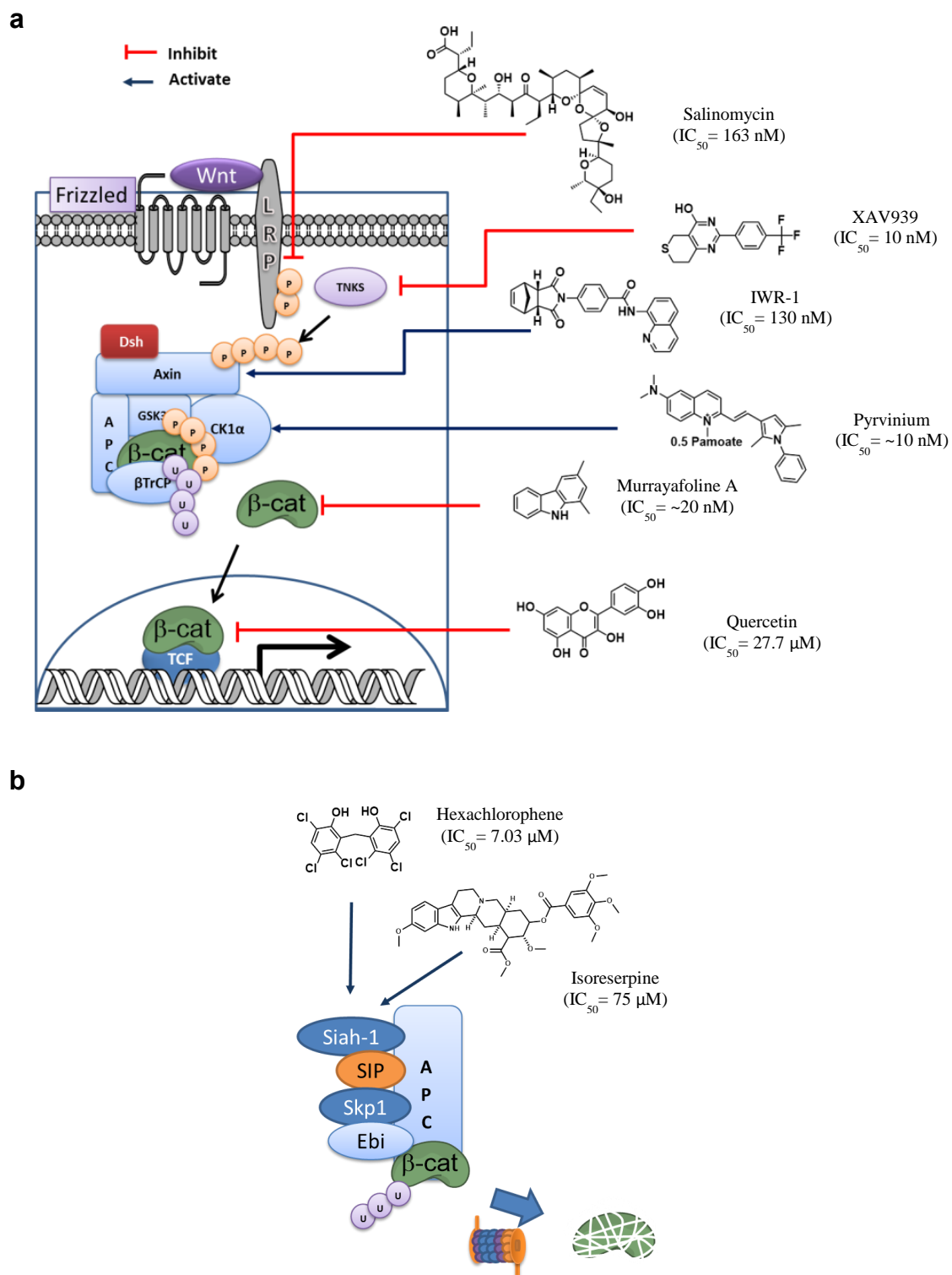


Figure 1.3. Wnt signal inhibition of some reported compounds via the (a) conventional pathway and (b) via an alternative pathway, Siah-1 mechanism.

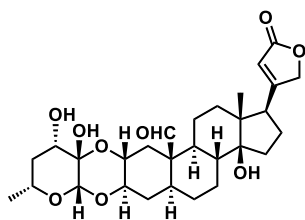
independent of GSK3 β and β -TrCP. On the other hand, murrayafoline A, a carbazole alkaloid derived from *Glycosmis stenocarpa*, was reported to promote β -catenin degradation independent of the phosphorylation and Siah-1 mechanism.²⁷

A number of natural compounds, isolated from either plants or bacteria (actinomycetes), have been reported by our group (Figure 1.4). Calotropin, a cardenolide from *Calotropis gigantea*, enhanced the level of CK1 α .²⁸ Xylogranin B, a new limonoid isolated from *Xylocarpus granatum*, inhibited the translocation of β -catenin to the nucleus.²⁹ These two compounds exhibited inhibition of the TCF/ β -catenin transcriptional activity as well as cytotoxicity activity against colon cancer cells. Moreover, calotropin showed to be cytotoxic against the colon cancer cells which are dependent on Wnt activity, and not in RKO cancer cells which do not possess active Wnt signal.²⁸ Chromomycin A₂³⁰ and nonactin³¹ are Wnt inhibitors isolated from actinomycetes.

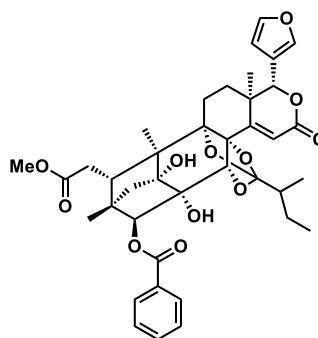
1.5. Screening of potential Wnt inhibitors: Cell-based luciferase assay system

A cell-based luciferase assay using the cell line HEK293 stably transfected with TCF reporter gene (SuperTopflash; TOP-TCF optimized binding site: CCTTTGATC) was used to determine the TCF/ β -catenin transcriptional activity (Figure 1.5). In order to stabilize β -catenin in HEK293 cells, they were treated with LiCl to inhibit the activity of the GSK3 β . The β -catenin translocates to the nucleus, complexes with TCF then binds to the TCF binding site of the TCF-luciferase construct, leading to the transcription of the luciferase gene. The luciferase activity is evaluated from the luminescence produced from the oxidation of the substrate luciferin catalysed by the luciferase protein. Viability assay is also conducted as lower luminescence reading can be due to low viability of the reporter cells.

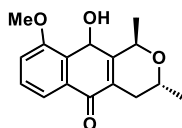
Plant-derived Wnt Inhibitors



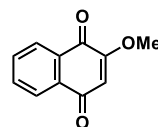
Calotropin (IC_{50} 1.3 nM)
(*Calotropis gigantea*)



Xylogranin B (IC_{50} 48.9 nM)
(*Xylocarpus granatum*)

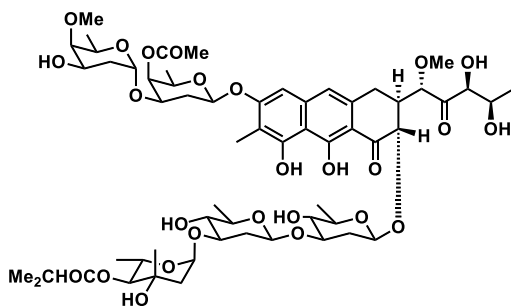


Isoeletherin (IC_{50} 9.5 μ M)
(*Eleutherine palmifolia*)

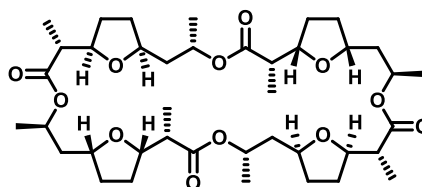


2-methoxy-1,4-naphthoquinone
(IC_{50} 48.9 μ M)
(*Impatiens balsamina*)

Actinomycete-derived Wnt Inhibitors



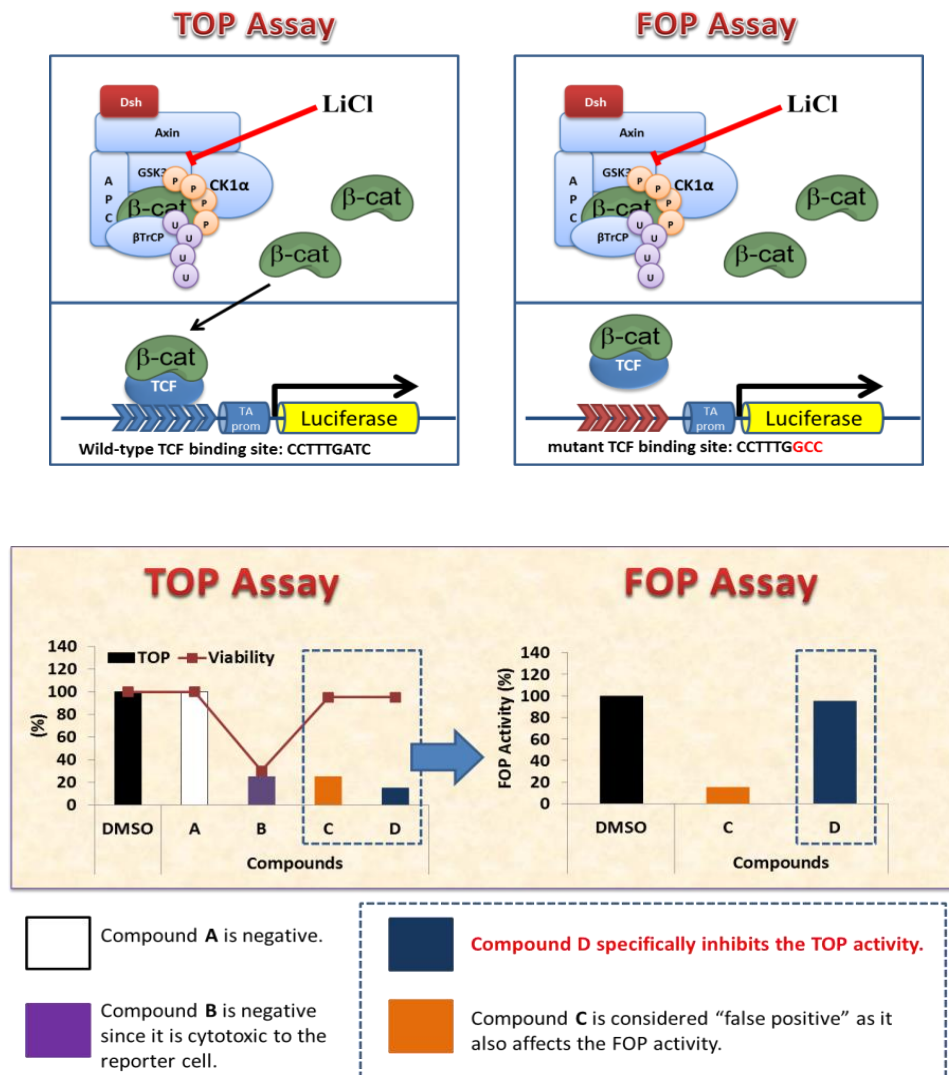
Chromomycin A₂
(IC_{50} 1.8 nM)



Nonactin
(IC_{50} 7.2 nM)

Figure 1.4. Wnt inhibitors reported by our group.

a



b

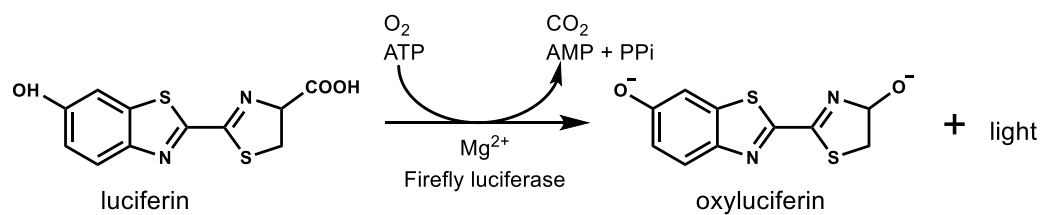


Figure 1.5. a. Cell-based luciferase assay system using TOP and FOP assays.
 b. Oxidative conversion of luciferin to oxyluciferin catalyzed by the enzyme luciferase.

Furthermore, in order to exclude the non-specific effects on luciferase activity, transfection with SuperFOPflash (far from optimized TCF-binding site: CCTTTGGCC) is also conducted. FOP plasmid contains a mutant TCF-binding site, and does not respond to active Wnt signalling activity. Compounds that inhibit the TOP activity without affecting viability of reporter assay cell, and do not significantly affect the FOP activity are considered “hits” (Figure 1.6).

1.6. Cytotoxicity assay using FMCA

Fluorometric microculture cytotoxicity assay (FMCA) is a simple method to determine cytotoxic and/or cytostatic effect *in vitro*.³² In this assay, fluorescein diacetate (FDA) is used as the probe. When added to live cells, FDA is hydrolyzed by the esterases to produce fluorescein, a fluorescent compound (Figure 1.6).

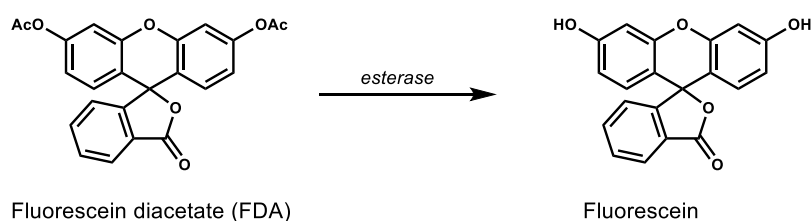


Figure 1.6. Enzymatic hydrolysis of fluorescein diacetate to fluorescein.

1.7. Aim of the study

As we continue our efforts to discover other inhibitors, a screening study identified three plants KKP261 *Curcuma comosa*, KKB304 *Scoparia dulcis*, and KKB302 *Azadirachta excelsa* as potent sources of Wnt inhibitors. In this study, we aim to isolate and identify compounds from these identified plants that could be responsible for the inhibition of the Wnt pathway.

Specifically, our objectives are:

- a. To elucidate the structure of the isolated compounds based on their spectroscopic data (NMR, mass, UV, IR, and optical rotation)
- b. To determine the TCF/ β -catenin transcriptional activity of the isolated compound by using the TOP and FOP assay.
- c. To investigate the cytotoxicity of the compounds against a panel of gastrointestinal cancer cells.
- d. To identify the putative mode of mechanism on the inhibitory activity by Western blot analysis.

References

1. Newman, D. J.; Cragg, G. M., Natural Products As Sources of New Drugs over the 30 Years from 1981 to 2010. *J. Nat. Prod.* **2012**, 75, 311-335.
2. McChesney, J. D.; Venkataraman, S. K.; Henri, J. T., Plant natural products: Back to the future or into extinction? *Phytochemistry* **2007**, 68, 2015-2022.
3. Nusse, R.; Varmus, H., Three decades of Wnts: a personal perspective on how a scientific field developed. *EMBO J.* **2012**, 31, 2670-2684.
4. Ferlay, J.; Soerjomataram, I.; Ervik, M.; Dikshit, R.; Eser, S.; Mathers, C.; Rebelo, M.; Parkin, D.; Forman, D.; Bray, F., GLOBOCAN 2012 v1.0, Cancer Incidence and Mortality Worldwide: IARC CancerBase No. 11 [Internet]. Lyon, France: International Agency for Research on Cancer; **2013**. Available from <http://globocan.iarc.fr>, accessed on 12 Jul 2014.
5. Matsuda, A.; Matsuda, T.; Shibata, A.; Katanoda, K.; Sobue, T.; Nishimoto, H.; The Japan Cancer Surveillance Research, G., Cancer Incidence and Incidence Rates in Japan in 2008: A Study of 25 Population-based Cancer Registries for the Monitoring of Cancer Incidence in Japan (MCIJ) Project. *Jpn. J. Clin. Oncol.* **2014**, 44, 388-396.
6. Anastas, J. N.; Moon, R. T., WNT signalling pathways as therapeutic targets in cancer. *Nat. Rev. Cancer* **2013**, 13, 11-26.
7. Clevers, H.; Nusse, R., Wnt/ β -Catenin Signaling and Disease. *Cell* **2012**, 149, 1192-1205.
8. Liu, C.; Li, Y.; Semenov, M.; Han, C.; Baeg, G.-H.; Tan, Y.; Zhang, Z.; Lin, X.; He, X., Control of β -Catenin Phosphorylation/Degradation by a Dual-Kinase Mechanism. *Cell* **2002**, 108, 837-847.
9. Aberle, H.; Bauer, A.; Stappert, J.; Kispert, A.; Kemler, R., β -Catenin is a target for the ubiquitin-proteasome pathway. *EMBO J.* **1997**, 16, 3797-3804.
10. He, X.; Semenov, M.; Tamai, K.; Zeng, X., LDL receptor-related proteins 5 and 6 in Wnt/ β -catenin signaling: arrows point the way. *Development* **2004**, 131, 1663-1677.
11. Li, Vivian S. W.; Ng, Ser S.; Boersema, Paul J.; Low, Teck Y.; Karthaus, Wouter R.; Gerlach, Jan P.; Mohammed, S.; Heck, Albert J. R.; Maurice, Madelon M.; Mahmoudi, T.; Clevers, H., Wnt Signaling Through Inhibition Of β -Catenin Degradation In An Intact Axin1 Complex. *Cell* **2012**, 149, 1245-1256.
12. He, T. C.; Sparks, A. B.; Rago, C.; Hermeking, H.; Zawel, L.; da Costa, L. T.; Morin, P. J.; Vogelstein, B.; Kinzler, K. W., Identification of c-MYC as a target of the APC pathway. *Science* **1998**, 281, 1509-1512.

13. Shtutman, M.; Zhurinsky, J.; Simcha, I.; Albanese, C.; D'Amico, M.; Pestell, R.; Ben-Ze'ev, A., The cyclin D1 gene is a target of the β -catenin/LEF-1 pathway. *Proc. Natl. Acad. Sci. USA* **1999**, 96, 5522-5527.
14. Zhang, T.; Otevrel, T.; Gao, Z.; Ehrlich, S. M.; Fields, J. Z.; Boman, B. M., Evidence that APC regulates survivin expression: a possible mechanism contributing to the stem cell origin of colon cancer. *Cancer Res.* **2001**, 61, 8664-8667.
15. Liu, J.; Stevens, J.; Rote, C. A.; Yost, H. J.; Hu, Y.; Neufeld, K. L.; White, R. L.; Matsunami, N., Siah-1 Mediates a Novel β -Catenin Degradation Pathway Linking p53 to the Adenomatous Polyposis Coli Protein. *Mol. Cell* **2001**, 7, 927-936.
16. Matsuzawa, S.-i.; Reed, J. C., Siah-1, SIP, and Ebi Collaborate in a Novel Pathway for β -Catenin Degradation Linked to p53 Responses. *Mol. Cell* **2001**, 7, 915-926.
17. Kolligs, F. T.; Bommer, G.; Göke, B., Wnt/ β -Catenin/Tcf Signaling: A Critical Pathway in Gastrointestinal Tumorigenesis. *Digestion* **2002**, 66, 131-144.
18. Barker, N.; Clevers, H., Mining the Wnt pathway for cancer therapeutics. *Nat. Rev. Drug Discov.* **2006**, 5, 997-1014.
19. Ikenoue, T.; Ijichi, H.; Kato, N.; Kanai, F.; Masaki, T.; Rengifo, W.; Okamoto, M.; Matsumura, M.; Kawabe, T.; Shiratori, Y.; Omata, M., Analysis of the β -Catenin/T Cell Factor Signaling Pathway in 36 Gastrointestinal and Liver Cancer Cells. *Cancer Sci.* **2002**, 93, 1213-1220.
20. Yang, J.; Zhang, W.; Evans, P. M.; Chen, X.; He, X.; Liu, C., Adenomatous Polyposis Coli (APC) Differentially Regulates β -Catenin Phosphorylation and Ubiquitination in Colon Cancer Cells. *J. Biol. Chem.* **2006**, 281, 17751-17757.
21. Park, C. H.; Chang, J. Y.; Hahm, E. R.; Park, S.; Kim, H.-K.; Yang, C. H., Quercetin, a potent inhibitor against β -catenin/Tcf signaling in SW480 colon cancer cells. *Biochem. Biophys. Res. Comm.* **2005**, 328, 227-234.
22. Huang, S. M.; Mishina, Y. M.; Liu, S.; Cheung, A.; Stegmeier, F.; Michaud, G. A.; Charlat, O.; Wiellette, E.; Zhang, Y.; Wiessner, S.; Hild, M.; Shi, X.; Wilson, C. J.; Mickanin, C.; Myer, V.; Fazal, A.; Tomlinson, R.; Serluca, F.; Shao, W.; Cheng, H.; Shultz, M.; Rau, C.; Schirle, M.; Schlegl, J.; Ghidelli, S.; Fawell, S.; Lu, C.; Curtis, D.; Kirschner, M. W.; Lengauer, C.; Finan, P. M.; Tallarico, J. A.; Bouwmeester, T.; Porter, J. A.; Bauer, A.; Cong, F., Tankyrase inhibition stabilizes axin and antagonizes Wnt signalling. *Nature* **2009**, 461, 614-620.
23. Thorne, C. A.; Hanson, A. J.; Schneider, J.; Tahinci, E.; Orton, D.; Cselenyi, C. S.; Jernigan, K. K.; Meyers, K. C.; Hang, B. I.; Waterson, A. G.; Kim, K.; Melancon, B.; Ghidu, V. P.; Sulikowski, G. A.; LaFleur, B.; Salic, A.; Lee, L. A.; Miller, D. M.; Lee, E., Small-molecule inhibition of Wnt signaling through activation of casein kinase 1 α . *Nat. Chem. Biol.* **2010**, 6, 829-36.

24. Venerando, A.; Girardi, C.; Ruzzene, M.; Pinna, L. A., Pyrvinium pamoate does not activate protein kinase CK1, but promotes Akt/PKB down-regulation and GSK3 activation. *Biochem. J.* **2013**, 452, 131-137.
25. Park, S.; Gwak, J.; Cho, M.; Song, T.; Won, J.; Kim, D.-E.; Shin, J.-G.; Oh, S., Hexachlorophene Inhibits Wnt/ β -Catenin Pathway by Promoting Siah-Mediated β -Catenin Degradation. *Mol. Pharmacol.* **2006**, 70, 960-966.
26. Gwak, J.; Song, T.; Song, J.-Y.; Yun, Y.-S.; Choi, I.-W.; Jeong, Y.; Shin, J.-G.; Oh, S., Isoreserpine promotes β -catenin degradation via Siah-1 up-regulation in HCT116 colon cancer cells. *Biochem. Biophys. Res. Comm.* **2009**, 387, 444-449.
27. Choi, H.; Gwak, J.; Cho, M.; Ryu, M.-J.; Lee, J.-H.; Kim, S. K.; Kim, Y. H.; Lee, G. W.; Yun, M.-Y.; Cuong, N. M.; Shin, J.-G.; Song, G.-Y.; Oh, S., Murrayafoline A attenuates the Wnt/ β -catenin pathway by promoting the degradation of intracellular β -catenin proteins. *Biochem. Biophys. Res. Comm.* **2010**, 391, 915-920.
28. Park, H. Y.; Toume, K.; Arai, M. A.; Sadhu, S. K.; Ahmed, F.; Ishibashi, M., Calotropin: a cardenolide from *Calotropis gigantea* that inhibits Wnt signaling by increasing casein kinase 1 α in colon cancer cells. *ChemBioChem* **2014**, 15, 872-878.
29. Toume, K.; Kamiya, K.; Arai, M. A.; Mori, N.; Sadhu, S. K.; Ahmed, F.; Ishibashi, M., Xylogranin B: A Potent Wnt Signal Inhibitory Limonoid from *Xylocarpus granatum*. *Org. Lett.* **2013**, 15, (23), 6106-6109.
30. Toume, K.; Tsukahara, K.; Ito, H.; Arai, M. A.; Ishibashi, M., Chromomycins A2 and A3 from marine actinomycetes with TRAIL resistance-overcoming and Wnt signal inhibitory activities. *Mar. Drugs* **2014**, 12, 3466-3476.
31. Tamai, Y.; Toume, K.; Arai, M. A.; Hayashida, A.; Kato, H.; Shizuri, Y.; Tsukamoto, S.; Ishibashi, M., Nonactin and Related Compounds Found in a Screening Program for Wnt Signal Inhibitory Activity. *Heterocycles* **2012**, 84, 1245-1250.
32. Lindhagen, E.; Nygren, P.; Larsson, R., The fluorometric microculture cytotoxicity assay. *Nat. Protocols* **2008**, 3, 1364-1369.

CHAPTER 2

Methods

2.1 General Experimental Procedure

^1H and ^{13}C NMR spectra: JEOL JNM-ECA600, ECP600 and ECP400 spectrometers with deuterated solvent

HRESIMS: JEOL JMS-T100LP spectrometer

Optical rotation: JASCO P-1020 polarimeter

UV spectra: Shimadzu UV mini-1240 spectrometer

CD spectra: JASCO J-720WI spectrophotometer

IR spectra: ATR in a JASCO FTIR 230 spectrophotometer.

Microplate reader: Thermo Luminoskan Ascent, Thermo Fluoroskan Ascent

HPLC: JASCO PU-2080, JASCO RI-2031 Plud (RI Detector), JASCO UV-2075 (UV Detector), JASCO OR-2090 (Chiral Detector)

Flow cytometer: Guava EasyCyte5

2.2. Cell culture

The STF/293 cell line was a generous gift from Prof. Jeremy Nathans (John Hopkins Medical School); HEK293, HCT116, DLD1, and RKO cells were purchased from ATCC; SW480 cells were derived from the Institute of Development, Aging, and Cancer, Tohoku University. STF/293, HEK293, SW480, DLD1, and HCT116 were cultured in Dulbecco's modified Eagle medium (DMEM) with 10% FBS. Cultures were maintained in a humidified incubator at 37 °C in 5% CO₂/95% air.

2.3. Reporter gene assay and transfection

The TCF/ β -catenin transcriptional activity was determined using the method previously described.¹ STF/293 cells which were stably transfected with SuperTOPflash, were seeded into 96-well plates (3×10^4 cells/well), and after 24 h incubation, treated with compounds combined with 15 mM LiCl. After 24 h, cells were lysed and luciferase activity was measured using Luciferase Assay System (Promega). Quercetin which was previously shown to possess β -catenin/TCF transcriptional inhibitory activity was used as a positive control.² For the negative reporter assay, HEK293 cells were briefly split into 24-well plates (1×10^5 cells/well). After 24 h, cells were transfected with 500 ng/well of the luciferase reporter construct (SuperFOPflash) and 50 ng/well of pRL-CMV (Promega, USA) for normalization. At 12 h post-transfection, the compounds combined with 15 mM LiCl were added. Cells were lysed after 24 h incubation, and luciferase activity was measured using the PICAGENE Dual Seapansy (Toyo Ink). SuperFOPflash plasmid was generously given by Prof. Randall T. Moon of the University of Washington.

For the TCF/ β -catenin transcriptional activity in AGS cells, 1×10^5 cells/well were seeded into each well of 24-well plate, and incubated for 24 h. Then, the cells were transfected with either SuperTOPflash or SuperFOPflash (500 ng/well) and pRL-CMV (25 ng/well). After 24-h post-transfection, the cells were treated with the compound for 24 h, lysed and the luciferase was measured using the PICAGENE Dual Seapansy (Toyo Ink).

To determine the relative luciferase activity (%) of each assay, the following formulas were used:

- a. Relative TOP Activity using STF/293 reporter cells:

$$Rel.TOP\ Activity\ (\%) = \frac{Luminescence\ of\ treated\ samples}{Luminescence\ of\ control} \times 100$$

- b. Transient transfection for both Relative TOP and FOP Activity

$$TOP \text{ or } FOP \text{ Activity} = \frac{FL \text{ of treated sample} - FL \text{ of blank}}{RL \text{ of control} - FL \text{ of blank}}$$

where: FL = luminescence reading for the Firefly luciferase (TOP or FOP)

RL = luminescence reading for the Renilla luciferase (pRL-CMV)

$$Rel. \text{ TOP or FOP Activity (\%)} = \frac{TOP \text{ or FOP activity of treated sample}}{TOP \text{ or FOP activity of control (DMSO)}} \times 100$$

2.4. Cell viability assay.

Cell viability was measured using the FMCA assay.³ STF/293 (3 x 10⁴ cells/well), AGS, HCT116, SW480, DLD1, RKO and HEK293 (5 x 10³ cells/well) were inoculated into 96-well plates for 24 h. Compounds were then added and incubated for another 24 h. After incubation, they were treated with fluorescein diacetate (0.35 mg/mL) (Wako) in PBS buffer. Fluorescence was detected after 1 h incubation. The percent viability (%) was calculated as follows:

$$Viability (\%) = \frac{Fluorescence \text{ of treated sample}}{Fluorescence \text{ of control}} \times 100$$

2.5. TRAIL-resistance overcoming activity assay

The TRAIL-resistance overcoming activity was determined using the method described previously.⁴ AGS cells were seeded in 96-well plates (6 x 10³ cells/well), incubated for 24 h and then, treated with different concentrations of the compounds,

either alone or in combination with TRAIL (100 ng/mL). After 24 h, viability was assessed using the FMCA method described above.

2.6. Western blot analysis

Whole cell extracts, cytoplasmic and nuclear fractions were prepared as described previously.⁵ The cytoplasmic and nuclear fractions were obtained using the NE-PER Nuclear and Cytoplasmic Extraction Reagent (Thermo Scientific) according to manufacturer's recommendations. Proteins were separated by 7.5-12.5% SDS-polyacrylamide gel and then transferred onto a nitrocellulose transfer membrane (Pall). The membranes were blocked with 5% nonfat milk in TBST and probed with anti- β -catenin (1:2000, BD Biosciences, #610153); anti- GSK3 β (1:1000, Santa Cruz Biotechnology, #sc-71186), anti- CK1 α (1:200, Santa Cruz Biotechnology, #sc-6477), anti-phospho- β -catenin (S33/S37/T41) (1:200, Cell Signaling Technology, #9561), anti-phospho- β -catenin (S45) (1:200, Cell Signaling Technology, #9564), anti-c-myc (1:200, Santa Cruz Biotechnology, #sc-40); anti-cyclin D1 (1:1000, Abcam, #ab6152); anti-survivin (1:500, Cell Signaling Technology, #71G4B7); anti-p53 (1:500, Sigma, #P5813); anti-Bcl2 (1:1000, Sigma, #B9804); anti-TNFRSF10A/DR4 (1:500, Sigma, #WH0008797M1); anti-DR5 (1:500, Sigma, #D3938); and, anti- β -actin (1:4000, Sigma, #A2228) primary antibodies overnight at 4°C. The anti- β -actin antibody served as internal control. Then, the membranes were washed with TBST and incubated with either horseradish peroxidase conjugated anti-mouse IgG (1:4000, GE Healthcare, NA931VS) or anti-rabbit (1:4000, Jackson Immuno Research, 705-035-003) for 1 h at room temperature. After washing the membranes with TBST, protein bands were visualized using the ECL advance Western detection system (GE Healthcare) or Immobilon Western chemiluminescent HRP substrate (Millipore).

2.7. Cell cycle analysis by flow cytometry

The distribution of cells, with treatment or without treatment, in the different phases of the cell cycle was estimated by measuring the cellular DNA using flow cytometry.⁶ Random population of cells was seeded in 12-well plate (1×10^5 cells/well) for 24 h and treated as described. The attached cells were washed with PBS and then detached with trypsin. All the washings and the medium were combined, centrifuged at 1000 rpm for 5 min, and the cells were then washed 2x with PBS. After washing, the cells were resuspended in 0.3 mL PBS and fixed in 70% ethanol overnight (>18 h) at 20°C. After fixation, the cells were washed with PBS, centrifuged and resuspended in 0.25 mL PBS. It was then added with 5 µL RNase (10 mg/mL, Sigma) and incubated for 1 h at 37 °C. Then, 10 µL PI (10 mg/mL, Sigma) was added and incubated for 15 min in the dark. Stained cells were run in Guava EasyCyte5 (Millipore) and analysed using Guava InCyte software (Millipore).

2.8. Apoptosis study by flow cytometric analysis

Cells were seeded in 12-well plate (1×10^5 cells/well) for 24 h, and treated as described. After the incubation period, both the floating and attached cells were collected. The cells were harvested and washed using the same process as described in the cell cycle analysis. The cells were then stained with propidium iodide (PI) and Annexin-V-fluos staining kit (Roche) according to the manufacturer's protocol and run in Millipore Guava EasyCyte5. Data were analysed using Guava InCyte software (Millipore).

References

1. Li, X.; Ohtsuki, T.; Koyano, T.; Kowithayakorn, T.; Ishibashi, M., New Wnt/ β -Catenin Signaling Inhibitors Isolated from *Eleutherine palmifolia*. *Chem. Asian J.* **2009**, 4, 540-547.
2. Park, C. H.; Chang, J. Y.; Hahm, E. R.; Park, S.; Kim, H.-K.; Yang, C. H., Quercetin, a potent inhibitor against β -catenin/Tcf signaling in SW480 colon cancer cells. *Biochem. Biophys. Res. Comm.* **2005**, 328, 227-234.
3. Lindhagen, E.; Nygren, P.; Larsson, R., The fluorometric microculture cytotoxicity assay. *Nat. Protocols* **2008**, 3, 1364-1369.
4. Minakawa, T.; Toume, K.; Arai, M. A.; Koyano, T.; Kowithayakorn, T.; Ishibashi, M., Prenylflavonoids isolated from *Artocarpus champeden* with TRAIL-resistance overcoming activity. *Phytochemistry* **2013**, 96, 299-304.
5. Toume, K.; Kamiya, K.; Arai, M. A.; Mori, N.; Sadhu, S. K.; Ahmed, F.; Ishibashi, M., Xylogranin B: A Potent Wnt Signal Inhibitory Limonoid from *Xylocarpus granatum*. *Org. Lett.* **2013**, 15, 6106-6109.
6. van Engeland, M.; Nieland, L. J.; Ramaekers, F. C.; Schutte, B.; Reutelingsperger, C. P., Annexin V-affinity assay: a review on an apoptosis detection system based on phosphatidylserine exposure. *Cytometry* **1998**, 31, 1-9.

CHAPTER 3

Diarylheptanoids from *Curcuma comosa* with Wnt/ β -catenin signal inhibitory activity

3.1. Plant description

C. comosa belongs to the Zingiberaceae family. It is distributed in Thailand, Indonesia and Malaysia. The rhizome has been used by local folks as an anti-inflammatory agent. Previous chemical studies showed that the rhizome of this plant contained diarylheptanoids and sesquiterpenes.^{1, 2} The diarylheptanoids of this plant had been reported to have estrogenic³ and anti-inflammatory activities.⁴ The plant sample (rhizome) used in this study was collected from Thailand and, a reference specimen (KKP261) has been deposited in the laboratory. During the screening, the MeOH of *C. comosa* showed a decrease in TOP activity by 82% at 50 $\mu\text{g/mL}$ (Figure 3.1). The viability of STF/293 reporter cells at the same concentration was 84%.

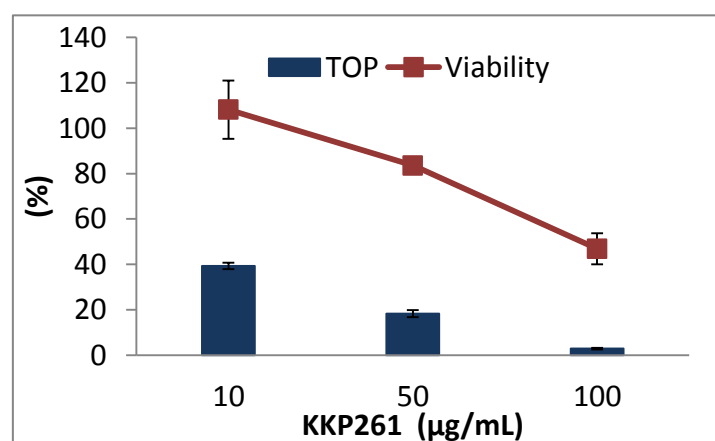


Figure 3.1. Bar graphs showing the dose-dependent TOP activity of KKP261 MeOH extract. The line graph represents cell viability. All data are presented as the mean \pm s.d. (n=3).

3.2. Isolation of the constituents

Figure 3.2 shows the isolation scheme of *C. comosa*. The dried rhizome of *C. comosa* (226 g) was extracted using MeOH. The MeOH crude extract (6.6 g) of *C. comosa* was directly subjected to silica gel column chromatography (ϕ 50 x 270 mm) eluting with the hexane-EtOAc gradient system (1:0 to 0:1) to give fractions 1A-1L. Fraction 1E (76.5 mg) eluted with hexane:EtOAc (8:2) was recrystallized to give compound **9** (28.4 mg). Fraction 1J (548 mg), which showed high activity on the TOP assay, was then subjected to ODS flash column chromatography (ϕ 25 x 180 mm) to yield fractions 3A-3H. Active fraction 3D (59 mg) eluted with MeOH:H₂O (1:1) was further purified using silica gel column chromatography (ϕ 25 x 170 mm; CHCl₃:MeOH gradient system (1:0 - 0:1)) to give compound **4** (11.2 mg). Another fraction from 3D was further purified by preparative HPLC [Cosmosil 5C₁₈-AR-II; ϕ 10 x 250 mm; 60% MeOH] to give compounds **1** (5.7 mg) and **5** (4.9 mg). Fraction 3B (58.2 mg) was subjected to flash silica column chromatography (ϕ 25 x 230 mm) using CHCl₃: MeOH (1:0 to 0:1) to give fractions 6A-6H. Fraction 6B was identified as compound **10** (6.2 mg). Fraction 6F was further purified by preparative HPLC [Cosmosil 5C₁₈-AR-II; ϕ 10 x 250 mm; 53% MeOH] to afford compound **6** (2.9 mg). Fraction 6C gave compound **3** (1.1 mg) after purification by HPLC [Cosmosil 5C₁₈-AR-II; ϕ 10 x 250 mm; 45% MeOH]. The active fraction 1K was subjected to ODS flash column chromatography (ϕ 45 x 180 mm) and eluted with increasing MeOH (67-100%), followed by silica gel column chromatography (ϕ 30 x 235 mm) using CHCl₃:MeOH (1:0 to 0:1) yielded ten fractions (11A-11J). Fraction 11H was identified as compound **7** (14.8 mg). Fraction 11E, which showed weak activity, was further purified using by preparative HPLC [Cosmosil π -NAP; ϕ 10 x 250 mm; 60% MeOH] to give a mixture (6.8 mg) of compound **2** and an unknown compound.

KKP261 *C. comosa* (rhizome)

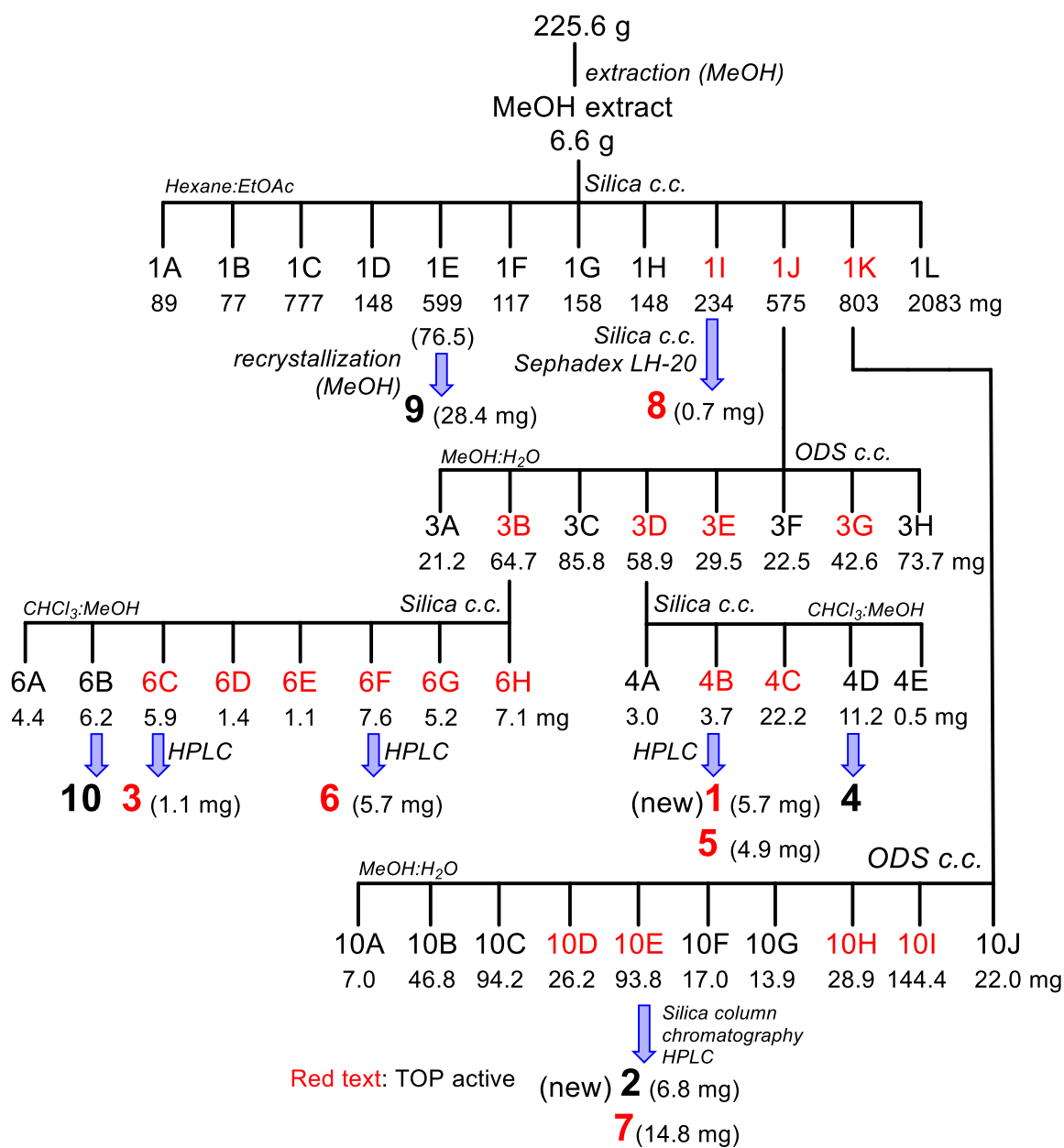


Figure 3.2. Isolation chart of *C. comosa*.

Another active fraction, 1I (203.2 mg), was subjected to ODS flash column chromatography (ϕ 40 x 170 mm) and eluted with increasing MeOH (60%-80%) to give 11 fractions (15A-15K). Fraction 15F (18.3 mg), which showed strong activity, was subjected to silica gel column chromatography using CHCl_3 :MeOH (10:1-0:1) and yielded 8 fractions (16A-16H). Fraction 16D (7.1 mg) was further purified using Sephadex LH-20, followed by silica gel column chromatography [ϕ 25 x 150 mm; CHCl_3 :MeOH (1:0-0:1)] to afford compound **8** (0.7 mg).

3.3. Characterization of the isolated compounds

Compound **1**, isolated as a colorless solid, gave a molecular formula of $\text{C}_{21}\text{H}_{26}\text{O}_5$ with HRESIMS at m/z 381.1634 ($[\text{M}+\text{Na}]^+$, $\text{C}_{21}\text{H}_{26}\text{O}_5\text{Na}$, Δ -4.4 mmu. The ^1H and ^{13}C NMR data (Table 3.1) of **1** are similar to the NMR spectra its reported enantiomer (**ent-1**).⁵ Compound **1** gave a negative optical rotation, which suggests a $3S,5S$ configuration, while its reported $3R,5R$ enantiomer (**ent-1**) had a positive value. To further confirm the configuration of **1**, we conducted deacetylation to produce hannokinol (**7**). The identity of the deacetylated product was verified by comparison of its NMR spectra with the isolated compound **7**.^{6, 7} Optical rotation of the deacetylated product was determined using reversed phase HPLC equipped with an optical rotation detector (ORD) and its response was compared with the isolated (-)-hannokinol (**7**). The $3R,5R$ form (**ent-7**) was previously reported to be $[\alpha]_{\text{D}}^{26} +4.0$ (c 0.10 MeOH),⁷ while the $3S,5S$ form (**7**) was found to be $[\alpha]_{\text{D}}^{25} -19.0$.⁶ Compound **7** and the deacetylated product of **1** both gave a negative response in the ORD. These findings suggest that the deacetylated product of **1** had a negative optical rotation. Therefore, the structure of compound **1** was determined to be (-)-($3S,5S$)-3-acetoxy-5-hydroxy-1,7-bis(4-hydroxyphenyl)heptane.

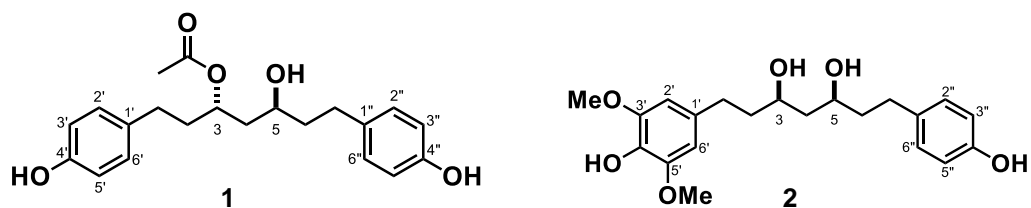


Table 3.1. ^1H (600 MHz) and ^{13}C (150 MHz) spectral data for compounds **1** and **2**.

Position	1 ^a		2 ^b	
	^1H (δ , ppm; J , Hz)	^{13}C (δ , ppm)	^1H (δ , ppm; J , Hz)	^{13}C (δ , ppm)
1	2.48 (2H, m)	32.0	2.56 (2H, m)	30.7
2	1.87 (2H, m)	38.0	1.74 (2H, m)	40.0
3	5.06 (1H, m)	73.0	3.85 (1H, m)	72.4
4	1.72 (1H, m)	43.0	1.56 (2H, m)	42.8
	1.60 (1H, m)			
5	3.51 (1H, m)	68.1	3.85 (1H, m)	72.5
6	1.63 (2H, m)	41.0	1.74 (2H, m)	39.9
7	2.63 (1H, m)	31.8	2.66 (2H, m)	31.9
	2.54 (1H, m)			
1'		133.7		132.9
2'	6.96 (1H, d, 8.7)	130.3	6.39 (1H, s)	104.9
3'	6.67 (1H, d, 8.7)	116.1		146.9
4'		156.4		132.8
5'	6.67 (1H, d, 8.7)	116.1		146.9
6'	6.96 (1H, d, 8.7)	130.3	6.39 (1H, s)	104.9
1''		134.2		133.3
2''	6.98 (1H, d, 8.7)	130.3	6.99 (1H, d, 8.3)	129.4
3''	6.68 (1H, d, 8.7)	116.1	6.73 (1H, d, 8.3)	115.3
4''		156.4		154.2
5''	6.68 (1H, d, 8.7)	116.1	6.73 (1H, d, 8.3)	115.2
6''	6.98 (1H, d, 8.7)	130.3	6.99 (1H, d, 8.3)	129.4
3-OAc	1.98 (3H, s)	21.1		
		173.1		
3',5'-OMe			3.82 (6H, s)	56.2
3,5,4',4''-OH			4.40 (4H, br s)	

^a measured in CD_3OD

^b measured in CDCl_3

Compound **2** was obtained as a colorless compound. An intense peak at m/z 399.1762 ($[M+Na]^+$, $C_{21}H_{28}O_6Na$ Δ -2.1 mmu) was observed in HRESIMS, which is consistent with the molecular formula of $C_{21}H_{28}O_6$. A singlet peak at δ 3.82 (6H) was due to the two symmetric methoxy groups and were assigned at C-3' and C-5'. The presence of two symmetric benzene protons was indicated by the correlations observed between a singlet proton peak at δ 6.39 and carbon peak at δ 104.9 in both HMBC (Figure 3.2) and HMQC. They were assigned at H-2' and H-6'. The two doublets at δ 6.99 ($J = 8.3$ Hz) and 6.73 ($J = 8.3$ Hz) suggested the presence of 1,4-disubstituted aromatic protons and were assigned to four aromatic protons, H-2''/H-6'' and H-3''/H-5'', respectively. From these results, **2** was assigned as 3,5-dihydroxy-1-(4-hydroxy-3,5-dimethoxyphenyl)-7-(4-hydroxyphenyl)heptane.

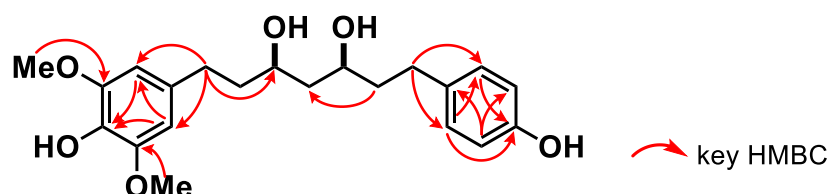


Figure 3.3. Selected key HMBC of **2**

Since compound **2** contains a 1,3-diol group, we employed the Rychnovsky's method to determine its relative configuration. In the Rychnovsky's method, *syn*-isomer has carbon resonances for the acetonide methyl groups at 30 and 19 ppm, while the anti-isomers have methyl resonances in the range of 24-25 ppm.⁸ Acetonidation of **2** produced the acetonide **2a** which gave an intense peak at m/z 439.2070 ($[M+Na]^+$, $C_{24}H_{32}O_6Na$, Δ -2.7 mmu) based on HRESIMS. The HMQC data of the acetonide **2a** showed correlations between the two methyl peaks at δ 1.32 and δ 1.62, and ^{13}C peaks at δ 21.9 and δ 32.5,

respectively (Figure 3.3). These results suggested that **2a** was produced from a *syn*-1,3-diol.¹⁵ The absolute stereochemistry of **2** remains undefined.

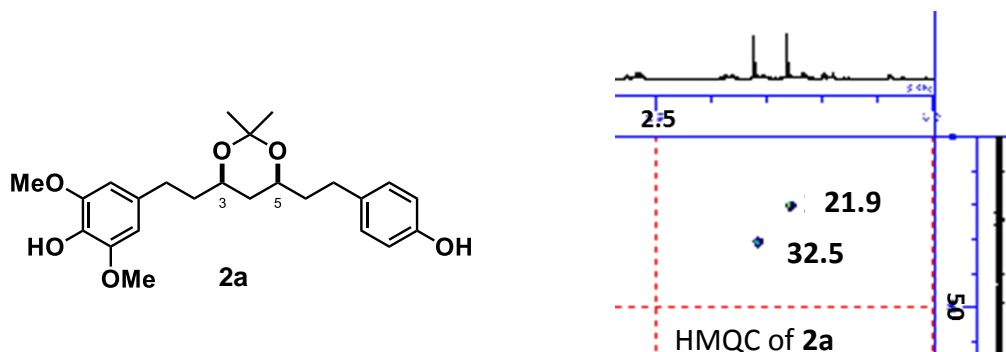


Figure 3.4. Acetonide derivative (**2a**) of compound **2** and its HMQC.

The structures of the five known diarylheptanoids were identified by comparing their spectral values and optical rotations with those in the literature.

(5*R*)-5-hydroxy-7-(4-hydroxyphenyl)-1-(4-hydroxy-3-methoxyphenyl)-3-heptanone

(3)^{5, 9}:

¹H and ¹³C NMR see Table 3.2; ESIMS: *m/z* 367 [M + Na]⁺

(3*R*,5*R*)-3,5-diacetoxy-1,7-bis(3,4-dihydroxyphenyl)heptane (4)¹⁰:

¹H and ¹³C NMR see Table 3.2; [α]_D²⁵ +8.3 (*c* 1.2 EtOH), lit. [α]_D²⁵ +1.5 (*c* 1.3 EtOH);

ESI-MS: *m/z* 455 [M + Na]⁺

(3*R*,5*R*)-3,5-diacetoxy-1-(3,4-dihydroxyphenyl)-7-(4-hydroxyphenyl)heptane (5)⁵:

¹H and ¹³C NMR see Table 3.2; [α]_D²⁶ +12.2 (*c* 0.5 MeOH), lit. [α]_D²⁵ +17.2 (*c* 0.1

MeOH); ESI-MS: *m/z* 439 [M + Na]⁺

(5*S*)-5-hydroxy-1,7-bis(4-hydroxyphenyl)heptan-3-one (6)^{11, 12}

¹H and ¹³C NMR see Table 3.3; ESI-MS: *m/z* 337 [M + Na]⁺

(-)-hannokinol (7)⁶

¹H and ¹³C NMR see Table 3.3; [α]_D²³ -34.1 (*c* 0.1 MeOH), lit. [α]_D²⁵ -19 (not indicated);

ESI-MS: *m/z* 339 [M + Na]⁺

1,7-bis(4-hydroxyphenyl)hepta-4*E*,6*E*-dien-3-one (8)¹³

¹H and ¹³C NMR see Table 3.3; ESI-MS: *m/z* 293 [M-H]⁻

zederone (9)¹⁴

¹H and ¹³C NMR see Table 3.4; [α]_D³¹ +240 (*c* 1.00, CHCl₃) lit. [α]_D³¹ +290 (*c* 1.14

CHCl₃); ESI-MS: *m/z* 515 [2M + Na]⁺

aerugidiol (10)^{15, 16}

¹H and ¹³C NMR see Table 3.4; [α]_D²⁴ -3.3 (*c* 1.0, MeOH; lit. [α]_D²⁶ -17.0 *c* 1.0 MeOH);

ESI-MS: *m/z* 273 [2M + Na]⁺

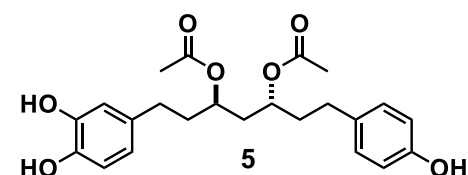
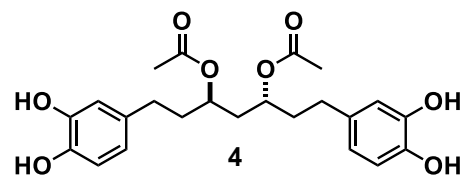
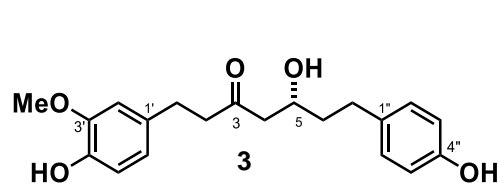


Table 3.2. ^1H (600 MHz) and ^{13}C (150 MHz) spectral data for compounds **3**, **4** and **5**.

Position	3		4		5	
	^1H (δ , ppm; J , Hz)	^{13}C (δ , ppm)	^1H (δ , ppm; J , Hz)	^{13}C (δ , ppm)	^1H (δ , ppm; J , Hz)	^{13}C (δ , ppm)
1	2.74 (2H, m)	30.3	2.44 (2H, t, 8.4)	32.0	2.44 (2H, t, 8.0)	32.0
2	2.74 (2H, m)	46.4	1.76 (2H, m)	37.7	1.76 (2H, m)	37.8
3		211.9	4.91 overlapped	71.5	4.85 overlapped	71.5
4	2.50 (1H, m), 2.58 (1H, m)	51.3	1.83 (2H, m)	39.5	1.83 (2H, m)	39.5
5	3.99 (1H, m)	68.3	4.91 overlapped	71.5	4.85 overlapped	71.5
6	1.65 (2H, m)	40.5	1.76 (2H, m)	37.7	1.76 (2H, m)	37.8
7	2.53 (1H, m), 2.63 (1H, m)	31.9	2.44 (2H, t, 8.4)	32.0	2.50(2H, d, 8.0)	31.7
1'		134.1		134.3		134.3
2'	6.75 (1H, d, 1.8)	113.1	6.59 (1H, d, 1.8)	116.5	6.59 (1H, d, 2.0)	116.5
3'		149.0		146.1		146.2
4'		145.8		144.4		144.4
5'	6.67 (1H, d, 7.8)	116.1	6.65 (1H, d, 8.4)	116.3	6.68 (1H, d, 8.7)	116.3
6'	6.60 (1H, dd, 1.8, 7.8)	121.7	6.47 (1H, dd, 8.4, 1.8)	120.6	6.46 (1H, dd, 8.7, 2.0)	120.6
1''		134.1		134.3		133.5
2''	6.98 (1H, d, 7.8)	130.3	6.59 (1H, d, 1.8)	116.5	6.97 (1H, d, 8.4)	130.3
3''	6.67 (1H, d, 7.8)	116.1		146.1	6.68 (1H, d, 8.7)	116.3
4''		156.4		144.4		156.5
5''	6.67 (1H, d, 7.8)	116.1	6.65 (1H, d, 8.4)	116.3	6.68 (1H, d, 8.7)	116.2
6''	6.98 (1H, d, 7.8)	130.3	6.47 (1H, dd, 8.4, 1.8)	120.6	6.97 (1H, d, 8.4)	130.3
3-OAc			1.961 (3H, s)	21.1	1.958 (3H, s)	21.1
				172.8		172.73
5-OAc			1.961 (3H, s)	21.1	1.961 (3H, s)	21.1
				172.8		172.75
3'-OCH ₃	3.80 (3H, s)	56.5				

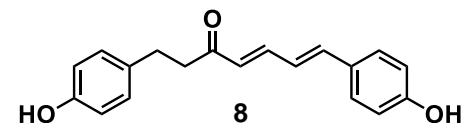
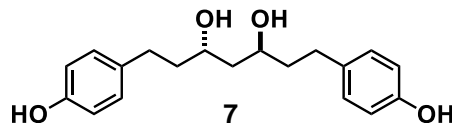
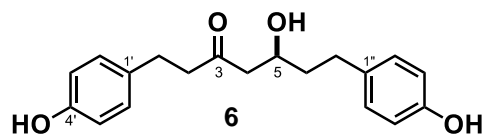
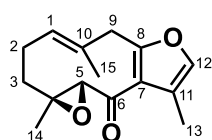
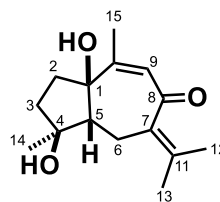


Table 3.3. ^1H (600 MHz) and ^{13}C (150 MHz) spectral data for compounds **6**, **7** and **8**.

Position	6		7		8	
	^1H (δ , ppm; J , Hz)	^{13}C (δ , ppm)	^1H (δ , ppm; J , Hz)		^{13}C (δ , ppm)	
1	2.72 (2H, m)	29.8	2.55 (1H, m)		2.87 (2H, t, 7.2)	
2	2.72 (2H, m)	46.4	2.67 (1H, m)		2.82 (2H, t, 7.2)	
3		211.9	3.88 (2H, m)			
4	2.52 (1H, m)	51.3	1.58 (2H, m)		6.23 (1H, d, 16.2)	
	2.59 (1H, m)					
5	3.99 (1H, m)	68.3	3.88 (2H, m)		7.38 (1H, dd, 16.2, 10.8)	
6	1.65 (2H, m)	40.5	1.68 (2H, m)		6.82 (1H, dd, 15.6, 10.8)	
7	2.64 (1H, m)	32.0	2.55 (1H, m)		6.96 (1H, d, 15.6)	
	2.72 (1H, m)		2.67 (1H, m)			
1'		133.3				
2'	6.98 (1H, d, 8.4)	130.2	6.72 (1H, d, 8.8)		7.02 (1H, d, 9)	
3'	6.67 (1H, d, 8.8)	116.2	7.02 (1H, d, 8.8)		6.68 (1H, d, 9)	
4'		156.6				
5'	6.67 (1H, d, 8.8)	116.2	7.02 (1H, d, 8.8)		6.68 (1H, d, 9)	
6'	6.98 (1H, d, 8.4)	130.2	6.72 (1H, d, 8.8)		7.02 (1H, d, 9)	
1''		134.1				
2''	6.98 (1H, d, 8.4)	130.3	6.72 (1H, d, 8.8)		7.39 (1H, d, 9)	
3''	6.67 (1H, d, 8.8)	116.1	7.02 (1H, d, 8.8)		6.76 (1H, d, 9)	
4''		156.4				
5''	6.67 (1H, d, 8.8)	116.1	7.02 (1H, d, 8.8)		6.76 (1H, d, 9)	
6''	6.98 (1H, d, 8.4)	130.3	6.72 (1H, d, 8.8)		7.39 (1H, d, 9)	



9



10

Table 3.4. NMR spectroscopic data of compound **9** and **10** (in CDCl₃).

Position	9		10	
	¹ H (δ, ppm; <i>J</i> , Hz)	¹³ C (δ, ppm)	¹ H (δ, ppm; <i>J</i> , Hz)	¹³ C (δ, ppm)
1	5.46 (1H, br d, 9.6)	131.0		87.0
2 α	2.5 (1H, dddd, 3.6, 12, 12.9, 13.2)	24.6		37.7
2 β	2.21 (1H, br d, 12.6)			
3 α	2.28 (1H, ddd, 3, 3, 13)	38.0		37.5
3 β	1.26 (1H, ddd, 3, 12.6, 13.2)			
4		64.0		83.7
5	3.79 (1H, s)	66.5		61.5
6		192.2	2.63 (1H, d, 14.4)	27.7
7		122.2		133.3
8		157.1		n.d.
9	3.67 (1H, d, 16.2) 3.73 (1H, d, 16.2)	41.9	5.83 (1H, t, 1.8)	128.5
10		131.0		151.5
11		123.2		n.d.
12	7.06 (1H, s)	138.0	1.99 (3H, s)	23.2
13	2.09 (3H, s)	10.3	1.85 (3H, s)	22.5
14	1.32 (3H, s)	15.7	1.41 (3H, s)	24.6
15	1.58 (3H, s)	15.1	1.99 (3H, s)	22.4

3.4. TCF/ β -catenin transcriptional inhibitory activity

Compounds **1**, **6**, **7**, and **8** showed the highest inhibitory activity in the TOP assay with IC_{50} values of 3.0, 1.0, and 2.9 μ M, respectively (Figure 3.5). However, only **1** and **8** did not affect FOP activity up to 5 μ M, which suggests that their inhibitory activity was specific to the TOP activity. The other diarylheptanoids (**2-6**) as well as zederone (**9**) also showed dose-dependent inhibitory activity against the TOP assay; however, since their IC_{50} values were higher than 10 μ M, they were not subjected to further assays. Aerugidiol (**10**), on the other hand, was inactive.

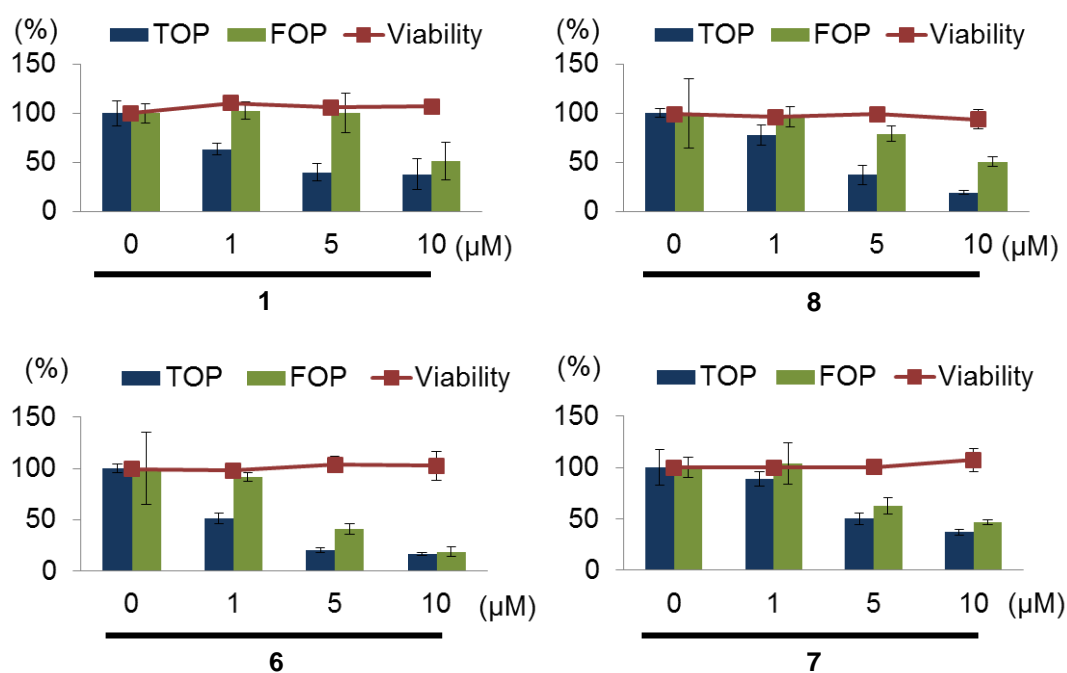


Figure 3.5. TOP and FOP activity of compounds **1**, **6**, **7** and **8**. TOP was measured using HEK293 cells stably transfected with SuperTOPflash reporter gene (STF/293) while the FOP activity was measured using HEK293 cells transiently transfected with SuperFOPflash reporter gene. Line graph represents the viability of STF/293 cells. Data were from one experiment representative of at least two independent experiments (mean \pm s.d). All data are presented as the mean \pm s.d. (n=3).

Since the assay involved the addition of LiCl, an inhibitor of glycogen synthase kinase-3 (GSK3), the data may suggest that **1** and **8** act downstream of the Wnt signaling pathway or on β -catenin itself. However, western blot analysis using SW480 cells showed that β -catenin levels in both cytoplasmic and nuclear fractions were not affected. Some curcumin derivatives exhibiting Wnt/ β -catenin pathway inhibitory activity were also reported to have no effect on β -catenin levels. Instead, they showed to decrease the level of p300, which is a positive regulator of the Wnt signal pathway.¹⁷ The FMCA was used to determine the effect of **1** and **8** on the viability of colon cancer cells, SW480, HCT116, and DLD1. Several studies previously reported that inhibiting TCF/ β -catenin transcriptional activity decreased the viability of colon cancer cells.^{17, 18} However, after 24 hr incubation, neither compounds exhibited inhibitory activity on the growth of these three colon cancer cells.

References

1. Suksamrarn, A.; Ponglikitmongkol, M.; Wongkrajang, K.; Chindaduang, A.; Kittidanairak, S.; Jankam, A.; Yingyongnarongkul, B.-e.; Kittipanumat, N.; Chokchaisiri, R.; Khetkam, P.; Piyachaturawat, P., Diarylheptanoids, new phytoestrogens from the rhizomes of *Curcuma comosa*: Isolation, chemical modification and estrogenic activity evaluation. *Bioorg. Med. Chem.* **2008**, *16*, 6891-6902.
2. Qu, Y.; Xu, F.; Nakamura, S.; Matsuda, H.; Pongpiriyadacha, Y.; Wu, L.; Yoshikawa, M., Sesquiterpenes from *Curcuma comosa*. *J. Nat. Med.* **2009**, *63*, 102-104.
3. Winuthayanon, W.; Suksen, K.; Boonchird, C.; Chuncharunee, A.; Ponglikitmongkol, M.; Suksamrarn, A.; Piyachaturawat, P., Estrogenic Activity of Diarylheptanoids from *Curcuma comosa* Roxb. Requires Metabolic Activation. *J. Agr. Food Chem.* **2009**, *57*, 840-845.
4. Sodsai, A.; Piyachaturawat, P.; Sophasan, S.; Suksamrarn, A.; Vongsakul, M., Suppression by *Curcuma comosa* Roxb. of pro-inflammatory cytokine secretion in phorbol-12-myristate-13-acetate stimulated human mononuclear cells. *Int. Immunopharmacol.* **2007**, *7*, 524-531.
5. Li, J.; Liao, C.-R.; Wei, J.-Q.; Chen, L.-X.; Zhao, F.; Qiu, F., Diarylheptanoids from *Curcuma kwangsiensis* and their inhibitory activity on nitric oxide production in lipopolysaccharide-activated macrophages. *Bioorg. Med. Chem. Lett.* **2011**, *21*, 5363-5369.
6. Alegrio, L. V.; Braz-filho, R.; Gottlieb, O. R., Diarylheptanoids and isoflavonoids from *Centrolobium* species. *Phytochemistry* **1989**, *28*, 2359-2362.
7. Yokosuka, A.; Mimaki, Y.; Sakagami, H.; Sashida, Y., New Diarylheptanoids and Diarylheptanoid Glucosides from the Rhizomes of *Tacca chantrieri* and Their Cytotoxic Activity. *J. Nat. Prod.* **2002**, *65*, 283-289.
8. Rychnovsky, S. D.; Richardson, T. I.; Rogers, B. N., Two-Dimensional NMR Analysis of Acetonide Derivatives in the Stereochemical Assignment of Polyol Chains: The Absolute Configurations of Dermostatins A and B. *J. Org. Chem.* **1997**, *62*, 2925-2934.
9. Shin, D.; Kinoshita, K.; Koyama, K.; Takahashi, K., Antiemetic principles of *Alpinia officinarum*. *J. Nat. Prod.* **2002**, *65*, 1315-8.
10. Kikuzaki, H.; Kobayashi, M.; Nakatani, N., Diarylheptanoids from rhizomes of *Zingiber officinale*. *Phytochemistry* **1991**, *30*, 3647-3651.
11. Ohta, S.; Koyama, M.; Aoki, T.; Suga, T., Absolute Configuration of Platyphylloside and (-)-Centrolobol. *Bull. Chem. Soc. Jpn.* **1985**, *58*, 2423-2424.

12. Giang, P. M.; Son, P. T.; Matsunami, K.; Otsuka, H., One new and several minor diarylheptanoids from *Amomum muricarpum*. *Nat. Prod. Res.* **2011**, 26, 1195-1200.
13. Ali, M. S.; Tezuka, Y.; Awale, S.; Banskota, A. H.; Kadota, S., Six New Diarylheptanoids from the Seeds of *Alpinia blepharocalyx*. *J. Nat. Prod.* **2001**, 64, 289-293.
14. Shibuya, H.; Hamamoto, Y.; Cai, Y.; Kitagawa, I., A reinvestigation of the structure of zederone, a furanogermacrane-type sesquiterpene from zedoary. *Chem. Pharm. Bull.* **1987**, 35, 924-927.
15. Masuda, T.; Jitoe, A.; Nakatani, N., Structure of Aerugidiol, a New Bridge-head Oxygenated Guaiane Sesquiterpene. *Chem. Lett.* **1991**, 20, 1625-1628.
16. Hu, D.; Ma, N.; Lou, Y.; Qu, G.-x.; Qiu, F., Guaiane sesquiterpenes of *Curcuma wenyujin*. *Shenyang Yao Ke Da Xue Xue Bao* **2008**, 25, 188-190.
17. Ryu, M.-J.; Cho, M.; Song, J.-Y.; Yun, Y.-S.; Choi, I.-W.; Kim, D.-E.; Park, B.-S.; Oh, S., Natural derivatives of curcumin attenuate the Wnt/ β -catenin pathway through down-regulation of the transcriptional coactivator p300. *Biochem. Biophys. Res. Comm.* **2008**, 377, 1304-1308.
18. Chen, B.; Dodge, M. E.; Tang, W.; Lu, J.; Ma, Z.; Fan, C.-W.; Wei, S.; Hao, W.; Kilgore, J.; Williams, N. S.; Roth, M. G.; Amatruda, J. F.; Chen, C.; Lum, L., Small molecule-mediated disruption of Wnt-dependent signaling in tissue regeneration and cancer. *Nat. Chem. Biol.* **2009**, 5, 100-107.

CHAPTER 4

Cytotoxicity of Scopadulciol isolated from *Scoparia dulcis* against Wnt-dependent cancer cells

4.1. Plant description

S. dulcis belongs to the Plantaginaceae family. It is distributed in Thailand, Indonesia and Malaysia. Pharmacological studies showed that it possessed antidiabetic, anti-inflammatory and analgesic activities.¹ Moreover, other studies had showed that scopadulciol isolated from this plant exhibited inhibitory activity against gastric H⁺, K⁺-ATPase which is responsible for acid secretion in the stomach,² and cytotoxicity against several gastric cancer cell lines.³ The plant sample (arial parts) used in this study was collected at Bangladesh and, a reference specimen (KKB304) has been deposited in the laboratory. The MeOH aerial plant extract of *S. dulcis* inhibited the TOP inhibitory activity by 73% at 5 µg/mL (Figure 4.1). At this concentration, it was not cytotoxic to the reporter cell (viability = 86%).

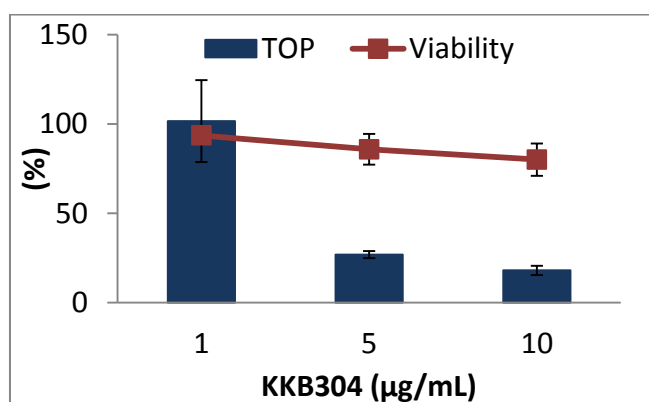


Figure 4.1. Bar graphs showing the dose-dependent TOP activity of KKB304 MeOH extract. The line graph represents cell viability. All data are presented as the mean \pm s.d. (n=3).

4.2. Isolation of the constituents

Figure 4.2 shows the isolation scheme of *S. dulcis*. The dried aerial parts of *S. dulcis* (128 g) were soaked in MeOH and left overnight at room temperature, homogenized, filtered and evaporated under reduced pressure to obtain a crude extract (3.0 g). The chlorophyll content of the MeOH crude extract was removed by Diaion HP-20 column chromatography (ϕ 40 x 230 mm) using acetone:MeOH (0:1-1:0) and yielded three fractions (1A-1C). Fraction 1B (0.5 g), which was eluted with 100% MeOH and showed potent decrease in TOP activity, was subjected to silica gel column chromatography (ϕ 40 x 275 mm) and eluted with CHCl₃:MeOH gradient system (1:0 to 0:1) to give fractions 2A-2K. Active fraction 2G (281.4 mg) eluted with CHCl₃:MeOH (95:5) was subjected to silica gel column chromatography (ϕ 40 x 280 mm) using CHCl₃:MeOH gradient system (9:1 to 0:1) to give fractions 3A-3L. Fraction 3J (25.8 mg) eluted with CHCl₃:MeOH (7:3) was further purified by preparative HPLC [Cosmosil 5C₁₈-AR-II; ϕ 10 x 250 mm; 85% MeOH; 2 mL/min] to give compound **11** (5.6 mg, t_R 20.4 min). Fraction 1A (2.2 g) eluted with 100% MeOH was re-suspended in 10% MeOH (300 mL) and partitioned between *n*-hexane, EtOAc, and *n*-BuOH (300 mL x 3). The hexane fraction was then subjected to Sephadex LH-20 column chromatography (ϕ 25 x 250 mm) with MeOH to give fractions 5A-5E. Purification of fraction 5D by HPLC [Cosmosil Cholester; ϕ 10 x 250 mm; 80% MeOH; 3 mL/min] yielded fractions 6A to 6D. Fraction 6B was identified as compound **12** (1.3 mg, t_R 21.2). Fraction 6A (1.8 mg) was further purified by silica gel column chromatography (ϕ 5 x 60 mm) and yielded compound **11** (1.5 mg). Recrystallization of fractions 2D, 2E and 3E in CHCl₃/MeOH yielded compounds **13** (0.8 mg), **14** (0.5 mg) and, a mixture of β -sitosterol and β -stigmasterol (0.8 mg), respectively.

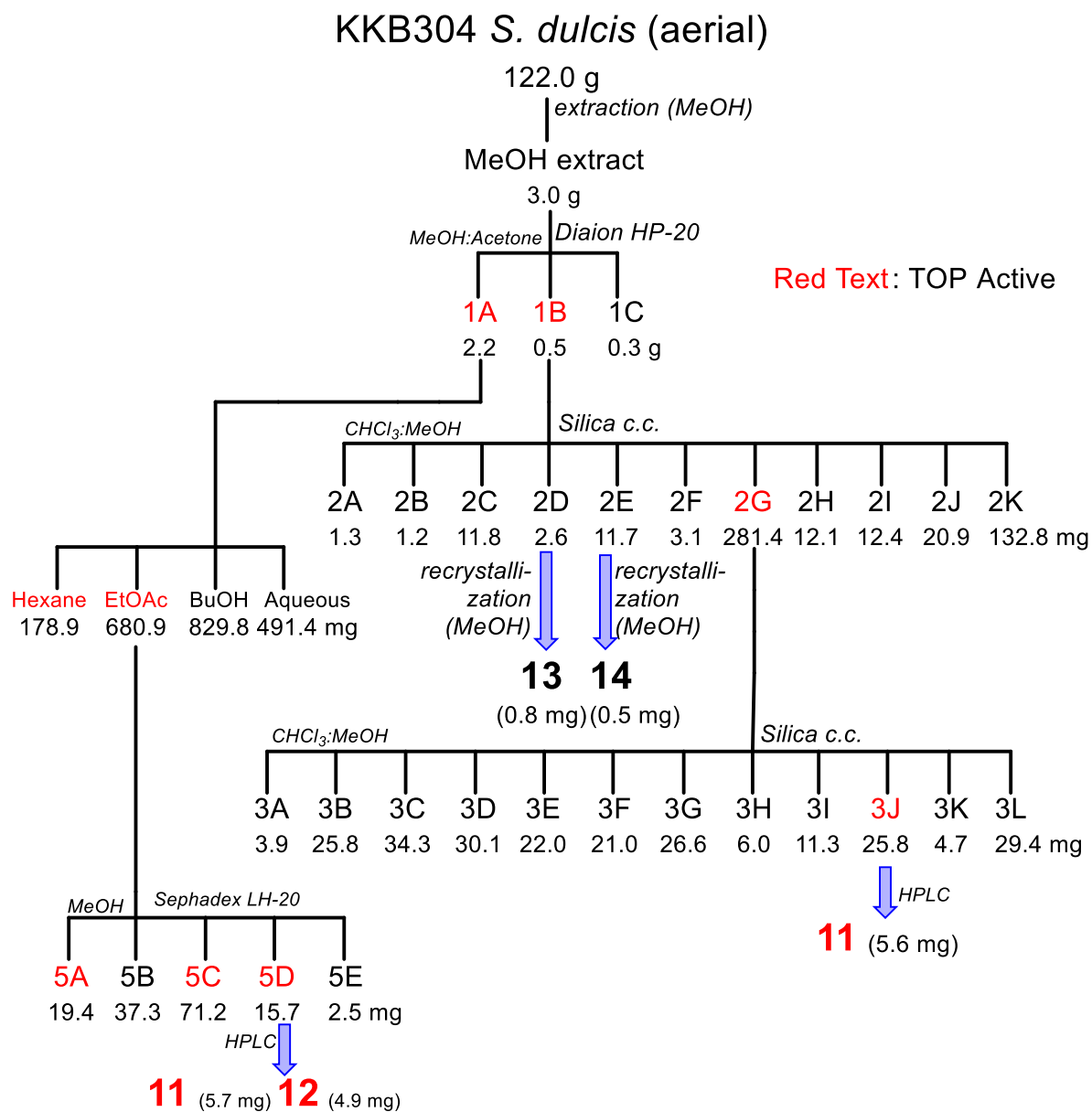


Figure 4.2. Isolation chart of *S. dulcis*.

4.3. Characterization of the isolated compounds

Purification of the compounds by silica gel, ODS column chromatography, and HPLC afforded two scopadulan-type diterpene scopadulciol (**11**)² and scopadiol (**12**)⁴, and two triterpenes friedelin (**13**) and glutinol (**14**). Their structures were identified by comparing their spectral values and optical rotations with those in the literature.

Scopadulciol (11)²

¹H and ¹³C NMR see Table 4.1; $[\alpha]_D^{25}$ -0.096 (*c* 0.5 CHCl₃), lit. $[\alpha]_D^{23}$ -2.3 (*c* 0.5 CHCl₃);

ESI-MS: *m/z* 447 [M+Na]⁺ 871 [2M+Na]⁺

Scopadiol (12)⁴

¹H and ¹³C NMR see Table 4.1; $[\alpha]_D^{25}$ -3.9 (*c* 0.5 CHCl₃), lit. $[\alpha]_D^{26}$ -2.7 (*c* 1.42 CHCl₃);

ESI-MS: *m/z* 449 [M+Na]⁺

Friedelin (13)

¹H and ¹³C NMR see Table 4.2; $[\alpha]_D^{25}$ -1.5 (*c* 0.5 CHCl₃), lit. $[\alpha]_D$ -21 (*c* 0.51 CHCl₃);

ESI-MS *m/z* 449 [M+Na]⁺

Glutinol (14)

¹H and ¹³C NMR see Table 4.2; ESIMS: *m/z* 449 [M+Na]⁺

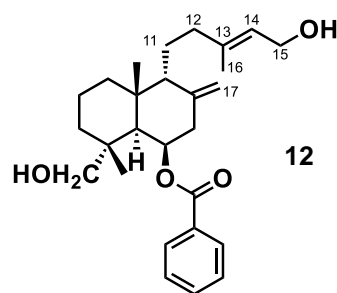
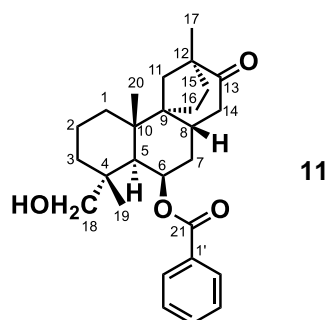


Table 4.1. NMR spectroscopic data of compounds **11** and **12** (in CDCl₃).

Position	11		12	
	¹ H (δ, ppm; <i>J</i> , Hz)	¹³ C (δ, ppm)	¹ H (δ, ppm; <i>J</i> , Hz)	¹³ C (δ, ppm)
1		34.2		38.5
2		18.1		18.5
3		38.4		38.3
4		37.6		38.1
5		43.0	2.03 (1H, br d, 3.0)	41.3
6	5.61 (1H, br d, 1.8)	70.2	5.60 (1H, br d, 2.4)	71.5
7		35.4	2.34 (1H, m)	36.9
8	2.45 (1H, m)	35.8		144.3
9		53.0		57.3
10		39.0		38.7
11		45.4		24.3
12		52.3		38.3
13		213.7		140.2
14		42.7	5.40 (1H, t, 5.4)	123.2
15		23.6	4.14 (2H, d, 7.2)	59.4
16		36.6	1.66 (3H, s)	16.6
17	0.90 (3H, s)	20.4	4.71 (2H, s)	113.0
18	3.10 (1H, d, 11.1)	71.2	3.58 (1H, d, 11.4)	71.3
	3.57 (1H, d, 11.1)		3.13 (1H, d, 11.4)	
19	1.06 (3H, s)	19.7	0.89 (3H, s)	20.3
20	1.51 (3H, s)	21.7	1.44 (3H, s)	25.9
21		166.3		166.2
1'		130.6		130.8
2',6'	8.01 (2H, d, 7.5)	129.6	8.01 (1H, d, 7.8)	129.6
3',5'	7.43 (2H, t, 7.5)	128.5	7.42 (1H, t, 7.8)	128.4
4'	7.55 (1H, t, 7.3)	133.0	7.54 (1H, t, 7.8)	132.8

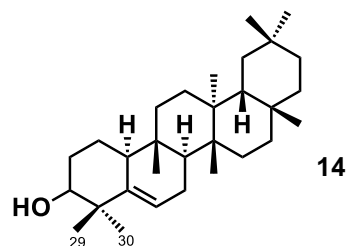
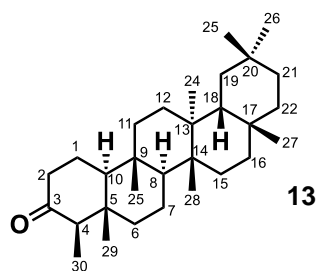


Table 4.2. NMR spectroscopic data of compounds **13** and **14** (in CDCl₃).

Position	13		14	
	¹ H (δ, ppm; <i>J</i> , Hz)	¹³ C (δ, ppm)	¹ H (δ, ppm; <i>J</i> , Hz)	¹³ C (δ, ppm)
1	1.66 (1H, m) 1.94 (1H, m)	22.3		18.2
2	2.28 (1H, m) 2.37 (1H, ddd, 5.4, 1.8)	41.5		27.8
3		Not detected	3.45 (1H, m)	76.3
4	2.23 (1H, m)	58.2		40.8
5		42.1		Not detected
6	1.26 (1H, m) 1.73 (1H, m)	41.3	5.61 (1H, br d, 6.6)	122.1
7	1.34 (1H, m) 1.46 (1H, m)	18.2		23.6
8	1.38 (1H, m)	53.1		47.4
9		37.4		34.9
10	1.53 (1H, m)	59.5		49.7
11	1.44 (2H, m)	35.6		34.6
12	1.32 (2H, m)	30.5		30.4
13		39.7		39.3
14		38.3		37.8
15	1.28 (1H, m) 1.48 (1H, m)	32.4		32.1
16		36.0		36.0
17		30.0		30.1
18	1.55 (1H, m)	42.8		43.1
19	1.18 (1H, m) 1.34 (1H, m)	35.3		35.1
20		28.2		28.2
21	1.42 (2H, m)	32.8		33.1
22	0.92 (2H, m)	39.2		39.0
23	0.86 (3H, d, 6.6)	6.8	1.02 (3H, s)	25.5
24	0.70 (3H, s)	14.7	1.12 (3H, s)	28.9
25	0.85 (3H, s)	17.9	0.83 (3H, s)	16.2
26	0.98 (3H, s)	20.3	1.07 (3H, s)	19.6
27	1.03 (3H, s)	18.7	0.98 (3H, s)	18.4
28	1.16 (3H, s)	32.1	1.14 (3H, s)	32.0
29	0.93 (3H, s)	35.0	0.93 (3H, s)	34.5

4.4. TCF/ β -catenin transcription inhibitory and cytotoxic activity of compound **11**.

The MeOH extract of *S. dulcis* (aerial part) was identified as a potential source of Wnt inhibitors during our screening of our plant extracts library using the TOP assay. Of the four isolated compounds, only **11** inhibited the TOP activity (Figure 4.3). However, **11** also inhibited our FOP assay indicating that the TOP activity-inhibition in HEK293 cells shown by **11** was not specific to TOP.

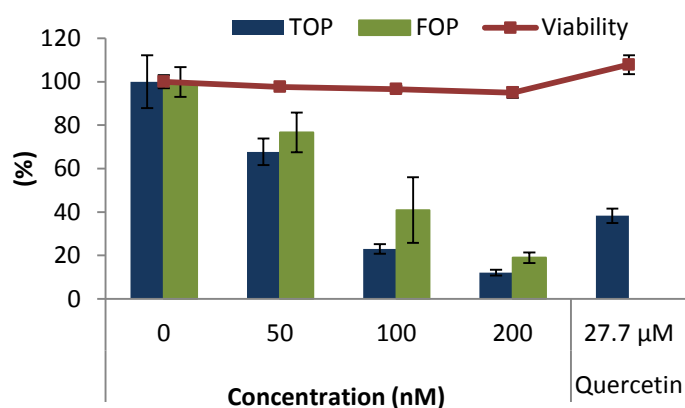


Figure 4.3. Columns show the TOP and FOP activity of **11**. TOP was measured using HEK293 cells stably transfected with SuperTOPflash reporter gene (STF/293) while the FOP activity was measured using HEK293 cells transiently transfected with SuperFOPflash reporter gene. Line graph represents the viability of STF/293 cells. Quercetin was used as the positive control for TOP assay. Data were from one experiment representative of at least two independent experiments (mean \pm s.d).

However, **11** was observed to decrease the viability of the gastrointestinal cancer cells SW480 (colon), HCT116 (colon), DLD1 (colon), and AGS (gastric) cells which are reported to have an active Wnt signal and, RKO (colon) cells which is independent on β -catenin for proliferation (Figure 4.4). It was also noted though that **11** showed some

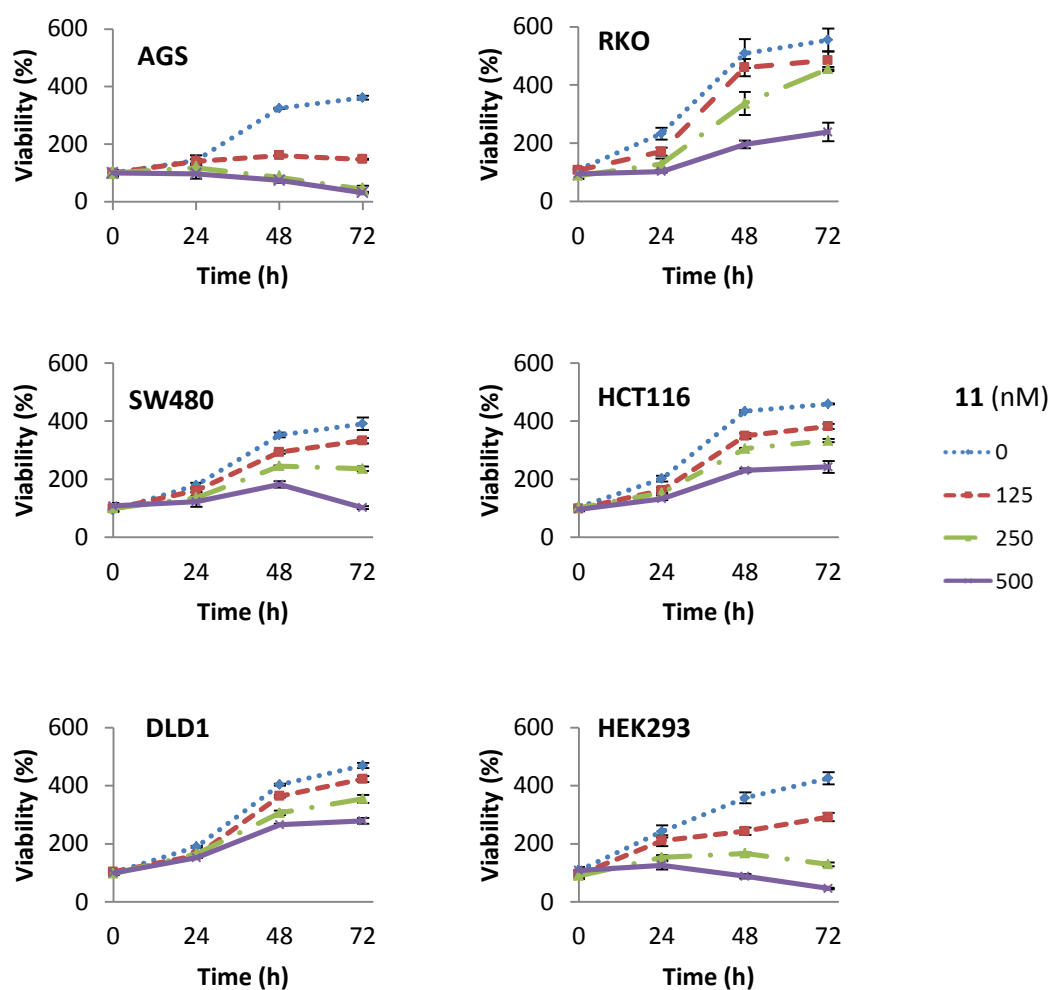


Figure 4.4. Effect of **11** on the viability of cancer cells AGS, RKO, SW480, HCT116, DLD1 and non-cancer cell HEK293. Cells were treated with **11** (300 nM) of different concentrations (125, 250 and 500 nM) for 24, 48 and 72 h. Viability was determined using FMCA and was calculated relative to 0 day.

cytotoxicity against the non-cancer cell HEK293. Viability assay using FMCA showed that **11** greatly decreased the viability of RKO and AGS cells. Compound **11** caused higher decrease of viability in RKO cells (IC₅₀ 359 nM) than in AGS cells (IC₅₀ 500 nM) after 24 h (Table 4.3). However, RKO was observed to increase its viability after 48 h but for AGS, viability started to decrease.

Table 4.3. IC₅₀ values for the cytotoxic activity of **11**.

Time (h)	IC ₅₀ (nM)					
	SW480	HCT116	DLD1	AGS	RKO	HEK293
24	>500	>500	>500	>500	359	>500
48	>500	>500	>500	101	374	227
72	296	>500	>500	70	479	181

In addition, cell cycle analysis showed that **11** increased G0/G1 population in RKO cells after 24 h (Figure 4.5). On the other hand, treatment of AGS cells with **11** resulted in a dose-dependent increase in Sub-G1 cell population suggesting that **11** induced apoptosis. Meanwhile there was no observed change in the sub-G1 cell population in RKO even at 300 nM. Since **11** had showed to induce apoptosis in AGS cells, we then investigated whether the cytotoxic activity of **11** was dependent on caspase activity. In the presence of z-VAD-fmk, a pan caspase inhibitor, the cytotoxic activity of **11** against AGS cells was not abolished indicating that the cytotoxic activity of **11** did not involve caspase activity (Figure 4.6).

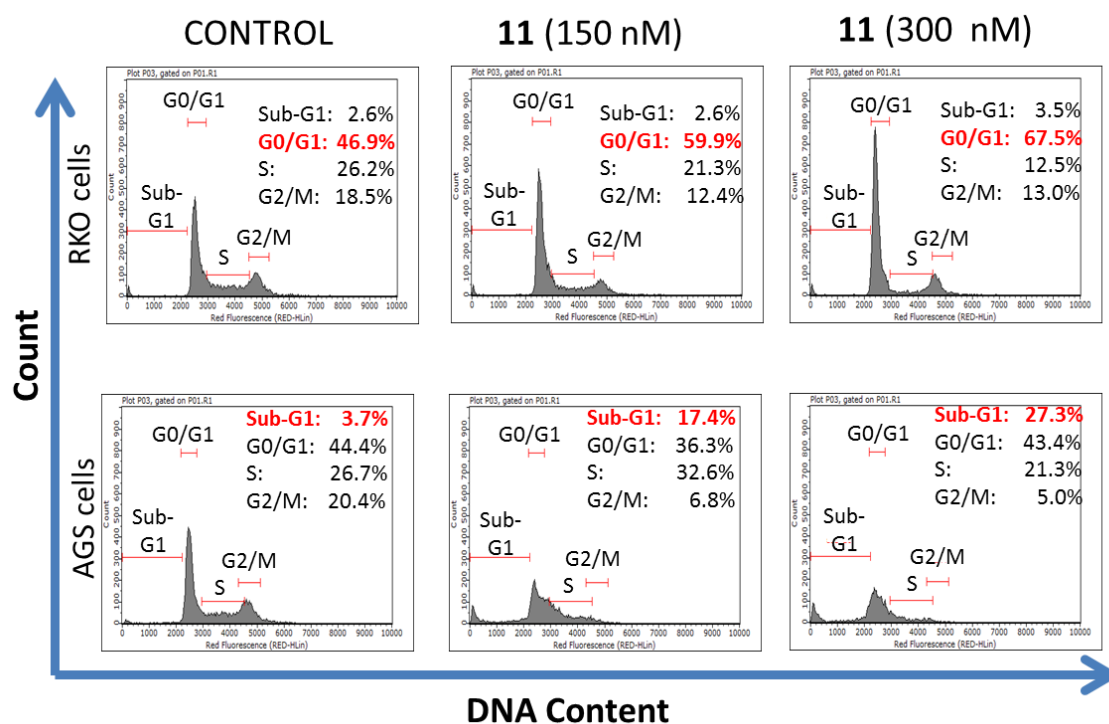


Figure 4.5. Effect of **11** on the cell cycle of RKO cells (upper panel) and AGS cells (lower panel). Cells were exposed to **11** (150 and 300 nM) for 24 h, stained with propidium iodide and analysed using FACS.

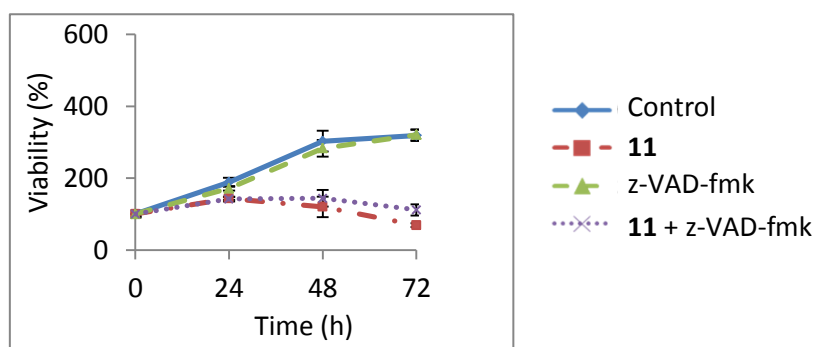


Figure 4.6. The involvement of caspase in the antiproliferative activity of **11** was determined by treating AGS cells with **11** in the absence or presence of z-VAD-fmk (50 μ M), a pan-caspase inhibitor. Viability in both experiments was determined using FMCA and was normalized to 0 day.

References

1. Murti, K.; Panchal, M.; Taya, P.; Singh, R., Pharmacological Properties of *Scoparia Dulcis*: A Review. *Pharmacologia* **2012**, 3, 344-347.
2. Hayashi, T.; Asano, S.; Mizutani, M.; Takeguchi, N.; Kojima, T.; Okamura, K.; Morita, N., Scopadulciol, an inhibitor of gastric H⁺, K(+) -ATPase from *Scoparia dulcis*, and its structure-activity relationships. *J. Nat. Prod.* **1991**, 54, 802-809.
3. Ahsan, M.; Islam, S. K.; Gray, A. I.; Stimson, W. H., Cytotoxic diterpenes from *Scoparia dulcis*. *J. Nat. Prod.* **2003**, 66, 958-61.
4. Hayashi, T.; Okamura, K.; Tamada, Y.; Iida, A.; Fujita, T.; Morita, N., A new chemotype of *Scoparia dulcis*. *Phytochemistry* **1993**, 32, 349-352.

CHAPTER 5

Trichillins from *Azadirachta excelsa* inhibit Wnt/ β -catenin transcriptional activity

5.1. Plant description

A. excelsa, commonly called marrango or Philippine Neem tree, belongs to the mahogany (Meliaceae) family. Similar to *A. indica*, it is also considered as a good source of compounds with antiinsecticidal properties such as azadirachtin and marrangin.¹ Pharmacological studies showed that it possessed antipyretic, antibacterial, antifungal and cytotoxic activities.² Fruits of *A. excelsa* were used in this study, and were collected from Bangladesh. A reference specimen (KKB302) has been deposited in the laboratory. The TOP activity was inhibited by 79% at 10 $\mu\text{g/mL}$ and the viability of the reporter cells was 97% (Figure 5.1).

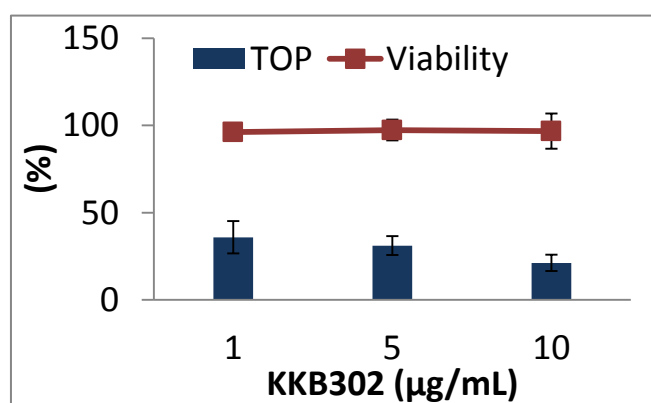


Figure 5.1. Bar graphs showing the dose-dependent TOP activity of KKB302 MeOH extract. The line graph represents cell viability. All data are presented as the mean \pm s.d. (n=3).

5.2. Isolation of the constituents

Figure 5.2 shows the isolation scheme of *A. excelsa*. The dried fruits of *A. excelsa* (204 g) were extracted with MeOH and yielded MeOH extract (30.5 g). The MeOH extract was resuspended in 10% methanol (300 mL) and partitioned between *n*-hexane, EtOAc, and *n*-BuOH (300 mL x 3) to give hexane (1.9 g), EtOAc (3.2 g), BuOH (6.5 g), and aqueous (14.7) extracts. The EtOAc fraction, which showed TOPflash inhibitory activity, was subjected to silica gel column chromatography (ϕ 50 x 320 mm) using hexane:EtOAc gradient system (1:0 to 6:1) to give fractions 1A-1J, then followed by EtOAc-MeOH (1:1-0:1) to yield 1K-1M. Active fraction 1I (503.1 mg) eluted with hexane:EtOAc (0:1) was subjected to ODS column chromatography (ϕ 40 x 230 mm) using MeOH (40-100%) to afford twelve fractions (2A-2L). Purification of fraction 2H (24.8 mg), from the eluate of 70-80% MeOH, by preparative HPLC [YMC-Pak-ODS-AM; ϕ 10 x 250 mm; 60% MeOH; 3 mL/min] gave compound **15** (1.5 mg, t_R 18.0 min). Fraction 2F (29.2 mg) eluted with MeOH (50%) was further purified by HPLC [Cosmosil Cholester; ϕ 10 x 250 mm; 60% MeOH; 3 mL/min], and yielded compound **17** (8.5 mg, t_R 15.0 min; 3.9 mg, 17.6 min). Fraction 2I (135 mg), from the eluate of 80% MeOH was further purified by sephadex column chromatography to give fractions 10A-10G. Fraction 10D (31.4 mg) was subjected to HPLC [Cosmosil Cholester; ϕ 10 x 250 mm; 65% MeOH; 3 mL/min] to give compounds **16** (0.5 mg, t_R 21.6 min), **18** (2.4 mg, t_R 32.8 min), **21** (1.7 mg, t_R 37.6 min), and **22** (1.0 mg, t_R 25.6 min). Fraction 10E (17.6 mg) was also subjected to HPLC [Cosmosil Cholester; ϕ 10 x 250 mm; 65% MeOH; 2 mL/min] to give compounds **16** (0.3 mg, t_R 26.0 min), **19** (1.1 mg, t_R 48.0 min), **20** (1.1 mg, t_R 57.0 min), **21** (1.1 mg, t_R 42.8 min), and **22** (0.8 mg, t_R 30.2 min).

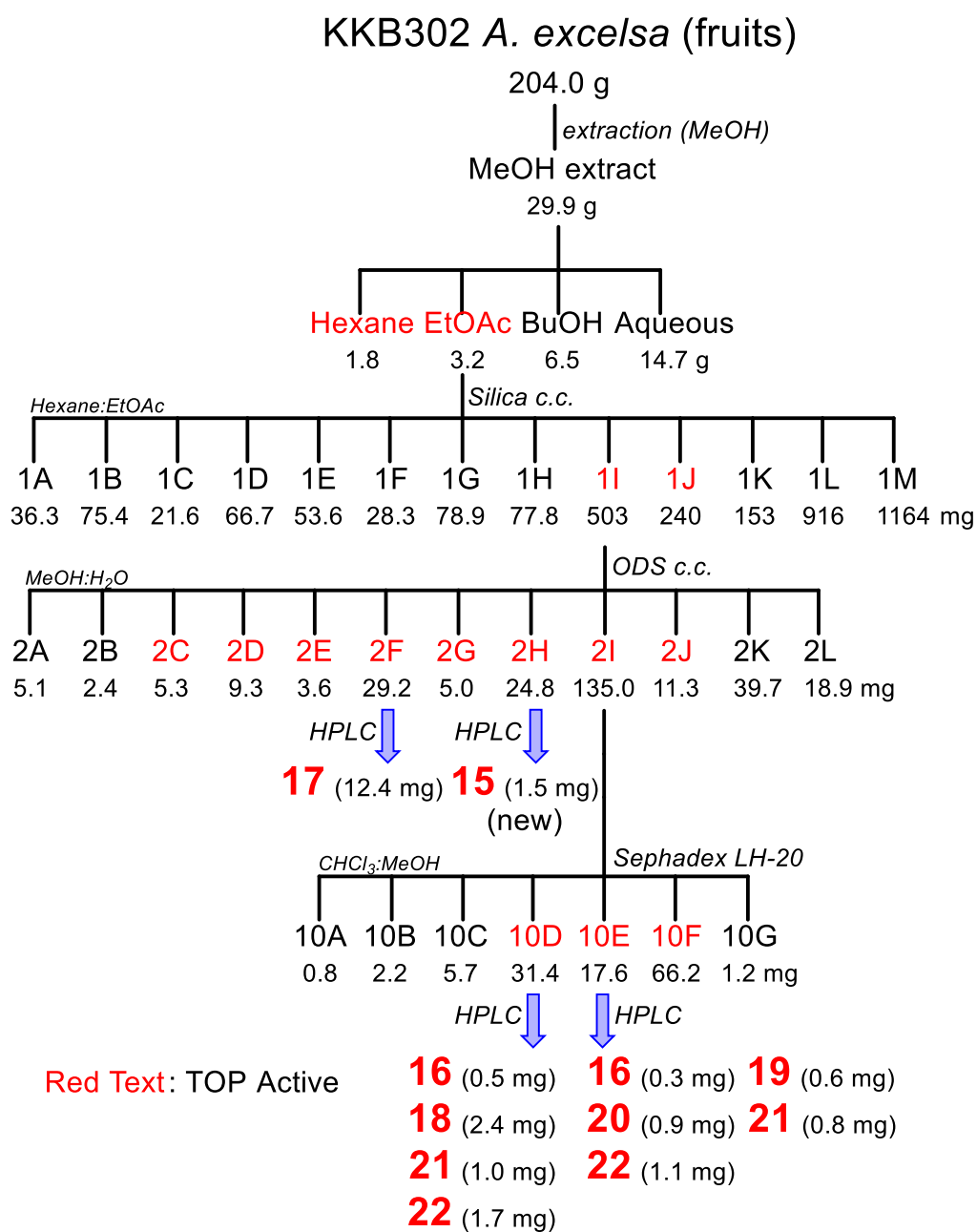
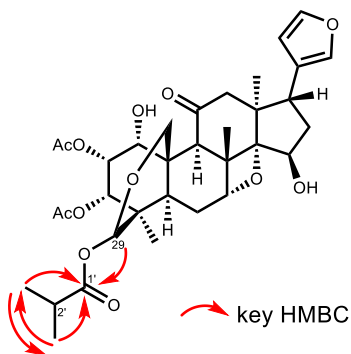


Figure 5.2. Isolation chart of *A. excelsa*.

5.3. Characterization of the isolated compounds

Compound **15** was obtained as a colorless solid with a molecular formula of $C_{34}H_{44}O_{12}$ based on HRESIMS (m/z 667.2742 $C_{34}H_{44}O_{12}Na$, $\Delta +1.1$ mmu). Based from its IR spectra, absorption peaks at 3489 and 1743 cm^{-1} indicated the presence of hydroxyl and carbonyl groups, respectively. Its H and C NMR spectra had signals for a typical tetranortriterpenoid. The presence of peaks δ_H 7.17 (s), 7.36 (t), and 6.17 (brs) suggested the presence of a β -furan-ring. The presence of two acetate groups is indicated by signals at δ_H 1.99 (3H, s) and 2.08 (3H, s). Comparison of the NMR spectra of **15** and the reported compound **16**, known as meliatoosenin I, showed that they had similar skeleton except for the ester moiety at C-29. In meliatoosenin I, 2-methylbutanoyl is attached to C-29 while **15** had methylpropionyl group at this position. The attachment of the methylpropionyl group to C-29 was indicated by the HMBC correlation between H-29 and C-1'.



Based from the report of Fukuyama *et al.* (2006),³ downfield shifts of C-7 (81.2), C-14 (97.5) and C-15 (77.0), from the shifts shown by compounds having 14,15-epoxide groups, indicated presence of an oxetane ring. On the other hand, the presence of 1-OH and 3-OAc was substantiated from the peak of 9-H at δ 4.48 which is due to the 1-OH in a 1,3-diaxial interaction. Compounds acetylated in H-1 were reported to show peak for H-9 at δ 4.0-4.2. The small J values in H-1 and H-3 suggested that the 1-OH and 3-OAc

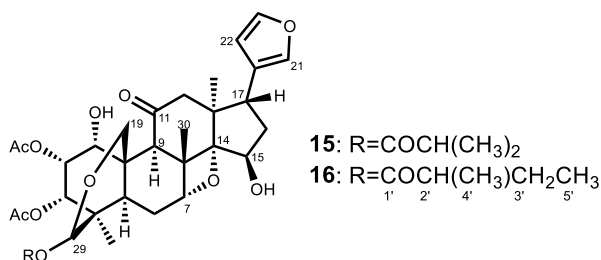


Table 5.1. NMR spectroscopic data of compound **15** and **16** (in CDCl₃).

Position	15		16	
	¹ H (δ, ppm; <i>J</i> , Hz)	¹³ C (δ, ppm)	¹ H (δ, ppm; <i>J</i> , Hz)	¹³ C (δ, ppm)
1	4.72 (1H, brs)	70.7	4.71 (1H, t, 3.6)	70.7
2	5.87 (1H, t, 4.8)	68.8	5.87 (1H, t, 4.8)	68.8
3	5.52 (1H, d, 4.8)	72.7	5.52 (1H, d, 4.8)	72.8
4		41.5		41.5
5	2.73 (1H, dd, 13.2, 5.4)	31.5	2.73 (1H, dd, 13.2, 6.0)	31.5
6	1.78 (1H, m)	23.1	1.78 (1H, m)	23.1
	1.92 (1H, m)		1.92 (1H, m)	
7	4.95 (1H, d, 3)	81.2	4.95 (1H, d, 2.4)	81.2
8		45.2		45.2
9	4.48 (1H, s)	52.1	4.48 (1H, s)	52.1
10		39.8		39.8
11		208.5		208.5
12a	2.31 (1H, d, 19)	52.0	2.31 (1H, m)	52.0
12b	2.48 (1H, d, 19)		2.48 (1H, m)	
13		46.2		46.3
14		97.5		97.5
15	4.89 (1H, s)	77.0	4.89 (1H, t, 4.2)	77.0
16	1.97 (1H, m)	37.6	1.95 (1H, m)	37.7
	1.87 (1H, m)		1.87 (1H, m)	
17	3.16 (1H, dd, 11.4, 5.4)	45.0	3.16 (1H, dd, 11.1, 5.4)	45.0
18	1.03 (3H, s)	21.6		21.6
19	4.05, 4.02 (2H, ABq, 12)	64.2	4.05, 4.02 (2H, d, ABq, 12)	64.2
20		124.1		Not detected
21	7.17 (1H, s)	139.5	7.16 (1H, s)	139.5
22	6.17 (1H, brs)	110.9	6.17 (1H, s)	110.9
23	7.36 (1H, t, 1.8)	143.1	7.36 (1H, t, 1.2)	143.1
28	0.77 (3H, s)	17.1		17.0
29	5.69 (3H, s)	92.7	5.70 (1H, s)	92.6
30	1.23 (3H, s)	17.0	1.23 (3H, s)	17.0
2-CH ₃ CO	1.99 (3H, s)	20.7	1.99 (3H, s)	20.7
2-CH ₃ CO		168.9		168.8
3-CH ₃ CO	2.08 (3H, s)	20.9	2.08 (3H, s)	20.9
3-CH ₃ CO		170.1		170.1
1'		175.7		Not detected
2'	2.59 (1H, quin, 7)	34.1	2.47 (1H, m)	41.0
3'	1.20 (3H, d, 7)	18.7	1.68 (1H, quin, 7.8)	26.5
			1.53 (1H, m)	
4'	1.18 (3H, d, 7)	18.6	1.16 (3H, d, 6.6)	16.3
5'			0.91 (3H, t, 7.8)	11.3
1-OH	2.29 (1H, brs)		2.31 (1H, overlapped)	

functional groups were in axial and α -configuration.³ The *S*-configuration at C-29 was determined based from the chemical shift at H-3. The chemical shift in **15** at H-3 is δ 5.52 which would suggest that the methylpropanoyl group is at the *exo*-position. As discussed by Huang *et al.* (1994),⁴ in general, 3-H signal appears upfield (example δ 4.87 *endo*-toosendanin) in the *endo*-configuration as compared to the *exo*-isomer (δ 5.33 *exo*-toosendanin) (Table 5.2).

The structures of the other known limonoids were identified by comparing their spectral values and optical rotations with those in the literature.

Meliatoosenin I (16)⁵

¹H and ¹³C NMR see Table 5.1; $[\alpha]_D^{25}$ -55.7 (*c* 0.10 MeOH), lit. $[\alpha]_D^{18}$ -51.0 (*c* 0.14 MeOH); ESIMS: *m/z* 681 [M+Na]⁺

Toosendanin [C-29 epimeric mixture (1:1), **17**]⁶

¹H and ¹³C NMR see Table 5.2; ESI-MS: *m/z* 597 [M+Na]⁺ 1171 [2M+Na]⁺

Trichillin H (18)⁷

¹H and ¹³C NMR see Table 5.2; $[\alpha]_D^{25}$ -76.1 (*c* 0.19 MeOH), lit. $[\alpha]_D$ -20.2 (*c* 0.12 MeOH); ESIMS: *m/z* 725 [M+Na]⁺

12-O-acetylarachin B (19)⁴

¹H and ¹³C NMR see Table 5.3; $[\alpha]_D^{24}$ -16.2 (*c* 0.10 MeOH), lit. $[\alpha]_D^{18}$ -55.0 (*c* 0.13 MeOH); ESIMS: *m/z* 667 [M+Na]⁺ 1311 [2M+Na]⁺

Meliatoxin A₁ (20)^{8,9}

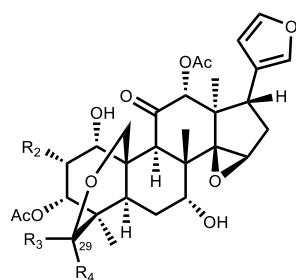
¹H and ¹³C NMR see Table 5.3; $[\alpha]_D^{25}$ -144.5 (*c* 0.10 MeOH); CD (MeOH): 230 nm ($\Delta\epsilon$ +0.7), 299 ($\Delta\epsilon$ -4.8), lit. CD (MeOH): 222 nm ($\Delta\epsilon$ +1), 294 ($\Delta\epsilon$ -4.8); ESIMS: *m/z* 681 [M+Na]⁺ 1339 [2M+Na]⁺

Meliatoxin B₂ (21)^{8,9}

¹H and ¹³C NMR see Table 5.4; $[\alpha]_D^{24}$ -37.8 (*c* 0.19 MeOH); CD (MeOH): 214 nm ($\Delta\epsilon$ +6.9), 299 ($\Delta\epsilon$ -3.0), lit. CD (MeOH): 225 nm ($\Delta\epsilon$ +6), 293 ($\Delta\epsilon$ -4.8); ESIMS: *m/z* 667 [M+Na]⁺

Meliatoxin B₁ (22)^{8,9}

¹H and ¹³C NMR see Table 5.4; $[\alpha]_D^{24}$ -47.7 (*c* 0.14 MeOH); CD (MeOH): 209 nm ($\Delta\epsilon$ +6.2), 298 ($\Delta\epsilon$ -3.8), lit. CD (MeOH): 224 nm ($\Delta\epsilon$ +5), 293 ($\Delta\epsilon$ -4.7); ESIMS: *m/z* 681 [M+Na]⁺

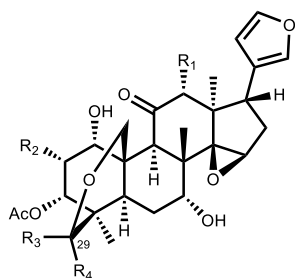


17: R₂=H,
R₃=H, R₄=OH or R₃=OH, R₄=H

18: R₂=OAc
R₃=OCOCH(CH₃)₂, R₄=H

Table 5.2. NMR spectroscopic data of compounds **17** and **18** (in CDCl₃).

Position	17 (<i>endo</i> -) [29-epimer (<i>exo</i> -)] (1:1)		18
	¹ H (δ, ppm; <i>J</i> , Hz)	¹³ C (δ, ppm)	¹ H (δ, ppm; <i>J</i> , Hz)
1	4.25 (1H,brm) [4.30 (1H,br m)]	70.3	4.40 (1H, brt, 4.2)
2	2.82 (2H,dt,16.8, 4.5)	35.4 [36.1]	5.88 (1H, t, 4.8)
3	4.87 (1H,d,4.5) [5.33 1H,d,4.5]	73.6 [76.3]	5.51 (1H, d, 4.8)
4		40	
5	2.48-2.617 m	25.5 [27.9]	2.79 (1H, dd, 13.8,3.6)
6		25.4 [27.3]	1.71 (1H, dt, 14.4,3.6)
			2.01 (1H, m)
7	3.58 (1H,brm) [3.62 (1H,brm)]	70.5	3.66 (1H, s)
8		42.4 [42.5]	
9	4.56 (1H, s)	48.3 [48.6]	4.61 (1H, s)
10		41.7	
11		206.8	
12	5.29 (1H, s)	78.4 [78.7]	5.40 (1H, s)
13		45.7	
14		72.1 [72.3]	
15	3.74 s	58.7	3.75 (1H, s)
16	2.21 (2H,dd, 13.5, 7.2)	33.6	2.22 (1H, dd, 13.6, 6.6)
			1.88 (1H, dd, 13.6, 11.4)
17	2.94 (1H, dd, 11.4, 7.2)	38.2	2.97 (1H, dd, 11.4, 6.0)
18	1.29 (3H, s) [1.30 (3H, s)]	20.7	1.33 (3H, s)
19	4.16 (1H, d, 12.3) [4.29 (1H, d, 12.3)] 4.22 (1H, d, 12.3) [4.47 (1H, d, 12.3)]	58.7 [63.8]	4.29,4.36 (2H, ABq, 13.6)
20		122.5	
21	7.10 (1H, s)	142.4	7.11 (1H, s)
22	6.11 (1H, s)	111.9	6.11 (1H, s)
23	7.31 (1H, s)	140.6	7.32 (1H, t, 1.2)
28	0.86 (3H, s) [0.87 (3H, s)]	15.6	0.82 (3H, s)
29	4.76 (1H, s) [4.86 (1H, s)]	96.1 [96.4]	5.73 (1H, s)
30	1.13 (3H, s) [1.16 (3H, s)]	18.5 [19.6]	1.15 (3H, s)
2-COCH ₃			2.00 (3H, s)
3-COCH ₃	2.07 (3H, s) [2.08 (3H, s)]	22.5 [22.7]	2.11 (3H, s)
3-COCH ₃		170.2 [170.1]	
12-COCH ₃	1.96 (3H, s) [1.97 (3H, s)]	21.4 [21.5]	1.96 (3H, s)
12-COCH ₃		169.8	
2'			2.67 (1H, hept, 7.0)
3'			1.22 (3H, d, 7.0)
4'			1.21 (3H, d, 7.0)
1-OH	2.27 (1H,d,7.2) [2.31 (1H,d,7.2)]		2.51 (1H, d, 4.0)



- 19:** R₁=OAc R₂=H
R₃=OCOCH(CH₃)₂, R₄=H
20: R₁=H R₂=OAc
R₃=OCOCH(CH₃)CH₂CH₃, R₄=H

Table 5.3. NMR spectroscopic data of compounds **19** and **20** (in CDCl₃).

Position	19	20
	¹ H (600 MHz)	¹ H (600 MHz)
1	4.25 (1H, t, 4.2)	4.22 (1H, t, 4.2)
2	1.89 (1H, m)	5.89 (1H, t, 4.2)
	2.80 (1H, dt, 16.8, 4.8)	
3	5.29 (1H, d, 3.6)	5.50 (1H, d, 4.2)
4		
5	2.70 (1H, dd, 14.7, 4.2)	2.73 (1H, m)
6	1.71 (1H, dt, 13.8, 4.8)	1.70 (1H, m)
	2.00 (1H, m)	~2.0 (1H, m)
7	3.67 (1H, m)	3.67 (1H, brs)
8		
9	4.59 (1H, s)	4.58 (1H, s)
10		
11		
12	5.26 (1H, s)	2.44 (2H, s)
13		
14		
15	3.74 (1H, s)	3.69 (1H, s)
16	2.22 (1H, dd, 6.9, 0.6)	2.24 (1H, dd, 13.2, 6.3)
	1.89 (1H, m)	1.86 (1H, dd, 13.2, 11.4)
17	2.96 (1H, dd, 11.0, 7.2)	2.73 (1H, m)
18	1.30 (3H, s)	1.22 (3H, s)
19	4.27, 4.4.30 (2H, ABq, 13.2)	4.37, 4.4.45 (2H, ABq, 13.2)
20		
21	7.11 (1H, brd, 0.6)	7.12 (1H, s)
22	6.13 (1H, t, 0.6)	6.11 (1H, s)
23	7.30 (1H, t, 1.8)	7.36 (1H, t, 1.5)
28	0.81 (3H, s)	0.82 (3H, s)
29	5.78 (1H, s)	5.76 (1H, s)
30	1.15 (3H, s)	1.07 (3H, s)
2-COCH ₃		2.01 (3H, s)
3-COCH ₃	2.08 (3H, s)	2.11 (3H, s)
12-COCH ₃	1.97 (3H, s)	
2'	2.60 (1H, hept, 6.6)	2.49 (1H, m)
3'	1.18 (3H, d, 7.2)	1.53 (1H, m)
		1.70 (1H, m)
4'	1.17 (3H, d, 7.2)	1.17 (3H, d, 6.6)
5'		0.92 (3H, t, 7.1)
1-OH		2.37 (1H, d, 4.2)

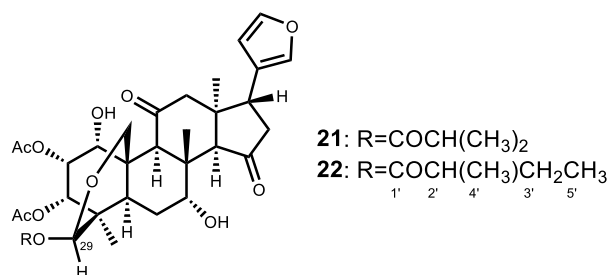


Table 5.4. NMR spectroscopic data of compounds **21** and **22** (in CDCl₃).

Position	21		22	
	¹ H (δ, ppm; <i>J</i> , Hz)	¹³ C (δ, ppm)	¹ H (δ, ppm; <i>J</i> , Hz)	¹³ C (δ, ppm)
1	4.25 (1H, d, 4.8)	71.9	4.26 (1H, d, 4.2)	71.9
2	5.88 (1H, t, 4.8)	68.7	5.88 (1H, t, 4.2)	68.7
3	5.55 (1H, d, 4.8)	73.3	5.56 (1H, d, 4.2)	73.3
4		40.6		40.7
5	2.65 (1H, m)	28.1	2.63 (1H, m)	28.1
6	1.82 (1H, dt, 14.4, 4.2)	23.0	1.81 (1H, dt, 13.8, 4.2)	23.0
7	3.96 (1H, brs)	69.2	3.96 (1H, m)	69.2
8		43.1		43.1
9	3.46 (1H, s)	51.4	3.46 (1H, s)	51.4
10		42.6		42.6
11		209.9		209.9
12	2.29, 2.65 (2H, ABq, 17.4)	43.3	2.29, 2.65 (2H, ABq, 17.4)	43.3
13		44.8		44.8
14	3.14 (1H, s)	62.4	3.14 (1H, s)	62.4
15		219.4		219.4
16	2.56 (2H, d, 10.4)	50.5	2.56 (2H, d, 10.2)	50.5
17	3.32 (1H, t, 10.4)	41.8	3.32 (1H, t, 10.2)	41.8
18	1.02 (3H, s)	28.1	1.03 (3H, s)	28.1
19	4.16, 4.62 (2H, ABq, 12.6)	63.8	4.16, 4.64 (2H, ABq, 13.2)	63.8
20		121.7		121.7
21	7.30 (1H, d, 0.6)	140.2	7.3 (1H, s)	140.2
22	6.22 (1H, dd, 1.8, 0.6)	110.2	6.28 (1H, s)	110.2
23	7.40 (1H, t, 1.8)	143.4	7.40 (1H, t, 1.2)	143.4
28	0.84 (1H, s)	18.5	0.84 (3H, s)	18.4
29	5.76 (1H, s)	93.0	5.74 (1H, s)	93.1
30	0.97 (3H, s)	20.2	0.97 (3H, s)	20.2
2-CH ₃ CO	2.01 (3H, s)	20.8	2.01 (3H, s)	20.8
2-CH ₃ CO		169.0		169.0
3-CH ₃ CO	2.12 (3H, s)	20.9	2.11 (3H, s)	20.9
3-CH ₃ CO		169.9		169.9
1'		175.3		n.d.
2'	2.46 (1H, m)	41.0	2.63 (1H, m)	34.1
3'	1.53, 1.68 (2H, m)	26.5	1.20 (3H, d, 6.9)	18.8
4'	1.17 (3H, d, 7.2)	11.3	1.19 (3H, d, 6.9)	18.7
5'	0.92 (3H, t, 7.8)	16.3		
1-OH	2.45 (1H, d, 4.8)		2.44 (1H, d, 4.8)	
6-OH	2.74 (1H, brs)		2.73 (1H, d, 5.4)	

5.4. TCF/ β -catenin transcription inhibitory activity of the isolated compounds

All the limonoids isolated from *A. excelsa* showed inhibitory activity against TOP activity. Compounds **17-20** showed the strongest inhibitory activity with IC₅₀ values 127, 300, 252 and 121 nM, respectively (Figure 5.3 and Table 5.5). Moreover, these compounds did not significantly affect FOP indicating that they specifically inhibited TOP.

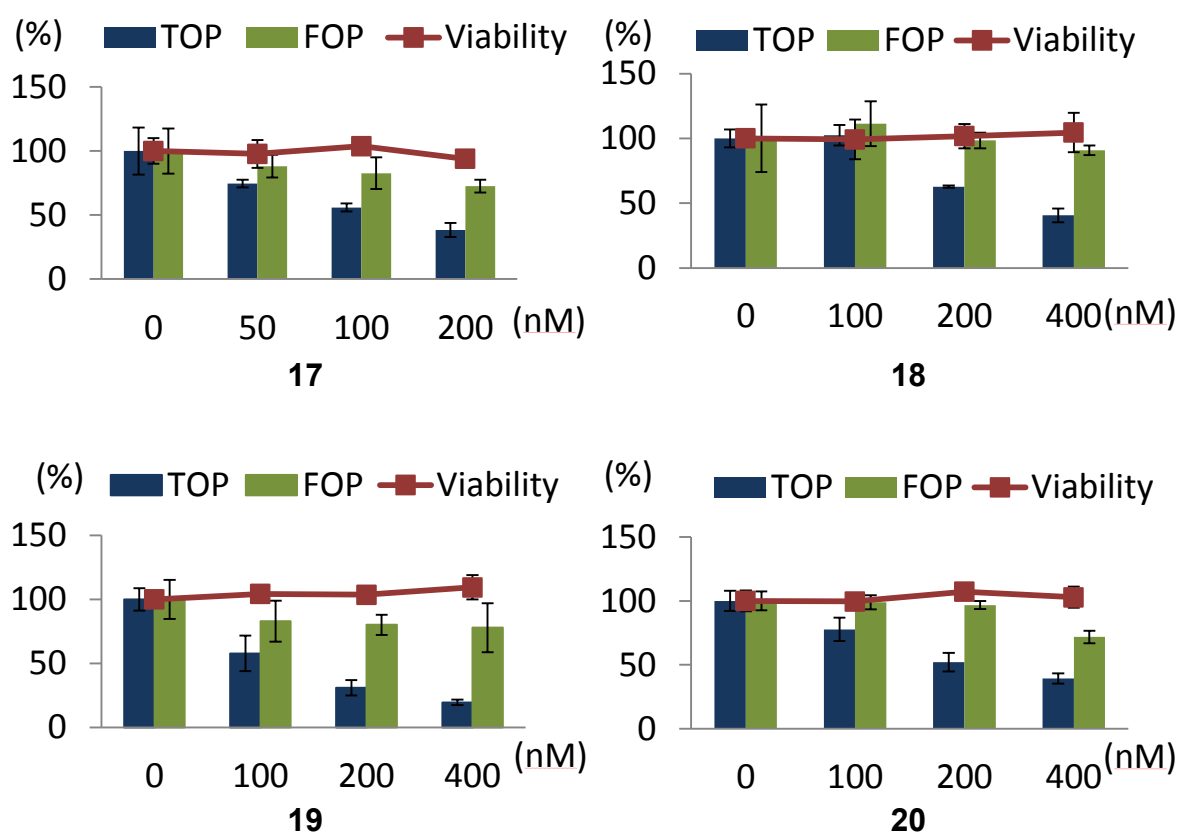
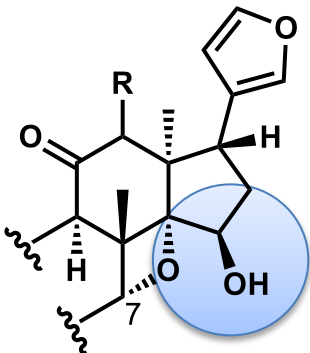
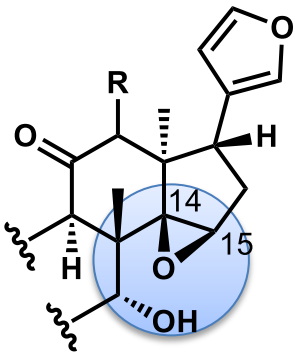
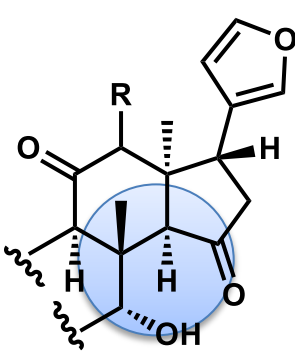


Figure 5.3. Columns show the TOP and FOP activity of **17-20**. TOP was measured using HEK293 cells stably transfected with SuperTOPflash reporter gene (STF/293) while the FOP activity was measured using HEK293 cells transiently transfected with SuperFOPflash reporter gene. Line graph represents the viability of STF/293 cells. Data were from one experiment representative of at least two independent experiments (mean \pm s.d.).

We then did simple structure-activity relationships study on the eight compounds isolated. It was observed that compounds bearing the 14,15-epoxide moiety had IC₅₀ values at the nanomolar scale, while the other compounds had IC₅₀ values at the micromolar scale. Possibly, the 14,15-epoxide moiety is an important functional group in the inhibition of the TOP activity.

Table 5.5. Structure-activity relations of compounds **15-22**.

  		
TOP inhibitory activity		
	IC ₅₀ (μM)	
15	33.7	17
16	20	18
		19
		20
		21
		22

5.5. Cytotoxic activity of compounds 17-19

We then investigated the cytotoxic activity of compounds **17-19** against gastrointestinal cancer cells SW480 (colon), HCT116 (colon), DLD1 (colon) and AGS (gastric) which all possess an active Wnt signal. We also determined their cytotoxic activity in Wnt-independent colon cancer RKO and a non-cancer cell line HEK293. It was observed that after 48 h treatment, the compounds had cytotoxicity against HCT116 (Figure 5.4). Compound **17** had the strongest cytotoxicity with IC_{50} 24.9 nM. But, it was

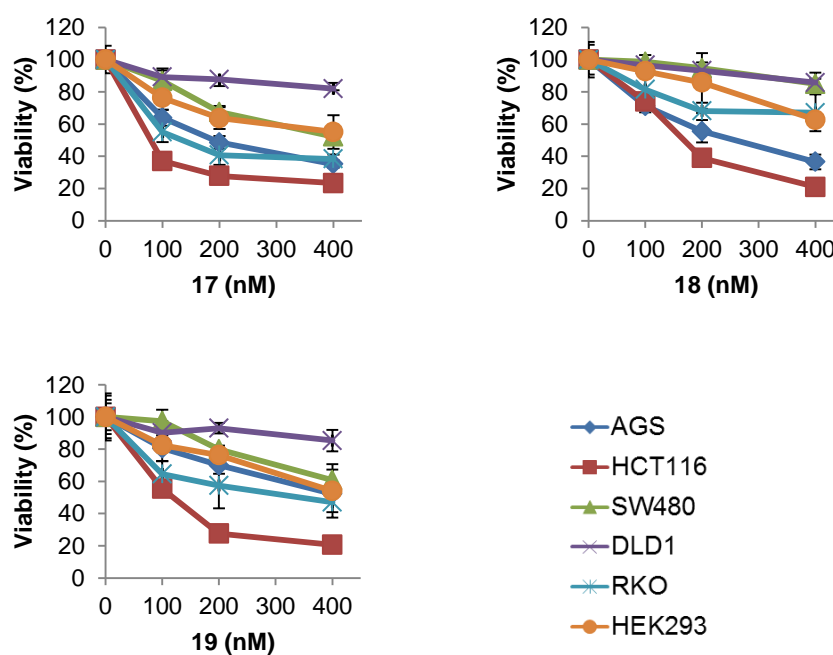


Figure 5.4. Effect of **17-19** on the viability of cancer cells AGS, RKO, SW480, HCT116, DLD1 and non-cancer cell HEK293. Cells were treated with the compounds of different concentrations (100, 200 and 400 nM) for 48 h. Viability was determined using FMCA.

also observed that **17** affect the viability of the Wnt-independent RKO. Compound **19** also decreased the viability of HCT116 and RKO. Compound **18** was observed to exhibit cytotoxicity in Wnt-dependent AGS and HCT116. Though its IC₅₀ values for these two cancer cells were lower than the observed IC₅₀ of the either compound **17** or **19**, its IC₅₀ for the Wnt-independent RKO as well as for the non-cancer cell line was >400 nM (Table 5.6). Furthermore, compounds **17-19** did not greatly decrease viability of SW480 and DLD1 (IC₅₀ >400 nM).

Table 5.6. IC₅₀ for the cytotoxic activity of compounds **17-19**.

	Non-cancer cell	Cancer cells				
		Wnt-independent		Wnt-dependent		
	HEK293	RKO	AGS	HCT116	SW480	DLD1
17	>400	129	192	24.9	>400	>400
18	>400	>400	239	161	>400	>400
19	>400	331	>400	108	>400	>400

5.6. Effect of **18** on the β -catenin and c-myc level in HCT116

Compound **18** showed cytotoxicity activity against HCT116, which harbor mutant β -catenin and wild-type APC, and not in SW480 and DLD1 which both have truncated APC and wild-type β -catenin. From this result, we inferred that the activity of **18** in HCT116 was possibly APC-mediated. However, western blot analysis showed that **18** did not degrade β -catenin, and also it did not affect the localization of β -catenin in HCT116 (Figure 5.5). This result suggested that APC may have not mediated the inhibition of Wnt signal by **18**. Wild-type APC has been reported to control nuclear accumulation of β -catenin by a combination of nuclear export and cytoplasmic degradation.¹⁰

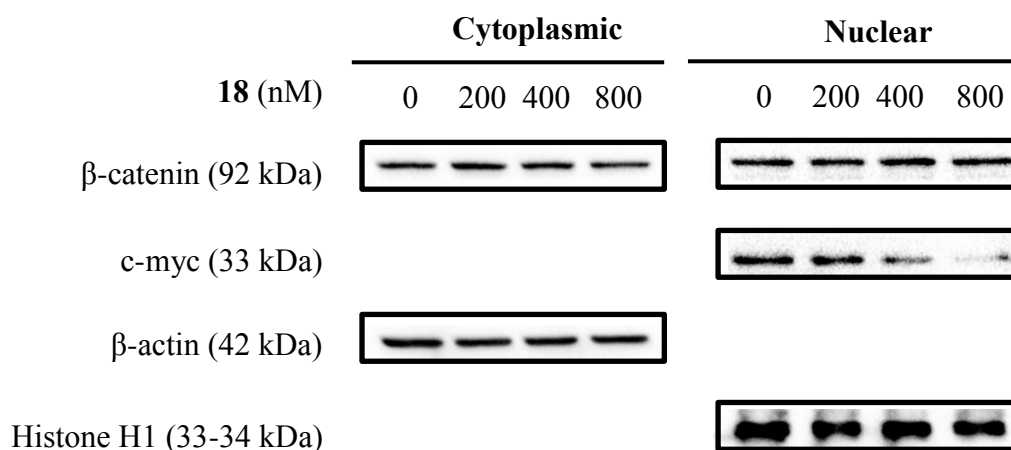


Figure 5.5. Western blot analysis of β -catenin and c-myc in HCT116 cells treated with **18** for 24 h. Cytoplasmic and nuclear lysates from HCT116 cells were obtained and subjected to Western blot analysis with anti- β -catenin and anti-c-myc antibodies. β -actin serves as protein control for full and cytoplasmic fractions while histone H1 for the nuclear fraction.

On the other hand, compound **18** decreased the level of the TCF/ β -catenin target protein, c-myc. This result indicated that even though there **18** did not affect level of β -catenin, possibly, it inhibited the Wnt signal affecting downstream of β -catenin. Moreover, the data suggested that the inhibitory activity of **18** was not mediated through induction of nuclear export and/or degradation of β -catenin. It can be implied that the action of **18** may have affected the downstream components of β -catenin. Inside the nucleus, β -catenin forms a complex with TCF which then recruits other co-activators pygopus, CBP and Bcl9 to activate the transcription process.¹¹ However, it was also reported that C-terminal binding protein (CtBP) can lower the available free nuclear β -catenin for binding to TCF by sequestering APC/ β -catenin complex.¹² Possibly, the Wnt signal inhibitory action of **18** could be targeting the TCF/ β -catenin complex formation. We assume also the possible involvement of nuclear CtBP as it was shown that CtBP preferentially binds to full-length APC, and not with truncated APC,¹³ which may explain why **18** did not affect the viability of SW480 and DLD1.

References

1. Schmutterer, H.; Doll, M., The marrango or Philippine Neem Tree, *Azadirachta excelsa*(=*A. integrifoliola*):A new source of insecticides with growth-regulating hormones. *Phytoparasitica* **1993**, 21, 79-86.
2. Cui, B.; Chai, H.; Constant, H. L.; Santisuk, T.; Reutrakul, V.; Beecher, C. W. W.; Farnsworth, N. R.; Cordell, G. A.; Pezzuto, J. M.; Kinghorn, A. D., Limonoids from *Azadirachta excelsa*. *Phytochemistry* **1998**, 47, 1283-1287.
3. Fukuyama, Y.; Nakaoka, M.; Yamamoto, T.; Takahashi, H.; Minami, H., Degraded and oxetane-bearing limonoids from the roots of *Melia azedarach*. *Chem. Pharm. Bull. (Tokyo)* **2006**, 54, 1219-1222.
4. Huang, R. C.; Okamura, H.; Iwagawa, T.; Nakatani, M., The Structures of Azedarachins, Limonoid Antifeedants from Chinese *Melia azedarach* Linn. *Bull. Chem. Soc. Jpn.* **1994**, 67, 2468-2472.
5. Zhang, Y.; Tang, C. P.; Ke, C. Q.; Li, X. Q.; Xie, H.; Ye, Y., Limonoids from the fruits of *Melia toosendan*. *Phytochemistry* **2012**, 73,106-113.
6. Itokawa, H.; Qiao, Z. S.; Hirobe, C.; Takeya, K., Cytotoxic limonoids and tetranortriterpenoids from *Melia azedarach*. *Chem. Pharm. Bull. (Tokyo)* **1995**, 43, 1171-1175.
7. Nakatani, M.; Chun Huang, R.; Okamura, H.; Naoki, H.; Iwagawa, T., Limonoid antifeedants from chinese *Melia azedarach*. *Phytochemistry* **1994**, 36, 39-41.
8. Oelrichs, P. B.; Hill, M. W.; Vallely, P. J.; MacLeod, J. K.; Molinski, T. F., Toxic tetranortriterpenes of the fruit of *Melia azedarach*. *Phytochemistry* **1983**, 22, 531-534.
9. Macleod, J. K.; Moeller, P. D.; Molinski, T. F.; Koul, O., Antifeedant activity against *Spodoptera litera* larvae and [(13)C]NMR spectral assignments of the meliatoxins. *J. Chem. Eco.* **1990**, 16, 2511-2518.
10. Henderson, B. R., Nuclear-cytoplasmic shuttling of APC regulates β -catenin subcellular localization and turnover. *Nat. Cell. Biol.* **2000**, 2, 653-660.
11. Clevers, H.; Nusse, R., Wnt/ β -Catenin Signaling and Disease. *Cell* **2012**, 149, 1192-1205.
12. Hamada, F.; Bienz, M., The APC tumor suppressor binds to C-terminal binding protein to divert nuclear β -catenin from TCF. *Dev. Cell* **2004**, 7, 677-85.
13. Sierra, J.; Yoshida, T.; Joazeiro, C. A.; Jones, K. A., The APC tumor suppressor counteracts β -catenin activation and H3K4 methylation at Wnt target genes. *Genes Dev.* **2006**, 20, 586-600.

CHAPTER 6

Scopadulciol (**11**) induces β -catenin degradation in AGS human gastric adenocarcinoma cells

6.1. Rationale

Compound **11** was not identified as a “positive” compound using the STF/293 assay system. In our study, however, we observed that **11** can affect the viability of AGS (gastric) and RKO (colon) cells. Previous report had shown that scopadulciol (**11**) exhibited cytotoxic activity against some gastric cancer cell lines.¹ However, its mechanism of action has not been reported. As discussed in Chapter 4, compound **11** caused a G0/G1 arrest in RKO cells while it induced apoptosis in AGS cells after 24 h. However, RKO was able to recover from the effect of **11** at 48 h while it caused decreased viability in AGS. But, z-VAD-fmk, a pan-caspase inhibitor, did not reverse the anti-proliferative activity of **11** in AGS which suggested that the apoptotic action of **11** was independent of the caspase activity. Because of these observed results, we then investigated the participation of the Wnt/ β -catenin signal in the antiproliferative activity of **11** in AGS.

6.2. Scopadulciol induces degradation of β -catenin level in AGS

AGS has an active Wnt signalling pathway due to mutation in β -catenin (G34E).² As shown in Figure 6.1, **11** decreased the β -catenin level in AGS cells after 24 h exposure in a concentration-dependent manner. Moreover, it inhibited the β -catenin accumulation in the nucleus as shown by the decrease in the level of nuclear β -catenin. From these results, we can infer that **11** could be affecting the Wnt signal. Then, we investigated the

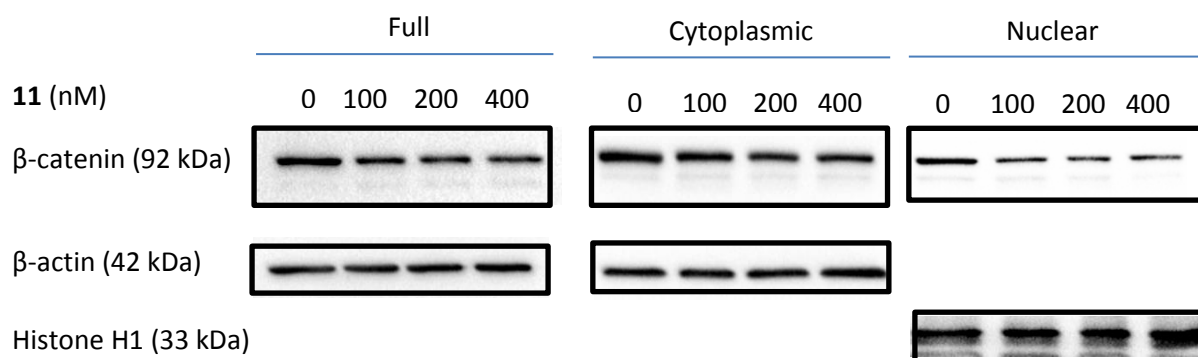


Figure 6.1. Effect of **11** on the level and localization of β -catenin in AGS after treatment with different concentrations of **11** (100, 200, 400 nM) for 24 h. Whole cell, cytoplasmic and nuclear lysates from AGS cells were obtained and subjected to Western blot analysis with anti- β -catenin antibody. β -actin serves as protein control for full and cytoplasmic fractions while histone H1 for the nuclear fraction.

possible mechanism involved in the β -catenin degradation by **11**. In the Wnt signalling pathway, the phosphorylation of β -catenin by CK1 α and GSK3 β is an important step in the ubiquitin/proteasome-mediated degradation of β -catenin.^{3, 4} However, we observed that the level of GSK3 β as well as the phosphorylated β -catenin was decreased in the presence of **11** (Figures 6.2a and 6.2b). CK1 α was not significantly affected by **11**. These results suggested that the degradation of β -catenin by **11** was independent of GSK3 β .

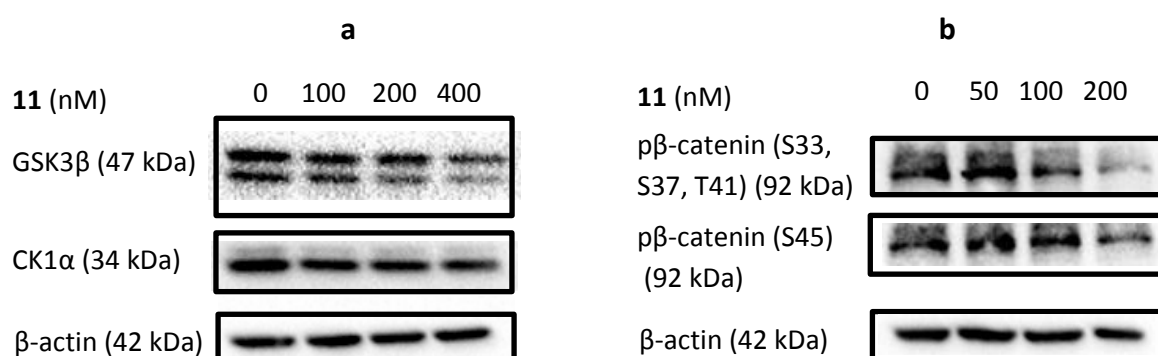


Figure 6.2. Western blot analysis on the level of (a) GSK3 β and CK1 α , and (b) phosphorylated β -catenin in AGS cells after treatment with different concentrations of **11** (100, 200, 400 nM) for 24 h.

6.3. Degradation of β -catenin by **11** is mediated by proteasome activity.

The mutation of β -catenin (G34E) in AGS is suggested to reduce the efficiency of the ubiquitin-proteasome degradation of β -catenin.² We then investigated if degradation of β -catenin in AGS by **11** is mediated by proteasomal activity. The proteasome activity was inhibited by pre-treatment of AGS with either MG132 or epoxomicin for 1 h. MG132 and epoxomicin are both 26S proteasome inhibitors, but epoxomicin is a more specific inhibitor.⁵ After pre-treatment with the proteasome inhibitors, the cells were treated with **11** for 24 h. Treatment with either MG132 or epoxomicin alone did not affect the level of β -catenin. In AGS treated with **11**, pre-treatment with MG132 or epoxomicin abolished the degradation of β -catenin. The result indicated that the **11**-induced degradation of β -catenin is proteasome-dependent (Figures 6.3a and 6.3b).

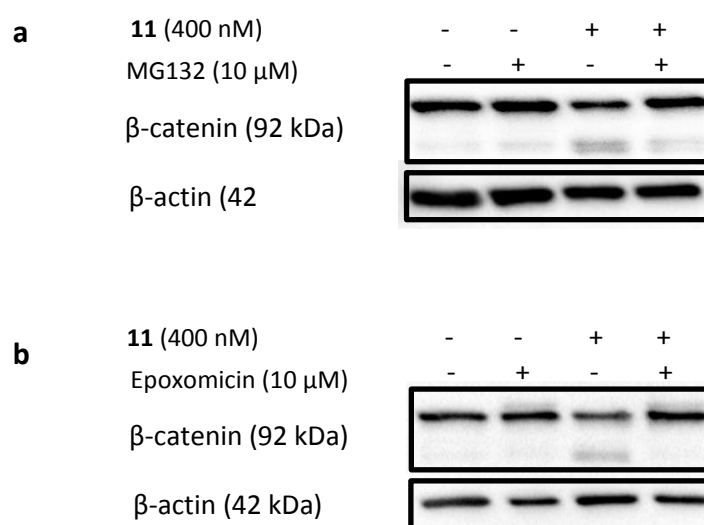


Figure 6.3. Effect of (a) MG132 and (b) epoxomicin on β -catenin level in AGS cells treated with **11**. Cells were pre-treated with either MG132 (10 μ M) or epoxomicin (10 μ M) for 1 h and treated with **11** (400 nM) for 24 h.

Moreover, β -catenin had been reported to be proteolytically cleaved by proteases calpain and calpase during apoptosis.⁶⁻⁸ To determine the participation of the proteases in β -catenin degradation, we pre-treated AGS with either a pan-caspase inhibitor, z-VAD-fmk, or with the calpain inhibitor calpastatin for 1 h. After the pretreatment, AGS cells were then treated with **11**. Pre-treatment with either caspase-inhibitor or the calpain inhibitor did not protect the degradation of β -catenin by **11** (Figure 6.4a and 6.4b). This indicated that caspase and calpain were not involved in the β -catenin degradation by **11**.

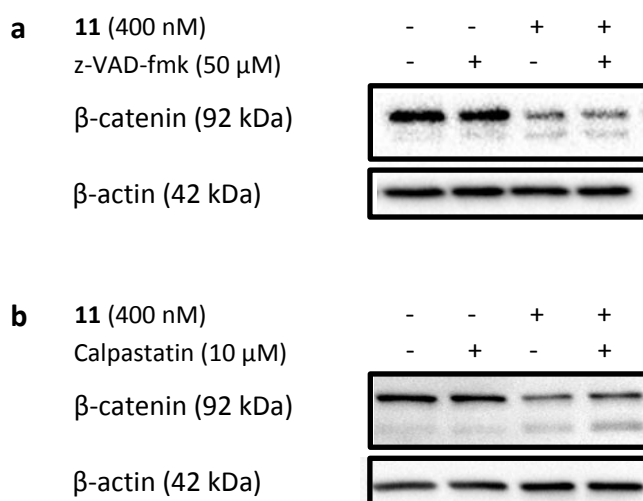


Figure 6.4. Effect of (a) z-VAD-fmk and (b) calpastatin pretreatment on β -catenin level in AGS cells treated with **11**. Cells were pre-treated with either z-VAD-fmk (50 μ M) or calpastatin (10 μ M) for 1 h and treated with **11** (400 nM) for 24 h.

6.4. p53 is involved in the degradation of β -catenin by scopadulciol (**11**)

p53 has been reported to decrease the stability of β -catenin independent of GSK3 β and β -TrCP via the Siah-1 mechanism.^{9, 10} We then investigated the possible role of p53 in the **11**-induced degradation of β -catenin. AGS cells were treated with **11** in the absence or presence of pifithrin- α , a p53 transcriptional activity inhibitor,¹¹ for 24 h. Western blot

analysis showed that pifithrin- α abolished the degradation of β -catenin by **11**, while β -catenin level in AGS cells treated with pifithrin- α alone was unaffected (Figure 6.5). The results suggested that p53 mediated the degradation of β -catenin induced by **11**.

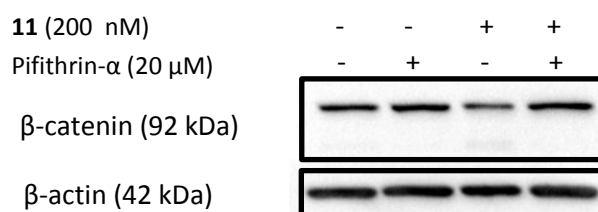


Figure 6.5. Level of β -catenin in AGS treated with **11** (200 nM) for 24 h in the absence or presence of pifithrin- α (20 μ M), p53 transcriptional activity inhibitor

Since the phosphorylation/ β -TrCP pathway was observed to be involved in the β -catenin degradation by **11** in AGS, **11** may have affected other mechanism that can induce degradation of β -catenin. One possible pathway is via the Siah-1 mechanism in which β -catenin is degraded independent of GSK3 β and β -TrCP and can be induced by the activity of p53.^{9, 10} Since we observed that p53 also mediated the degradation of β -catenin by **11**, possibly, the Siah-1 mechanism is involved.

6.5. Scopadulciol (11**) inhibits TCF/ β -catenin transcriptional activity and downregulates the expression of β -catenin target proteins in AGS.**

The decrease of β -catenin level by **11**, particularly in the nucleus, also suggested that TCF/ β -catenin transcriptional activity was also inhibited. The TCF/ β -catenin transcriptional activity regulates the expression of proliferation and survival proteins such

as c-myc, cyclin D1 and survivin. We then transfected AGS cell with the reporter plasmid TOPflash or the negative reporter, FOPflash, and treated the cells with **11**. As shown in Figure 6.6, the TOPflash activity was inhibited without a significant effect on the FOPflash activity suggesting that the inhibition was specific to TOPflash activity. This result indicated that the β -catenin/TCF activity was inhibited in the presence of **11** in AGS.

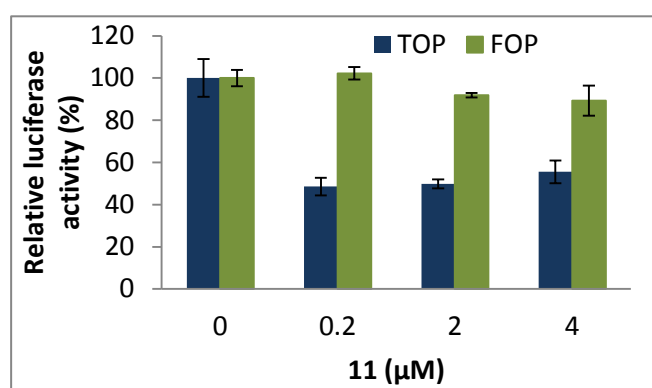


Figure 6.6. TOP and FOP activity of **11** in AGS cells. AGS cells were co-transfected with either TOP or FOP reporter gene and pRL-CMV plasmids for 24 h. After transfection, cells were incubated with **11**. Luciferase activities were measured after 24 h post-transfection.

We then determined the expression level of the β -catenin-dependent target proteins cyclin D1,¹² c-myc¹³ and survivin.¹⁴ Western blot analysis (Figure 6.7) showed that **11** decreased the level of cyclin D1, c-myc and survivin in a dose-dependent manner, suggesting further that **11** inhibited the TCF/ β -catenin transcriptional activity in AGS cells.

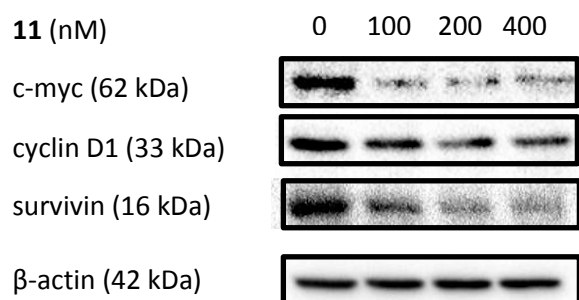


Figure 6.7. Western blot analysis using full lysate on the level of TCF/β-catenin target proteins in AGS cells after treatment with different concentrations (100, 200, 400 nM) of **11** for 24 h. Whole cell lysate were obtained and subjected to Western blot analysis.

6.6. Scopadulciol (**11**) exerted p53-dependent cytotoxicity in AGS

Since p53 was identified to mediate the degradation of β-catenin by **11**, we then determined if inhibition of the p53 activity will also affect the cytotoxic activity of **11**. We treated the AGS cells with **11** in the absence or presence of pifithrin-α for 48 h. Based from FMCA, we observed that pifithrin-α abrogated the cytotoxic activity of **11** in AGS (Figure 6.8). The result suggested that **11** exerted p53-dependent cytotoxic activity in AGS cells.

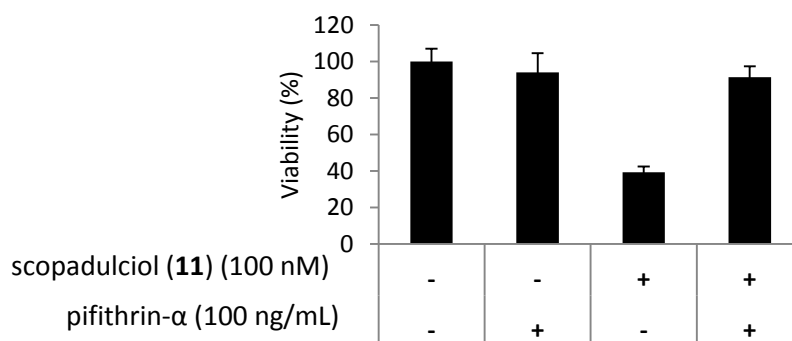


Figure 6.8. Effect pifithrin-α (20 μM) on the viability of AGS treated with **11** (100 nM) for 48 h. Viability of AGS was measured using FMCA.

References

1. Ahsan, M.; Islam, S. K.; Gray, A. I.; Stimson, W. H., Cytotoxic diterpenes from *Scoparia dulcis*. *J Nat. Prod.* **2003**, 66, 958-961.
2. Ikenoue, T.; Ijichi, H.; Kato, N.; Kanai, F.; Masaki, T.; Rengifo, W.; Okamoto, M.; Matsumura, M.; Kawabe, T.; Shiratori, Y.; Omata, M., Analysis of the β -Catenin/T Cell Factor Signaling Pathway in 36 Gastrointestinal and Liver Cancer Cells. *Cancer Sci.* **2002**, 93, 1213-1220.
3. Liu, C.; Li, Y.; Semenov, M.; Han, C.; Baeg, G.-H.; Tan, Y.; Zhang, Z.; Lin, X.; He, X., Control of β -Catenin Phosphorylation/Degradation by a Dual-Kinase Mechanism. *Cell* **2002**, 108, 837-847.
4. Aberle, H.; Bauer, A.; Stappert, J.; Kispert, A.; Kemler, R., β -catenin is a target for the ubiquitin-proteasome pathway. *EMBO J.* **1997**, 16, 3797-3804.
5. Kisselev, Alexei F.; van der Linden, W. A.; Overkleeft, Herman S., Proteasome Inhibitors: An Expanding Army Attacking a Unique Target. *Chem. Biol.* **2012**, 19, 99-115.
6. Van de Craen, M.; Berx, G.; Van den Brande, I.; Fiers, W.; Declercq, W.; Vandenabeele, P., Proteolytic cleavage of β -catenin by caspases: an in vitro analysis. *FEBS Lett.* **1999**, 458, 167-170.
7. Steinhusen, U.; Badock, V.; Bauer, A.; Behrens, J.; Wittman-Liebold, B.; Dörken, B.; Bommert, K., Apoptosis-induced cleavage of β -catenin by caspase-3 results in proteolytic fragments with reduced transactivation potential. *J. Biol. Chem.* **2000**, 275, 16345-16353.
8. Benetti, R.; Copetti, T.; Dell'Orso, S.; Melloni, E.; Brancolini, C.; Monte, M.; Schneider, C., The calpain system is involved in the constitutive regulation of β -catenin signaling functions. *J. Biol. Chem.* **2005**, 280, 22070-22080.
9. Matsuzawa, S.-i.; Reed, J. C., Siah-1, SIP, and Ebi Collaborate in a Novel Pathway for β -Catenin Degradation Linked to p53 Responses. *Mol. Cell* **2001**, 7, 915-926.
10. Liu, J.; Stevens, J.; Rote, C. A.; Yost, H. J.; Hu, Y.; Neufeld, K. L.; White, R. L.; Matsunami, N., Siah-1 Mediates a Novel β -Catenin Degradation Pathway Linking p53 to the Adenomatous Polyposis Coli Protein. *Mol. Cell* **2001**, 7, 927-936.
11. Murphy, P. J. M.; Galigniana, M. D.; Morishima, Y.; Harrell, J. M.; Kwok, R. P. S.; Ljungman, M.; Pratt, W. B., Pifithrin- α Inhibits p53 Signaling after Interaction of the Tumor Suppressor Protein with hsp90 and Its Nuclear Translocation. *J. Biol. Chem.* **2004**, 279, 30195-30201.

12. Shtutman, M.; Zhurinsky, J.; Simcha, I.; Albanese, C.; D'Amico, M.; Pestell, R.; Ben-Ze'ev, A., The cyclin D1 gene is a target of the β -catenin/LEF-1 pathway. *Proc. Natl. Acad. Sci. USA* **1999**, 96, 5522-5527.
13. He, T. C.; Sparks, A. B.; Rago, C.; Hermeking, H.; Zawel, L.; da Costa, L. T.; Morin, P. J.; Vogelstein, B.; Kinzler, K. W., Identification of c-MYC as a target of the APC pathway. *Science* **1998**, 281, 1509-1512.
14. Zhang, T.; Otevrel, T.; Gao, Z.; Ehrlich, S. M.; Fields, J. Z.; Boman, B. M., Evidence that APC regulates survivin expression: a possible mechanism contributing to the stem cell origin of colon cancer. *Cancer Res.* **2001**, 61, (24), 8664-8667.

CHAPTER 7

Scopadulciol (11) sensitizes AGS to TRAIL-induced apoptosis

7.1. Background of the study

Targeting β -catenin has also been suggested as another possible strategy to enhance the TRAIL-mediated apoptosis in resistant cancer cells.¹ The use of tumor necrosis factor-related apoptosis ligand (TRAIL) to induce cancer cell apoptosis has been considered an attractive strategy as it affects the cancer cell and not the normal cells.² When TRAIL binds to the death receptors (DR4 and DR5), it leads to the activation of Fas-associated death domain (FADD), followed by the activation of effector caspase (caspase-3) by the initiator caspase (caspase-8) (Figure 7.1).³ Also, TRAIL-induced apoptosis requires the mitochondrial pathway to completely activate caspase-3.⁴ When the caspase-8 is activated, truncated Bid (tBid) is generated which then translocates to the mitochondria. Interaction of the tBid with Bax and Bak results in the release of cytochrome c and SMAC/DIABLO, and induces apoptosis.

However, several cancer cells have developed resistance to the effect of TRAIL due to the overexpression of decoy receptors or of anti-apoptotic proteins such as Bcl2 and IAPs (e.g. survivin).⁵ Treatment with combination of TRAIL and compounds that can either upregulate DR4 or DR5 expression or downregulate the antiapoptotic protein level are possible strategies to overcome TRAIL-resistance in cancer cells. Several reports had shown that β -catenin can be a potential target to sensitize TRAIL-resistant cancer cells. In this study, we investigated to determine if **11** can sensitize AGS to TRAIL-induced apoptosis.

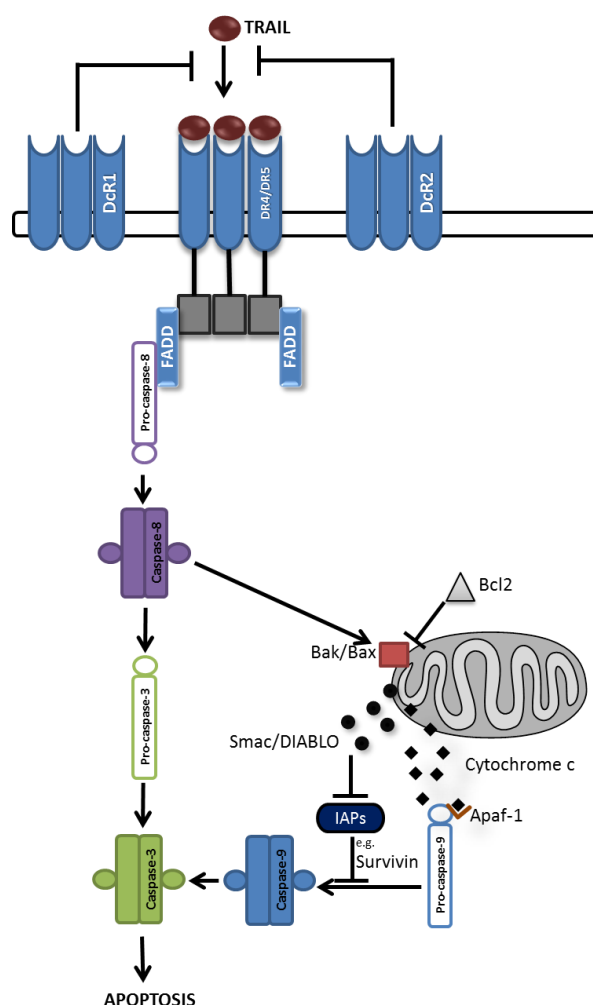


Figure 7.1. Intrinsic and extrinsic TRAIL (tumor necrosis-related apoptosis inducing ligand) signaling pathway.

7.2. Scopadulciol (11) has TRAIL-resistance overcoming activity.

The AGS cancer cell line is known to have a strong resistance to TRAIL. Treatment of AGS with TRAIL (100 ng/mL) did not significantly reduced the viability. When TRAIL was administered with luteolin⁶ (17.7 μ M), which was used as a positive control, the viability was further decreased to 41%. Combined treatment of **11** and TRAIL synergistically exhibited stronger apoptosis induction activity on AGS than in the

treatment with **11** alone (Figure 7.2). After 24 h exposure, combined treatment of **11** (200 nM) and TRAIL (100 ng/mL) showed about 93% reduction in AGS viability.

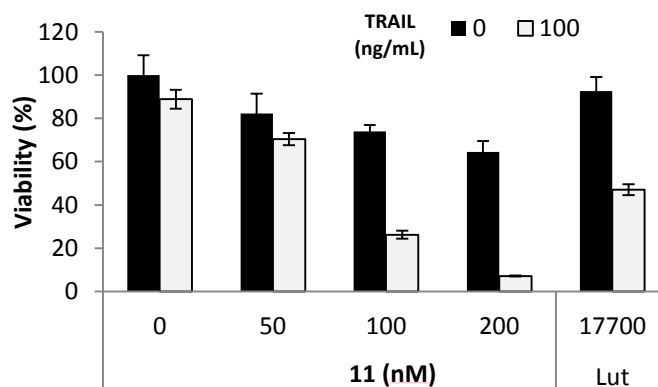


Figure 7.2. Compound **11** showed TRAIL-overcoming resistance activity in AGS cells. Cells were exposed to the different treatments as described for 24 h and assayed for viability using FMCA. Lut = Luteolin serves as control for the TRAIL-overcoming resistance activity assay.

FACS analysis showed that at 12 h exposure, 27.7% apoptotic cells were observed in **11**+TRAIL combined treatment while only 5.7% and 3.5% were observed in treatment with TRAIL or **11** alone, respectively (Figure 7.3). Furthermore, the number of early apoptotic cells in AGS with either TRAIL or **11** alone did not show significant difference with the control. These results suggested that **11** had a strong TRAIL-resistance overcoming activity. Furthermore, the combined treatment of non-cancer cell line HEK293 with **11** and TRAIL showed lower reduction in viability as compared with AGS (Figure 7.4).

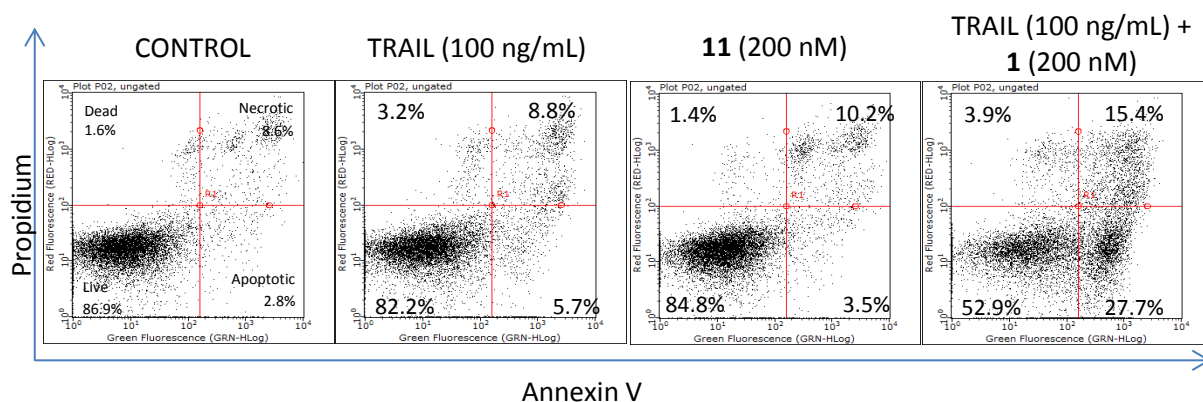


Figure 7.3. FACS analysis on the induction of apoptosis in AGS cells by TRAIL+**11** combined treatment. Cells were exposed to the different conditions as described for 12 h. Cells were collected and stained with annexin V and propidium iodide. The population of viable, apoptotic and dead cells were quantified by FACS analysis.

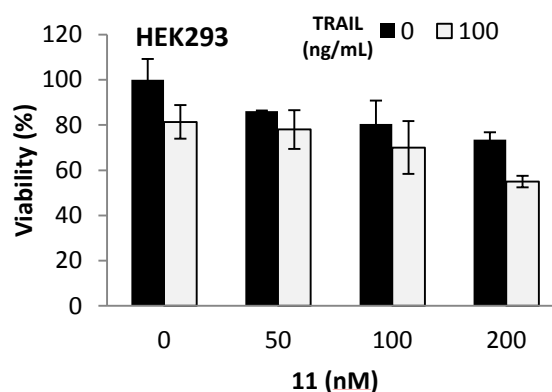


Figure 7.4. Effect of combined treatment of TRAIL and **11** against non-cancer cell HEK293. Cells were exposed to the different treatments as described for 24 h. Viability was determined using FMCA and was normalized to control (0 nM).

7.3. Scopadulciol (**11**) affected the level of the apoptosis-related proteins

Western blot analysis showed that **11** increased the level of DR4 and DR5 (Figure 7.5a), and decreased the level of the anti-apoptotic proteins Bcl2 (Figure 7.5a). Compound **11** was also observed to increase p53 level in AGS. Since in TRAIL-induced apoptosis caspase is responsible in initiating apoptosis, we then determined if the decrease in viability depends on the caspase activity. We pre-treated AGS cells with z-VAD-fmk, a pan-caspase inhibitor, for 1 h and then, treated with **11** in the absence or presence of TRAIL for 24 h. Results showed the caspase-inhibitor blocked the apoptosis induced by the combined treatment **11**+TRAIL, suggesting that the effect of **11** and TRAIL is caspase-dependent (Figure 7.5b).

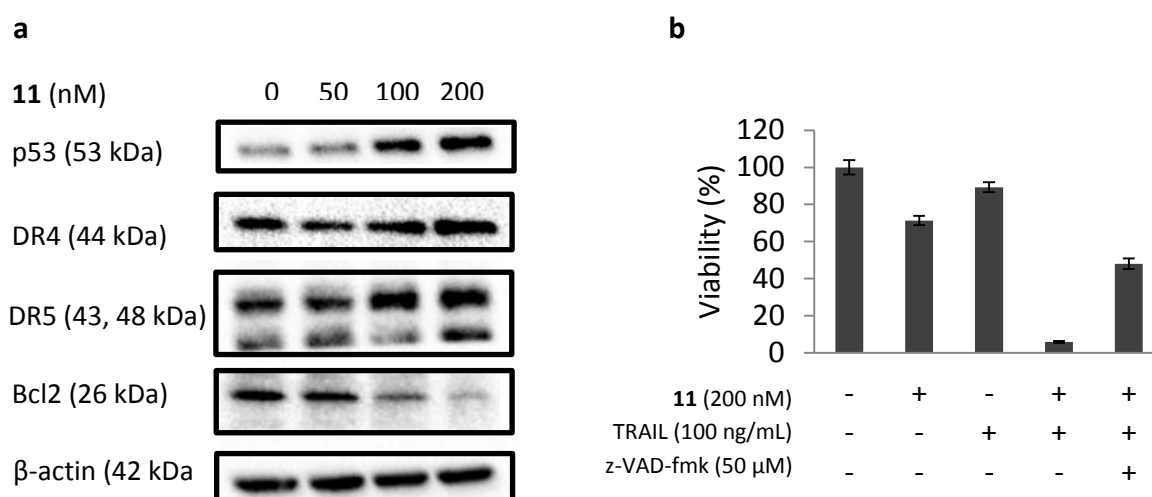


Figure 7.5. (a) Western blot analysis of p53, DR4, DR5 and Bcl2 in AGS treated with different concentration of **11**. Cells were treated with **11** at different concentrations (50, 200, 400 nM) for 24 hr and analyzed by Western blot. (b) Effect of z-VAD-fmk (50 μ M) on the viability of AGS cells treated with combined TRAIL and **11**. Cells were pretreated with z-VAD-fmk (50 μ M) for 1 h, then treated as described for 24 h. Viability was calculated relative to the control (no inhibitor and TRAIL) treatment. Data are from one experiment representative of at least two independent experiments (mean \pm s.d.).

The increase in the DR4 and DR5 level could lead to an enhance binding of TRAIL to the death receptors. The binding of TRAIL to the death receptors leads to the activation of caspase-8 which then activates caspase-3 to mediate apoptosis.³ Moreover, the mitochondrial pathway further enhanced the **11**+TRAIL induced apoptosis as **11** was observed to decrease the level of Bcl2 and survivin. Bcl2 is known to inhibit the pro-apoptotic protein Bax while survivin inhibits the activation of procaspase-9 to caspase-3.⁴ With the increase binding of TRAIL to the death receptors and decreased levels of the anti-apoptotic proteins, these possibly mediated AGS to overcome its resistance to TRAIL-induced apoptosis.

7.4. Combination of TRAIL and scopadulciol (11) enhanced degradation of β -catenin in AGS.

Western blot analysis also showed that the combined treatment **11**+TRAIL enhanced the degradation of β -catenin as early as 12 h (Figure 7.6a). Previous report had showed that combination of TRAIL with a Wnt inhibitor troglitazone had resulted in cleavage of β -catenin due to caspase activity.¹ In contrast to their results, in the presence of the pan-caspase inhibitor z-VAD-fmk, the degradation of the β -catenin induced by the combined TRAIL and **11** was not prevented (Figure 7.6b). This result suggested that β -catenin degradation by **11**+TRAIL was not caspase-mediated. There is no yet clear evidence on the direct relationship of decreased β -catenin level to TRAIL-mediated apoptosis. Decrease in β -catenin level was observed when AGS was treated with TRAIL and natural compound sanguinarine.⁷ The increased apoptosis in Huh-7 cells by the combined treatment of troglitazone, a β -catenin/TCF transcription inhibitor, and TRAIL was attributed to the disassembly of the adherens junction caused by β -catenin degradation.¹ Osteoprotogerin, which was reported to mediate resistance in colon cancer

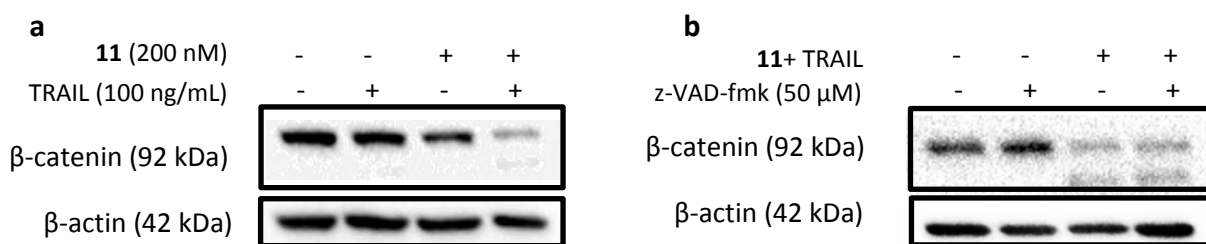


Figure 7.6. (a) Western blot analysis of β -catenin in AGS cells treated with **11** (200 nM) + TRAIL (100 ng/mL) for 12 h. (b) Effect of z-VAD-fmk pretreatment on β -catenin level in AGS treated with **11** and TRAIL. Cells were pre-treated with z-VAD-fmk (50 μ M) for 1 h and treated with **1** (200 nM) + TRAIL (100 ng/mL).

cell, was shown to be a target gene of β -catenin.^{8, 9} However a study also showed that downregulation of β -catenin was found to decrease TRAIL-sensitivity by lowering the expression of DR4 and DR5 in colon cancer cell.¹⁰ In this study, we were able to observe caspase-independent β -catenin degradation by the combined **11**+TRAIL which seems interesting, and warrant for further investigation. Since the function of Wnt/ β -catenin signalling pathway mediates cancer cell growth and survival, β -catenin degradation may, at least partly, contribute to the action of TRAIL in inducing apoptosis.

References

1. Senthivinayagam, S.; Mishra, P.; Paramasivam, S. K.; Yallapragada, S.; Chatterjee, M.; Wong, L.; Rana, A.; Rana, B., Caspase-mediated cleavage of β -catenin precedes drug-induced apoptosis in resistant cancer cells. *J. Biol. Chem.* **2009**, 284, 13577-13588.
2. Ashkenazi, A.; Holland, P.; Eckhardt, S. G., Ligand-based targeting of apoptosis in cancer: the potential of recombinant human apoptosis ligand 2/Tumor necrosis factor-related apoptosis-inducing ligand (rhApo2L/TRAIL). *J. Clin. Oncol.* **2008**, 26, 3621-3630.
3. Bodmer, J. L.; Holler, N.; Reynard, S.; Vinciguerra, P.; Schneider, P.; Juo, P.; Blenis, J.; Tschopp, J., TRAIL receptor-2 signals apoptosis through FADD and caspase-8. *Nat. Cell. Biol.* **2000**, 2, 241-243.
4. Deng, Y.; Lin, Y.; Wu, X., TRAIL-induced apoptosis requires Bax-dependent mitochondrial release of Smac/DIABLO. *Genes Dev.* **2002**, 16, 33-45.
5. Zhang, L.; Fang, B., Mechanisms of resistance to TRAIL-induced apoptosis in cancer. *Cancer Gene Ther.* **2005**, 12, 228-237.
6. Horinaka, M.; Yoshida, T.; Shiraishi, T.; Nakata, S.; Wakada, M.; Nakanishi, R.; Nishino, H.; Matsui, H.; Sakai, T., Luteolin induces apoptosis via death receptor 5 upregulation in human malignant tumor cells. *Oncogene* **2005**, 24, 7180-7189.
7. Choi, W. Y.; Jin, C. Y.; Han, M. H.; Kim, G. Y.; Kim, N. D.; Lee, W. H.; Kim, S. K.; Choi, Y. H., Sanguinarine sensitizes human gastric adenocarcinoma AGS cells to TRAIL-mediated apoptosis via down-regulation of AKT and activation of caspase-3. *Anticancer Res.* **2009**, 29, 4457-4465.
8. Glass Ii, D. A.; Bialek, P.; Ahn, J. D.; Starbuck, M.; Patel, M. S.; Clevers, H.; Taketo, M. M.; Long, F.; McMahon, A. P.; Lang, R. A.; Karsenty, G., Canonical Wnt Signaling in Differentiated Osteoblasts Controls Osteoclast Differentiation. *Developmental Cell* **2005**, 8, 751-764.
9. De Toni, E. N.; Thieme, S. E.; Herbst, A.; Behrens, A.; Stieber, P.; Jung, A.; Blum, H.; Göke, B.; Kolligs, F. T., OPG is regulated by beta-catenin and mediates resistance to TRAIL-induced apoptosis in colon cancer. *Clin. Cancer Res.* **2008**, 14, 4713-4718.
10. Jalving, M.; Heijink, D. M.; Koornstra, J. J.; Boersma-van Ek, W.; Zwart, N.; Wesseling, J.; Sluiter, W. J.; de Vries, E. G.; Kleibeuker, J. H.; de Jong, S., Regulation of TRAIL receptor expression by β -catenin in colorectal tumours. *Carcinogenesis* **2014**, 35, 1092-1099.

CHAPTER 8

Summary and Conclusion

The Wnt signal pathway plays a crucial role in many biological processes such as cell fate determination, proliferation and tissue maintenance. Abnormal activation of the Wnt signal can induce disease development, particularly cancer. Thus, targeting the Wnt signal offers a promising therapeutic strategy for the management of diseases. In our continued efforts to find for inhibitors from natural resources, we utilized a cell-based screen to identify potential plant sources of Wnt inhibitors. In this study, our objective is to isolate and identify the bioactive compounds from the “hit” plants. Furthermore, we aim to determine the putative mechanism through which the active compounds inhibit the Wnt signal.

Using the STF/293 reporter cell which is a HEK293 cell line stably transfected with TOPflash reporter plasmid (TOP assay), we identified one Thai plant, *Curcuma comosa* (Zingiberaceae), and two Bangladeshi plants *Scoparia dulcis* (Plantaginaceae), and *Azadirachta excelsa* (Meliaceae) to possess inhibitory activity against TOP assay, thus, making them potential sources of Wnt inhibitors. The extracts of the identified plants were subjected to an activity-guided multistep separation using chromatographic techniques (silica gel chromatography, ODS, sephadex LH-20, Diaion HP-20, and HPLC), and recrystallization. The identity of the isolated compounds was established from their spectroscopic data (NMR, MS, CD, and specific rotation), and by comparison with those of literature values for the known compounds. Two new (**1** and **2**) and six (**3-8**) known diarylheptanoids, and two known sesquiterpenoids (**9** and **10**) were isolated from *C. comosa*.¹ On the other hand, two scopadulan-type diterpenes (**11** and **12**), and two

triterpenes (**13** and **14**) were identified from *S. dulcis*. From *A. excelsa*, a new (**15**) and seven reported (**16-22**) trichillin-type limonoids were isolated.

From the isolated compounds, compounds **1**, **6-8** and **17-20** showed inhibitory activity against the TOP activity with $IC_{50} \leq 10 \mu M$. Compounds **1**, **8**, **17-19** did not significantly affect the FOP assay (negative reporter assay) which suggested that these compounds specifically inhibited the TOP activity. Among these identified potent Wnt inhibitors, **17-19** showed the strongest TOP inhibitory activity with IC_{50} of 127, 300, and 252 nM, respectively. Compound **18** decreased the viability of the Wnt-dependent cells HCT116 (IC_{50} 239 nM), and AGS (IC_{50} 161 nM) (Table 1). On the other hand, it did not affect the viability of SW480 and DLD1, also Wnt-dependent cancer cells.

Compound **11** did not inhibit TCF/ β -catenin transcription activity based on TOP assay using STF/293 cells but it exhibited cytotoxic activity against AGS cells, which has an active Wnt signal due to mutation in β -catenin. Western blot analysis showed that **11** can induce degradation as well as inhibit nuclear accumulation of β -catenin. In the presence of either proteasome inhibitor MG132 or p53 transcriptional inhibitor pifithrin- α , the degradation induced by **11** was abrogated. We also observed that **11** decreased GSK3 β level (Fig. 5b). These results indicated that β -catenin degradation by **11** in AGS is mediated by p53 and proteasome, and independent of GSK3 β . Transient transfection of AGS cells with either TOP or FOP plasmid showed that **11** decreased TOP activity in without affecting the FOP activity. Also, western blot analysis showed that **11** downregulated the level of the TCF/ β -catenin target proteins c-myc, cyclin D1 and survivin. Results indicated that **11** inhibited the TCF/ β -catenin transcription activity in AGS.

On the other hand, when combined with TRAIL (tumor necrosis-related apoptosis inducing ligand), **11** resulted in increase in cytotoxic activity but inducing caspase-

dependent apoptosis in AGS. The results showed that **11** had TRAIL-resistance overcoming activity. It sensitized AGS to TRAIL-induced apoptosis by increasing the level of DR4 and DR5, and downregulation of Bcl2. Furthermore, the **11**+TRAIL also enhanced β -catenin degradation, which may, at least, partly contribute to the induction of apoptosis by TRAIL.

In conclusion, using activity-guided isolation, ten compounds (**1-10**) were isolated from *C. comosa*, four (**11-14**) from *S. dulcis*, and eight (**15-22**) from *A. excelsa*. Compounds **1** and **2** are reported here as new diarylheptanoids, and **15** as new trichillin-type limonoid. Compounds **18** showed inhibitory activity against TCF/ β -catenin transcriptional activity in STF/293 reporter cells, and cytotoxicity against Wnt-dependent cancer cells AGS and HCT116. Compound **18** did not affect the level and localization of β -catenin in HCT116, but downregulated the level of the TCF/ β -catenin target protein, c-myc. Compound **11** attenuated the Wnt signal in AGS cells via p53- and proteasome-mediated degradation of β -catenin, and inhibition of the accumulation of β -catenin in the nucleus. Furthermore, it showed TRAIL-resistance overcoming activity in AGS. The observed enhanced degradation of β -catenin by **11**+TRAIL warrants for further investigation.

PROJECT 2

Search for Natural Compounds that
Enhance Ngn2 Promoter Activity

CHAPTER 9

Regulation of neurogenesis by the basic helix-loop-helix (bHLH) transcription factors

9.1. Overview

It is believed before that the ability of a brain to generate new neurons stops just after birth. However, studies showed that neural stem cells (NSCs) can also be found in the adult nervous system of all mammalian organisms, including humans.¹⁻³ NSCs are multipotent cells that can differentiate to neurons, astrocytes and glial cells (Figure 9.1).⁴

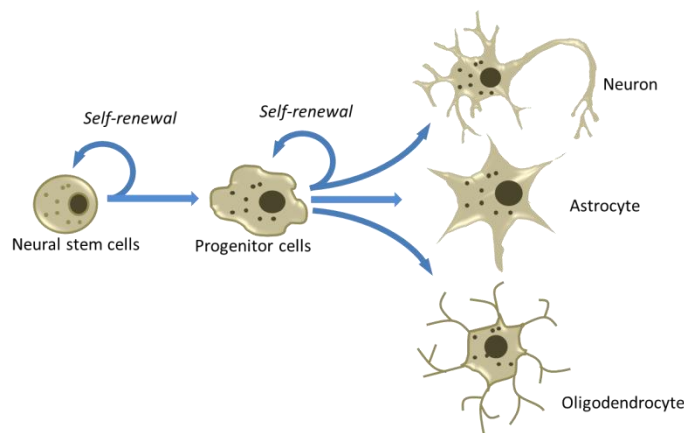


Figure 9.1. Differentiation of neural stem cells to neuron, astrocyte, and oligodendrocyte.

Neurogenesis in the adult nervous system is considered a significant discovery as it offers new strategies to develop treatment for neurodegenerative diseases. Some reports suggested that neurogenesis may replace lost neurons in Alzheimer's disease⁵, and is involved in the formation of trace memories.⁶ However, the adult neurogenesis is being

regulated by various factors such as the cell intrinsic programs and the environmental factors.⁷ Thus, the fate of NSCs can then be manipulated by regulating the pathway that is involved in neuronal fate specification. One of the factors that control neurogenesis is the basic helix-loop-helix genes (bHLH) which either repress or activate neurogenesis. The neurogenins (Ngn) are proneural genes that are key regulators of neurogenesis.⁸ In our study, we look for natural compounds that promote differentiation of NSCs to neurons by increasing the activity of Ngn2.

9.2. The Basic helix-loop-helix transcription factors

The bHLH transcription factors are responsible for the control of the neural stem cell differentiation. They are categorized as either the repressor type or the activator type. The repressor type genes maintain NSCs as well as control gliogenesis while the activator type initiate neurogenesis (Figure 9.2).⁹

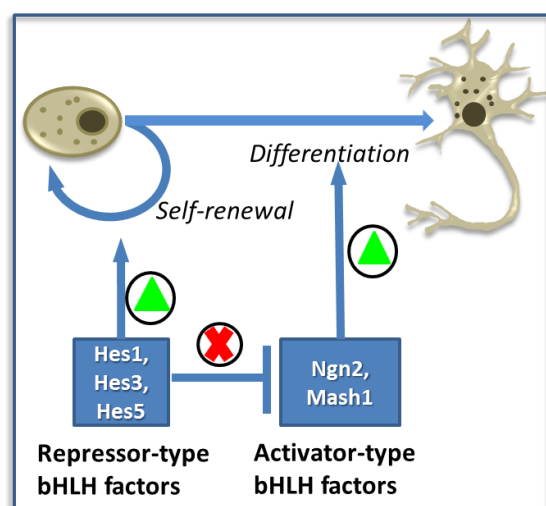


Figure 9.2. Role of bHLH factors in neurogenesis.

The repressor type bHLH factors which includes the *Hes* (*hairy and enhancer of split*) family (*Hes1*, *Hes3*, and *Hes5*) inhibits transcription via two mechanisms: active and passive repression.¹⁰ In active repression, Hes factors form a homodimer and binds to the N box (CACNAG). Then, a co-repressor TLE/Grg interacts with the dimer, and they actively repress transcription. In the passive repression, Hes1 forms a heterodimer with the bHLH activator E47, and inhibits transcriptional activation. On the other hand, some members of the neural bHLH or the activator type are *Ngn* family (*Ngn1*, *Ngn2*), *Mash1* and *Math*.⁸ They form a heterodimer with E47 and binds to the E box (CANNTG) to initiate transcription.

Moreover, neuronal differentiation is also dependent on the Notch pathway (Figure 9.3). Activation of the Notch pathway inhibits neuronal differentiation. It is said that expression of *Ngn2* and *Hes1* oscillates, thus maintaining a group of cells in undifferentiated state.¹¹ When the level of Hes1 is low, Ngn2 level increases. Ngn2 induces the expression of not only the proneural genes but also Notch ligands such as Dll1 which activates the Notch signal in the neighboring cells.¹² When the Notch is activated, it induces the expression of the bHLH repressors. Thus, the Ngn2 level must then be sustained to induce the NSCs to undergo neuronal differentiation.¹³

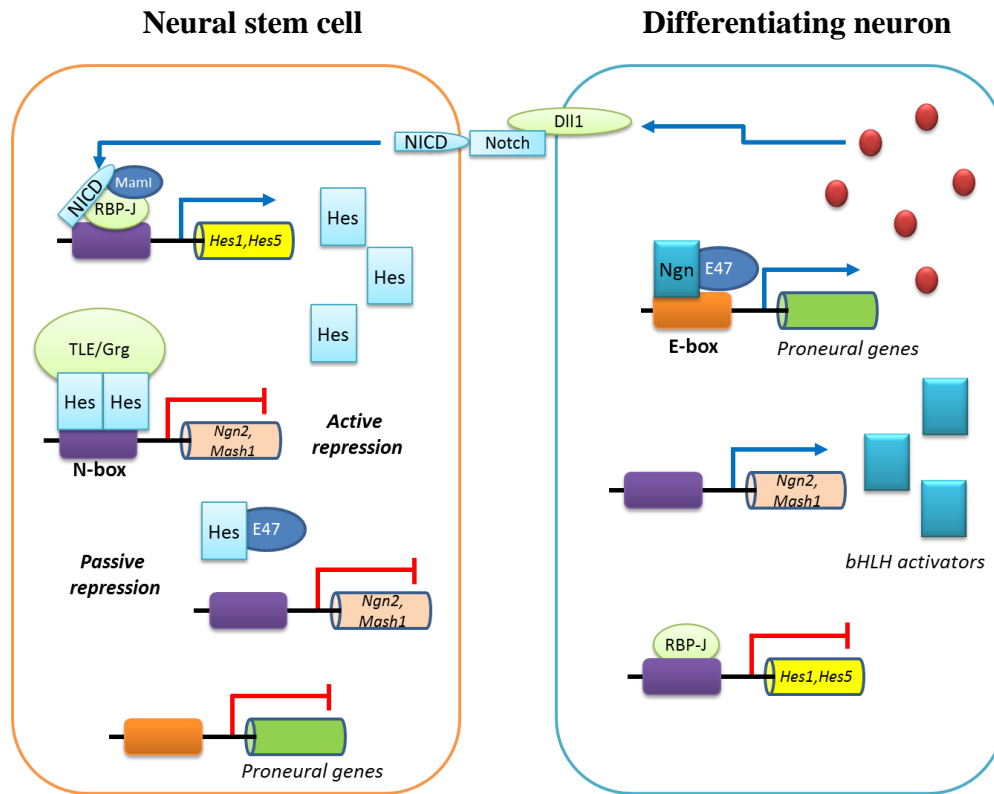


Figure 9.3. Regulatory pathways controlled by the activator and repressor bHLH. Figure adapted from Kageyama *et al.* (2005).⁹

9.3. Reported compounds that induce neuronal differentiation

There are several compounds which are reported to induce neuronal differentiation. Most of these compounds were observed to increase the expression of some bHLH activators and decrease *Hes1* expression (Figure 9.4). Docosahexanoic acid was reported to decrease the level of *Hes1* while the level of a bHLH activator *NeuroD* was upregulated.¹⁴ Baicalin was also reported to increase the level of *Ngn1*, *Ngn2*, and *NeuroD2*.¹⁵ Retinoic acid induced neuronal differentiation by increasing *NeuroD*.¹⁶ On the other hand, ginsenosides Rg5 induced neuronal differentiation by increasing Ca^{2+} -influx via voltage-gated channel resulted in increased bHLH activator expression.¹⁷ Our laboratory has also reported *Ngn2* activators from a plant *Butea superba*. Using our constructed *Ngn2* promoter assay, we were able to identify 3'-methoxydaidzein to enhance *Ngn2* promoter activity. Moreover, it also promoted neurite outgrowth in C17.2 and upregulated the mRNA expression of *Ngn2*, *Ngn1* and *NeuroD2*.¹⁸

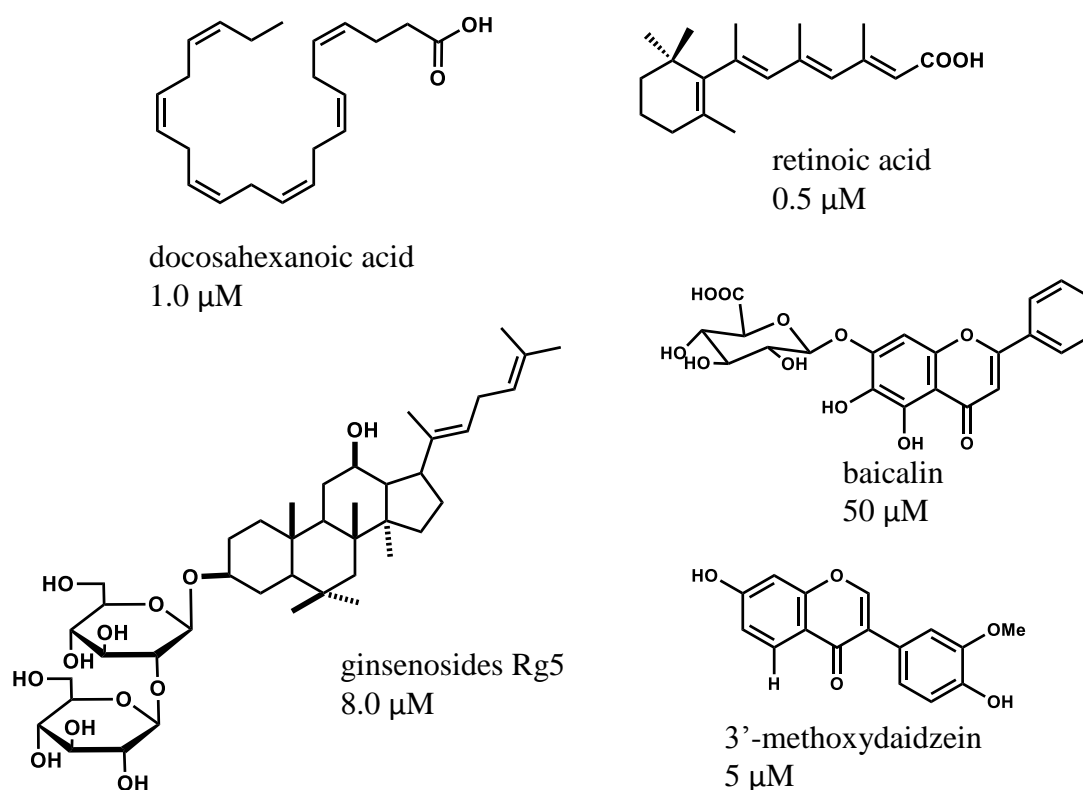


Figure 9.4. Reported compounds that induce neurogenesis and their respective effective concentrations.

References

1. Taupin, P.; Gage, F. H., Adult neurogenesis and neural stem cells of the central nervous system in mammals. *J. Neurosci. Res.* **2002**, 69, 745-749.
2. Baizabal, J.-M.; Furlan-Magaril, M.; Santa-Olalla, J.; Covarrubias, L., Neural stem cells in development and regenerative medicine. *Arch. Med. Res.* **2003**, 34, 572-588.
3. Reynolds, B. A.; Weiss, S., Generation of neurons and astrocytes from isolated cells of the adult mammalian central nervous system. *Science* **1992**, 255, 1707-1710.
4. Merkle, F. T.; Alvarez-Buylla, A., Neural stem cells in mammalian development. *Curr. Opin. Cell Biol.* **2006**, 18, 704-709.
5. Jin, K.; Peel, A. L.; Mao, X. O.; Xie, L.; Cottrell, B. A.; Henshall, D. C.; Greenberg, D. A., Increased hippocampal neurogenesis in Alzheimer's disease. *Proc. Natl. Acad. Sci. USA* **2004**, 101, 343-347.
6. Shors, T. J.; Miesegaes, G.; Beylin, A.; Zhao, M.; Rydel, T.; Gould, E., Neurogenesis in the adult is involved in the formation of trace memories. *Nature* **2001**, 410, 372-376.
7. Abrous, D. N.; Koehl, M.; Le Moal, M., Adult neurogenesis: from precursors to network and physiology. *Physiol. Rev.* **2005**, 85, 523-569.
8. Bertrand, N.; Castro, D. S.; Guillemot, F., Proneural genes and the specification of neural cell types. *Nat. Rev. Neurosci.* **2002**, 3, 517-530.
9. Kageyama, R.; Ohtsuka, T.; Hatakeyama, J.; Ohsawa, R., Roles of bHLH genes in neural stem cell differentiation. *Exp. Cell Res.* **2005**, 306, 343-348.
10. Kageyama, R.; Ohtsuka, T.; Kobayashi, T., The Hes gene family: repressors and oscillators that orchestrate embryogenesis. *Development* **2007**, 134, 1243-1251.
11. Shimojo, H.; Ohtsuka, T.; Kageyama, R., Oscillations in notch signaling regulate maintenance of neural progenitors. *Neuron* **2008**, 58, 52-64.
12. Kageyama, R.; Ohtsuka, T.; Shimojo, H.; Imayoshi, I., Dynamic Notch signaling in neural progenitor cells and a revised view of lateral inhibition. *Nature Neurosci.* **2008**, 11, 1247-1251.
13. Shimojo, H.; Ohtsuka, T.; Kageyama, R., Dynamic expression of notch signaling genes in neural stem/progenitor cells. *Front. Neurosci.* **2011**, 5, 78.
14. Katakura, M.; Hashimoto, M.; Shahdat, H. M.; Gamoh, S.; Okui, T.; Matsuzaki, K.; Shido, O., Docosaheptaenoic acid promotes neuronal differentiation by regulating basic helix-loop-helix transcription factors and cell cycle in neural stem cells. *Neuroscience* **2009**, 160, 651-660.

15. Li, M.; Tsang, K. S.; Choi, S. T.; Li, K.; Shaw, P. C.; Lau, K. F., Neuronal differentiation of C17.2 neural stem cells induced by a natural flavonoid, baicalin. *Chembiochem* **2011**, 12, 449-546.
16. Takahashi, J.; Palmer, T. D.; Gage, F. H., Retinoic acid and neurotrophins collaborate to regulate neurogenesis in adult-derived neural stem cell cultures. *J. Neurobiol.* **1999**, 38, 65-81.
17. Liu, J. W.; Tian, S. J.; de Barry, J.; Luu, B., Panaxadiol glycosides that induce neuronal differentiation in neurosphere stem cells. *J. Nat. Prod.* **2007**, 70, 1329-1334.
18. Arai, M. A.; Koryudzu, K.; Koyano, T.; Kowithayakorn, T.; Ishibashi, M., Naturally occurring Ngn2 promoter activators from *Butea superba*. *Mol. Biosyst.* **2013**, 9, 2489-2497.

CHAPTER 10

Ngn2 Promoter Assay Protocol

10.1. Cell-based luciferase assay system

The Ngn2 promoter activity was evaluated using our previously reported cell-based luciferase assay system.¹ The assay system utilized C3H10T1/2 cells stably transfected with pGL4.20 vector (Promega) containing Ngn2 promoter inserted upstream of the luciferase gene (Figure 10.1). The activation of the Ngn2 promoter leads to the transcription of the luciferase gene. This enzyme catalyzes the oxidative conversion of luciferin to oxyluciferin. In this chemical transformation, light also is being produced in which luminescence is measured and the relative activity is calculated.

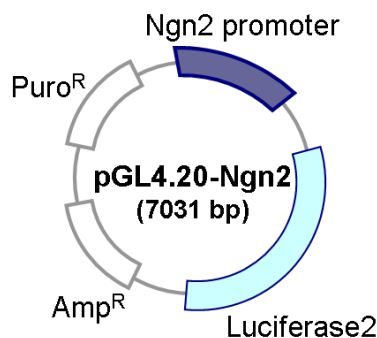


Figure 10.1. Ngn2 reporter plasmid.

10.2. Methods

10.2.1. Ngn2 reporter assay

The Ngn2 promoter activity assay was conducted using the methods described previously.¹ C3H10T1/2 cells stably transfected with a plasmid containing an Ngn2 promoter were seeded in 96-well plate at a density of 1×10^4 cells/well. After 24 h

incubation, different concentrations of compounds were added and incubated for 24 h. Then, cells were lysed with Glo Lysis Buffer. Luciferase activity was measured using Bright-Glo Luciferase Assay System (Promega) according to manufacturer's recommendations. Relative Ngn2 promoter activity of the control (50% EtOH only) is defined as 100% and the activity of the other treatments were calculated accordingly.

$$Rel. Ngn2 \text{ promoter activity (\%)} = \frac{Luminescence \text{ of treated samples}}{Luminescence \text{ of control}} \times 100$$

10.2.2. Neuronal differentiation activity

Briefly, cells at a density of 2×10^4 cells/well in proliferation medium [DMEM (high glucose with L-Glutamine); 5 μ g/mL insulin; 10 ng/mL EGF; 50 μ g/mL transferrin; 10 ng/mL biotin and 30 nM Na_2SeO_3] were seeded in 24 well plate with a poly-L-lysine/laminine-coated coverslip in each well. The cells were incubated for 24 h at 37 °C. After 24 h, the medium was removed and the cells were washed with DMEM only. Then the cells were treated with the samples prepared in differentiation medium [NeuroCult Basal Medium (mouse) with 10% NSC differentiation supplements (mouse)] for 4 d. After the treatment, the medium was removed and then washed with 500 μ L PBS twice for 5 min. Then, the cells were fixed with 500 μ L 4% paraformaldehyde for 30 min. The cells were then washed with 500 μ L PBS twice for 5 mins, and added with a blocking buffer (1% BSA+1% Triton-X in PBS) for 1 h. After blocking, the cells were washed with 300 μ L PBS twice for 5 min. Combined primary antibodies (200 μ L) [mouse anti-TUJ1 (1:400) + mouse anti-GFAP (1:400)] was added to the cells, and were incubated overnight at 4°C. Then, the primary antibodies were removed, and the cells were washed with 300 μ L PBS twice for 5 min. After washing, the cells were incubated with the secondary antibodies [anti-rabbit Alexa Fluor 555 (1:500) + anti-goat Alexa Fluor 488

(1:500) with 250 µg/mL RNase] in the dark for 1 h. Then, the secondary antibodies were removed, and the cells were washed with 300 µL PBS twice for 5 min. The cells were then counterstained with 200 µL TO-PRO (1µM) for 1 h. After counterstaining, the coverslips were removed from the 24-well plate and mounted in glass slide using a ProLong[®] Gold Antifade Reagent Special Packaging. The cells were viewed using Olympus FV500, and the cells were analyzed using ImageJ.²

References

1. Arai, M. A.; Koryudzu, K.; Koyano, T.; Kowithayakorn, T.; Ishibashi, M., Naturally occurring Ngn2 promoter activators from *Butea superba*. *Mol. Biosyst.* **2013**, 9, 2489-2497.
2. Rasband, W.S., ImageJ, U. S. National Institutes of Health, Bethesda, Maryland, USA, <http://imagej.nih.gov/ij/>, **1997-2014**.

CHAPTER 11

Phenolic compounds from *Oroxylum indicum* that activate Ngn2 promoter activity

11.1. Plant Description

Oroxylum indicum Linn., which belongs to family Bignoniaceae, is a known medicinal plant that grows in India, Japan, and Malaysia. Locals use it as treatment for common illnesses such as diarrhea, fever and jaundice.¹ Pharmacological studies showed that *O. indicum* contains antimicrobial,² antiinflammatory,² antimutagenic³ and antioxidant properties.⁴ Moreover, the flavanoid baicalein was isolated from *O. indicum*, and the compound showed antiproliferative activity against cancer cell.⁵ The bark sample of *O. indicum* used in this study was collected from Bangladesh. Its MeOH extract was screened by the previous student, and its Ngn2 promoter activity was 192% at 100 µg/mL.⁶ Liquid-liquid partition of its MeOH extract showed that its hexane extract showed the strongest activity with 250% at 50 µg/mL. It was followed by the EtOAc fraction (200%), and then BuOH fraction (150%). The water-soluble component of the extracts did not show induction of the Ngn2 promoter activity.

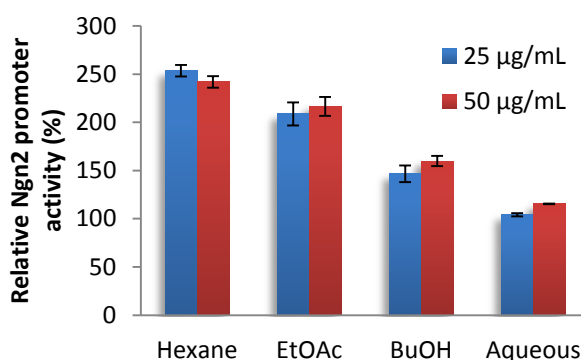


Figure 11.1 Ngn2 promoter activity of *O. indicum* hexane, EtOAc, BuOH and aqueous fractions.

11.2. Isolation of the constituents

Figure 11.2 shows the isolation scheme of *O. indicum*. The dried bark of *O. indicum* (336 g) was extracted in MeOH to give the crude extract (13.9 g). The extract was re-suspended in 10% MeOH (300 mL) and partitioned between *n*-hexane, EtOAc, and *n*-BuOH (300 mL x 3). The hexane fraction (3.9 g) was then subjected to silica gel column chromatography (ϕ 25 x 330 mm) with CHCl₃:MeOH (0:1-1:1) to give fractions nine fractions (1A-1I). Fraction 1C (40.3 mg) was subjected to ODS column chromatography (ϕ 15 x 250 mm) and eluted with H₂O:MeOH (1:1-0:1) to yield **23** (13.4 mg). Fraction 1E (ϕ 25 x 280 mm) was subjected to silica gel column chromatography (ϕ 25 x 280 mm) to afford **23** (10.8 mg), **24** (6.8 mg), **25** (13 mg) and **26** (58.1 mg). Fraction 1F (1161.1 mg) was subjected to ODS column chromatography (ϕ 20 x 270 mm) using H₂O:MeOH (1:1-0:1) as the eluent to yield ten fractions (6A-6J). The methanol-soluble of fraction 6E (11.0 mg) was then further purified by HPLC [Cosmosil 5C18-AR-II; ϕ 10 x 250 mm; 45% MeCN] to obtain **27** (1.4 mg). The BuOH fraction (2.8 g) was then subjected to ODS column chromatography (ϕ 30 x 270 mm) with H₂O:MeOH (9:1-1:1) and yielded fractions 8A-8I. Fraction 8D (92 mg) was subjected to HPLC [Cosmosil 5C18-AR-II; ϕ 10 x 250 mm; 30% MeOH] to afford **28** (t_R =16 min; 30.8 mg). Fraction 8G (30.2 mg) was further purified by ODS column chromatography (ϕ 230 x 120 mm) using 50% MeOH to yield compound **29** (9.0 mg).

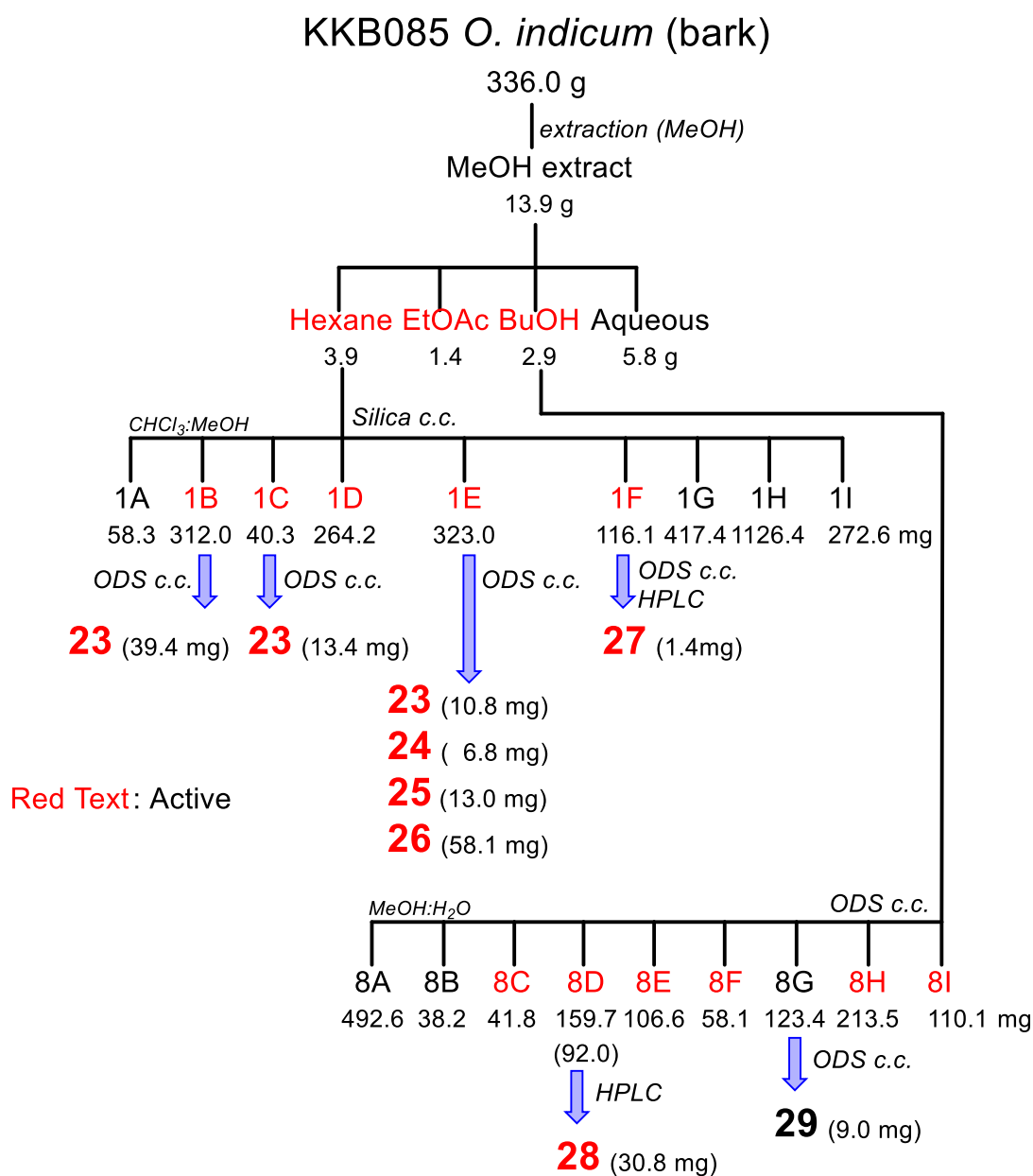


Figure 11.2. Isolation scheme of *O. indicum*

11.3. Characterization of the isolated compounds

Activity-guided multistep separation using chromatographic techniques (silica, ODS and HPLC) led to the isolation of six known flavonoids (**23-28**), and a phenyl ethyl glycoside (**29**). Their structures were identified by comparing their spectral values with those in literatures.

Oroxylin A (23)⁷

¹H and ¹³C NMR see Table 11.1; ESI-MS: m/z 284 [M+H]⁺

Chrysin (24)⁸

¹H and ¹³C NMR see Table 11.1; ESI-MS: m/z 253 [M+H]⁺

Hispidulin (25)⁹

¹H and ¹³C NMR see Table 11.1; ESI-MS m/z 270 [M+H]⁺

Baicalein (26)¹⁰

¹H and ¹³C NMR see Table 11.2; ESIMS: m/z 269 [M+H]⁺

Apigenin (27)¹¹

¹H and ¹³C NMR see Table 11.2; ESIMS: m/z 269 [M+H]⁺

Baicalin (28)¹²

¹H and ¹³C NMR see Table 11.2; ESIMS: m/z 445 [M-H]⁺

Verbascoside (29)¹³

¹H and ¹³C NMR see Table 11.3; ESIMS: m/z 623 [M-H]⁻

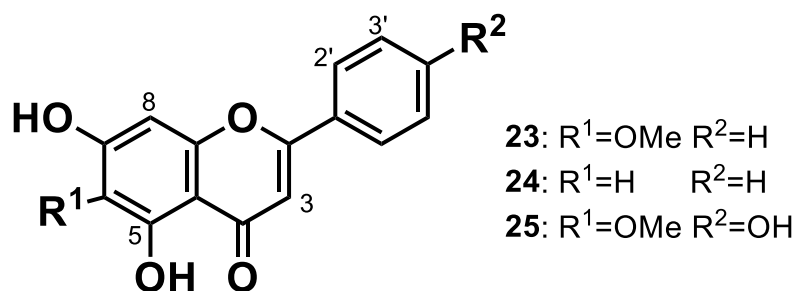


Table 11.1. NMR spectroscopic data of compounds **23**, **24** and **25** (DMSO-*d*₆, 400 MHz).

Position	23		24		25
	¹ H (δ, ppm; <i>J</i> , Hz)	¹³ C (δ, ppm)	¹ H (δ, ppm; <i>J</i> , Hz)		¹ H (δ, ppm; <i>J</i> , Hz)
1					
2		163.2			
3	5.61 (1H, s)	104.8	6.96 (1H, s)		6.58 (1H, s)
4		182.2			
5		152.6			
6		94.4	6.21 (1H, d, 2.4)		
7		157.8			
8	6.96 (1H, s)	130.8	6.52 (1H, d, 2.4)		6.77 (1H, s)
9		152.7			
10		104.4			
1'		131.5			
2'	8.06 (1H, d, 6.8)	126.4	8.05-8.07 (1H, m)		7.92 (1H, d, 8.6)
3'	7.62-7.55 (1H, m)	129.1	7.54-7.63 (1H, m)		6.91 (1H, d, 8.6)
4'	7.62-7.55 (1H, m)	132.0	7.54-7.63 (1H, m)		
5'	7.62-7.55 (1H, m)	129.1	7.54-7.63 (1H, m)		6.91 (1H, d, 8.6)
6'	8.06 (1H, d, 6.8)	126.4	8.05-8.07 (1H, m)		7.92 (1H, d, 8.6)
6-OMe	3.75 (3H, s)	59.9			3.74 (3H, s)
5-OH	12.92 (1H, s)		12.82 (1H, s)		13.07 (1H, s)
7-OH					10.70 (1H, s)
4'-OH					10.35 (1H, s)

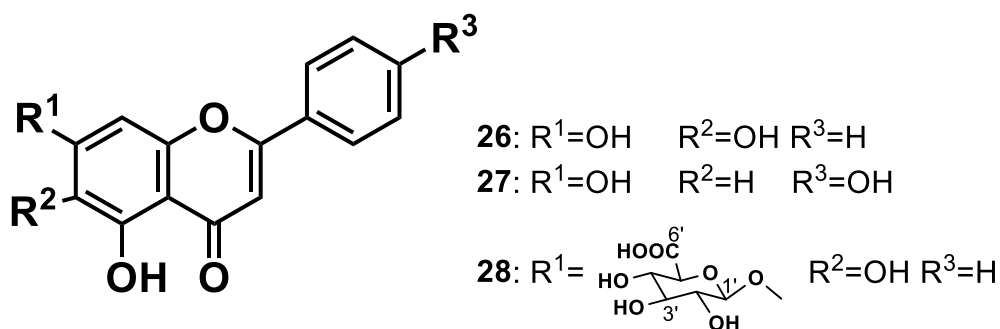


Table 11.2. NMR spectroscopic data of compounds **26**, **27**, and **28** (DMSO-*d*₆).

Position	26 (400 MHz)	27 (400 MHz)	28 (600 MHz)	
	¹ H (δ, ppm; <i>J</i> , Hz)	¹ H (δ, ppm; <i>J</i> , Hz)	¹ H (δ, ppm; <i>J</i> , Hz)	¹³ C (δ, ppm)
1				163.68
2				106.28
3	6.92 (1H, s)	6.55 (1H, s)	7.03 (1H, s)	182.78
4				146.81
5				130.02
6		6.15 (1H, d, 2)		154.94
7				94.49
8	6.62 (1H, d, 2.4)	6.40 (1H, d, 2)	6.98 (1H, s)	149.40
9				104.88
10				131.02
1'				126.58
2'	8.03 (1H, dd, 8.1, 1.1)	7.82 (1H, d, 8.8)	8.06 (1H, d, 8.4)	129.39
3'	7.58 (1H, m)	6.90 (1H, d, 8.8)	7.58 (1H, m)	132.23
4'	7.58 (1H, m)		7.58 (1H, m)	129.39
5'	7.58 (1H, m)	6.90 (1H, d, 8.8)	7.58 (1H, m)	126.58
6'	8.03 (1H, dd, 8.1, 1.1)	7.82 (1H, d, 8.8)	8.06 (1H, d, 8.4)	
5-OH	12.65 (1H, s)			
6-OH	8.80 (1H, s)			
7-OH	10.56 (1H, s)			
4'-OH				
<i>Glucoronide</i>				
1''			5.02 (1H, d, 7.2)	100.92
2''			3.22 (1H, m)	73.15
3''			3.22 (1H, m)	74.49
4''			3.22 (1H, m)	72.12
5''			3.64 (1H, d, 9.6)	76.02
6''				171.32

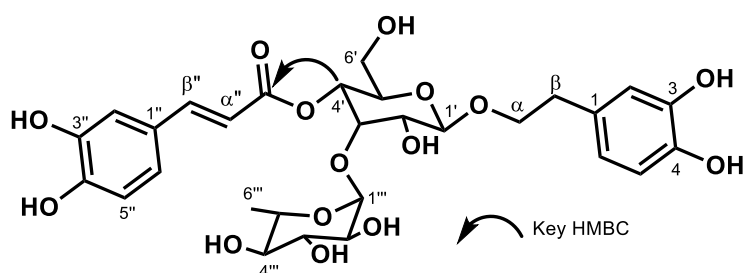


Table 11.3. NMR spectroscopic data of compound **29** (in CD₃OD, 600 MHz).

Position	29	
	¹ H (δ, ppm; <i>J</i> , Hz)	¹³ C (δ, ppm)
1		131.5
2	6.64 (1H, d, 1.8)	116.3
3		144.7
4		146.1
5	6.62 (1H, d, 8.1)	117.1
6	6.52 (1H, dd, 8.1, 1.8)	121.3
α	4.00 (1H, m)	72.4
β	3.67 (1H, m)	
	2.75 (2H, m)	36.6
<i>Glucose</i>		
1'	4.33 (1H, d, 7.2)	104.2
2'	3.57 (1H, m)	76.2
3'	3.50 (1H, m)	81.2
4'	4.85 (1H, m)	70.4
5'	3.65 (1H, m)	76.1
6'	3.87 (1H, m)	62.4
	3.69 (1H, m)	
<i>Caffeoyl</i>		
1''		127.7
2''	7.01 (1H, d, 2.1)	115.2
3''		148.0
4''		149.8
5''	6.73 (1H, d, 8.4)	116.5
6''	6.23 (1H, dd, 8.4, 2.1)	123.2
α''	6.23 (1H, d, 15.6)	114.7
β''	7.55 (1H, d, 15.6)	146.8
C=O		168.3
<i>Rhamnose</i>		
1'''	5.14 (1H, d, 1.2)	103.0
2'''	3.77 (1H, t, 18.6)	72.3
3'''	3.34 (1H, m)	72.1
4'''	3.25 (1H, m)	73.8
5'''	3.65 (1H, m)	70.6
6'''	1.04 (3H, d, 6)	18.4

11.4. Ngn2 promoter activity of compounds 23-28

The Ngn2 promoter activity of compounds **23-28** were determined based on concentration- and time-dependence. Compound **29** was not subjected to further assay as it was isolated from an inactive fraction. Result showed that all compounds were dose-dependent, that is, high activity is observed at high concentration (Figure 11.3). However, it is observed that at high concentration, their activities reached a plateau. Oroxylin A (**23**) and hispidulin (**25**) reached their highest activity at 10 μ M while chrysin (**24**) at 15 μ M. Oroxylin A (**23**) increased Ngn2 promoter activity by 2.6 folds while hispidulin (**25**) by 2.4 folds. Chrysin (**24**) exhibited 2.4-fold increase in activity. Baicalein (**26**) and apigenin (**27**) also induced Ngn2 promoter activity by 201% and 170%, respectively at 15 μ M. On the other hand, Baicalin (**28**) showed the weakest activity as their highest activity of 181% and 136%, respectively, was observed at 200 μ M. In the time-dependent activity, all compounds showed a time-dependent biphasic response (Figure 11.4). Their highest activity was observed after 24 h, but decreased after 48 h treatment.

11.5. Neuronal differentiation activity of 23

The neuronal differentiation activity of **23** was then determined using the multipotent cell line, MEB5 cells. Figure 11.5 shows MEB5 cells with or without **23** stained with TUJ1 (neuron marker), GFAP (astrocyte marker), and TO-PRO (nucleus marker). Immunostaining revealed that more neurons with a neurite length of about 200 μ m were observed in MEB5 cells treated with **23** as compared to control. The results suggested that **23** resulted in neuronal population with longer neurites. This means that **23** had neuronal differentiation activity. Compound **23** had been reported to induce adult neurogenesis in the hippocampal dentate gyrus region of mice.¹⁴ Possibly, induction of

the Ngn2 promoter by **23** may have participated in the stimulation of the neuronal differentiation.

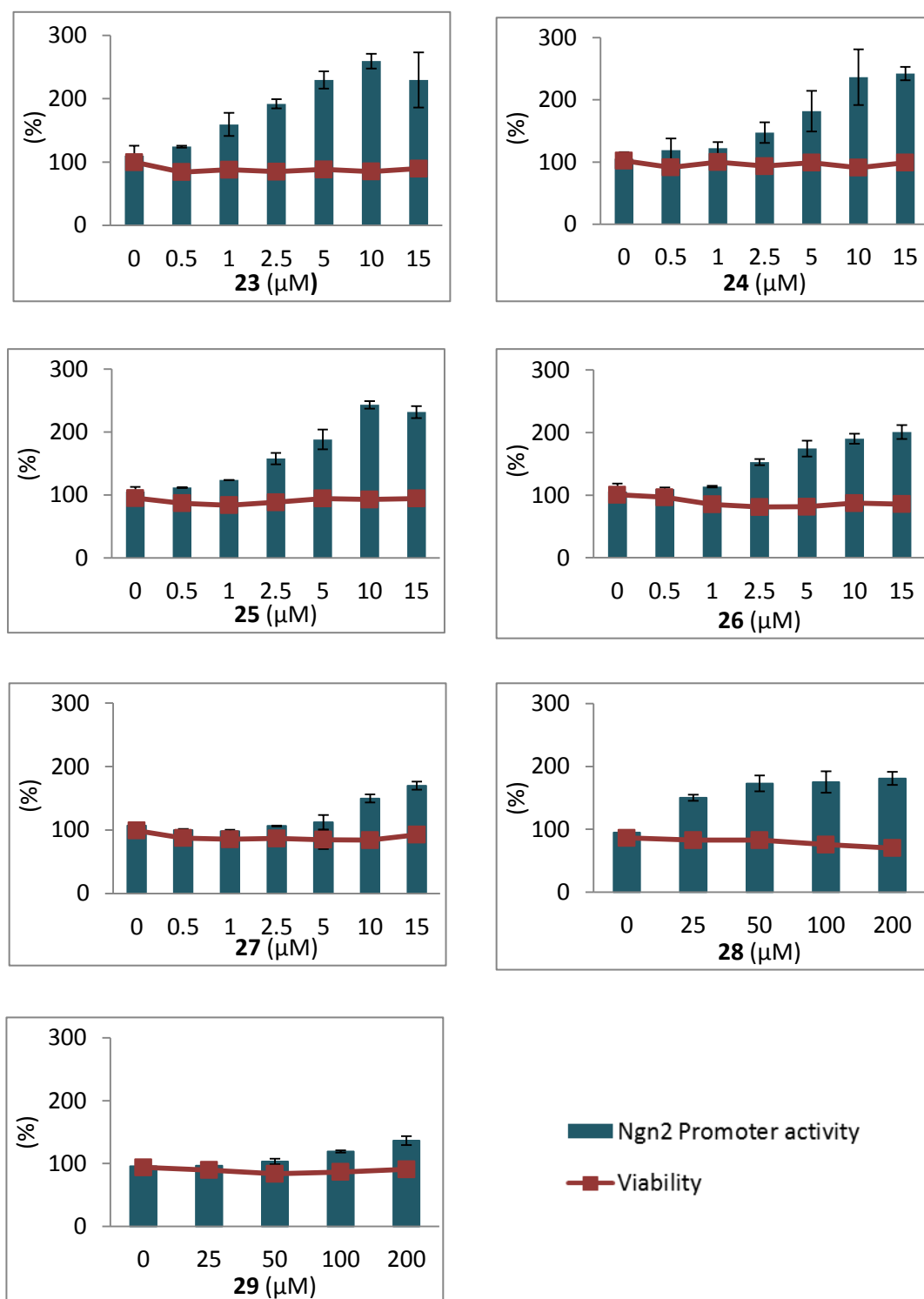


Figure 11.3. Concentration-dependent Ngn2 promoter activity of compounds **23-29**.

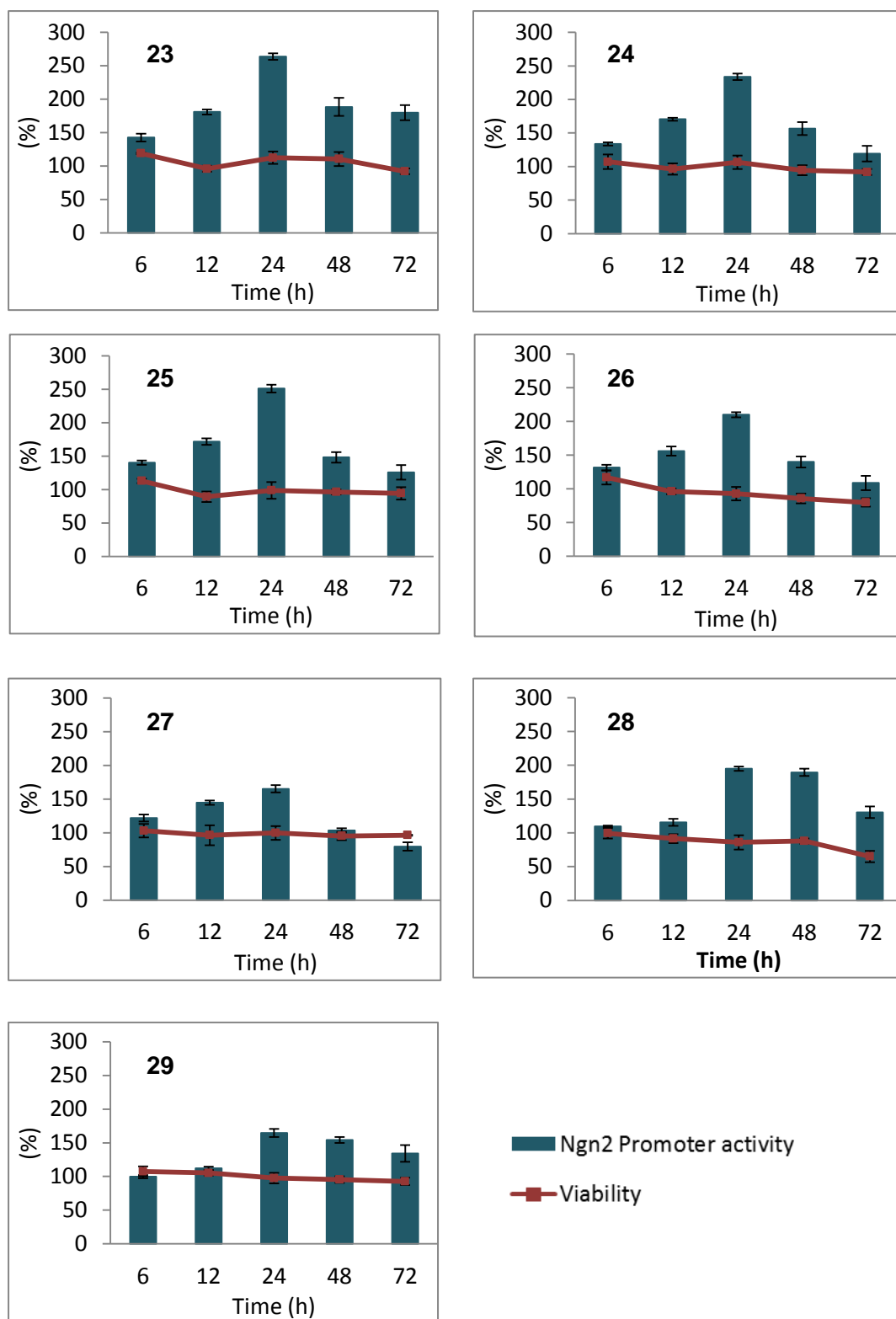


Figure 11.4. Time-dependent Ngn2 promoter activity of compounds **23-29**.

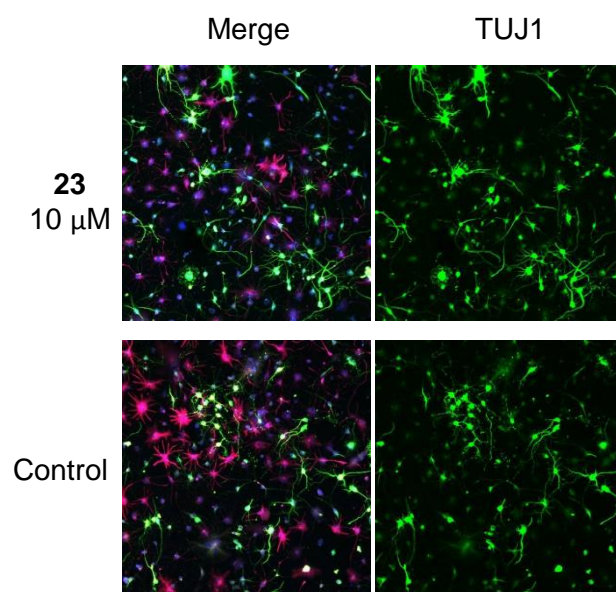


Figure 11.5. Neuronal differentiation activity of **23** using MEB5 cells.
 TUJ1 (Green): Neurons; GFAP (Red):Astrocytes;
 TO-PRO (blue):Nucleus.

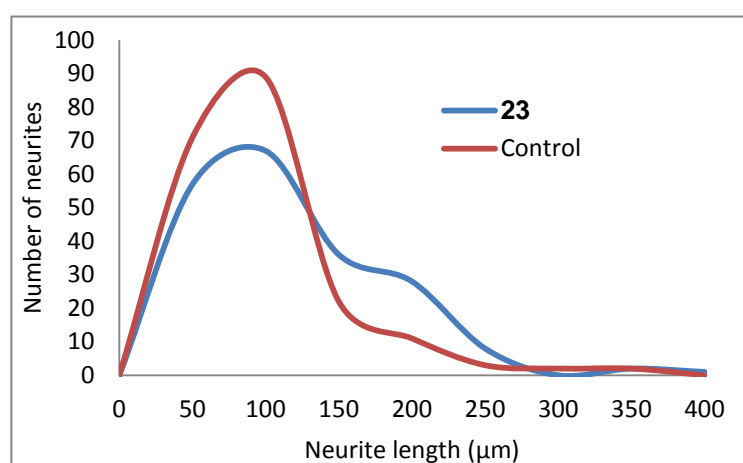


Figure 11.6. Histogram of neurite length of MEB5 treated with **23** for 4 d.

References

1. Harminder; Singh, V.; Chaudhary, A. K., A Review on the Taxonomy, Ethnobotany, Chemistry and Pharmacology of *Oroxylum indicum* Vent. *Indian J. Pharm. Sci.* **2011**, 73, 483-490.
2. Mat Ali, R.; Houghton, P. J.; Raman, A.; Hoult, J. R. S., Antimicrobial and antiinflammatory activities of extracts and constituents of *Oroxylum indicum* (L.) Vent. *Phytomedicine* **1998**, 5, 375-381.
3. Nakahara, K.; Onishi-Kameyama, M.; Ono, H.; Yoshida, M.; Trakoontivakorn, G., Antimutagenic activity against trp-P-1 of the edible Thai plant, *Oroxylum indicum* vent. *Biosci. Biotechnol. Biochem.* **2001**, 65, 2358-2360.
4. Mishra, S. L.; Sinhamahapatra, P. K.; Nayak, A.; Das, R.; Sannigrahi, S., In vitro Antioxidant Potential of Different Parts of *Oroxylum indicum*: A Comparative Study. *Indian J. Pharm. Sci.* **2010**, 72, 267-269.
5. Roy, M. K.; Nakahara, K.; Na, T. V.; Trakoontivakorn, G.; Takenaka, M.; Isobe, S.; Tsushida, T., Baicalein, a flavonoid extracted from a methanolic extract of *Oroxylum indicum* inhibits proliferation of a cancer cell line in vitro via induction of apoptosis. *Pharmazie* **2007**, 62, 149-153.
6. Koryudzu, K. *Butea superba* 等からの神経幹細胞分化活性化剤の探索. Chiba University, Chiba, Japan, **2013**.
7. Kim, D. H.; Jeon, S. J.; Son, K. H.; Jung, J. W.; Lee, S.; Yoon, B. H.; Lee, J. J.; Cho, Y. W.; Cheong, J. H.; Ko, K. H.; Ryu, J. H., The ameliorating effect of oroxylin A on scopolamine-induced memory impairment in mice. *Neurobiol. Learn. Mem.* **2007**, 87, 536-46.
8. Zeng, Y. B.; Yang, N.; Liu, W. S.; Tang, N., Synthesis, characterization and DNA-binding properties of La(III) complex of chrysin. *J. Inorg. Biochem.* **2003**, 97, 258-264.
9. Nazaruk, J.; Gudej, J., Flavonoid compounds from the flowers of *Cirsium rivulare* (Jacq.) All. *Acta Pol. Pharm.* **2003**, 60, 87-9.
10. Pegg, R. B.; Amarowicz, R.; Oszmiański, J., Confirming the chemical structure of antioxidative trihydroxyflavones from *Scutellaria baicalensis* using modern spectroscopic methods. *Pol. J. Food Nutr. Sci.* **2005**, 14/55, 43-50.
11. Ahn, D.; Lee, S. I.; Yang, J. H.; Cho, C. H.; Hwang, Y.-H.; Park, J.-H.; Kim, D. K., Superoxide radical scavengers from the whole plant of *Veronica peregrina*. *Nat. Prod. Sci.* **2011**, 17, 142-146.
12. Yuan, Y.; Hou, W.; Tang, M.; Luo, H.; Chen, L.-J.; Guan, Y. H.; Sutherland, I. A., Separation of Flavonoids from the Leaves of *Oroxylum indicum* by HSCCC. *Chromatographia* **2008**, 68, 885-892.

13. Olivier, D. K.; Shikanga, E. A.; Combrinck, S.; Krause, R. W. M.; Regnier, T.; Dlamini, T. P., Phenylethanoid glycosides from *Lippia javanica*. *S. Afr. J. Bot.* **2010**, 76, 58-63.
14. Lee, S.; Kim, D. H.; Lee, D. H.; Jeon, S. J.; Lee, C. H.; Son, K. H.; Jung, J. W.; Shin, C. Y.; Ryu, J. H., Oroxylin A, a flavonoid, stimulates adult neurogenesis in the hippocampal dentate gyrus region of mice. *Neurochem. Res.* **2010**, 35, 1725-1732.

CHAPTER 12

Ngn2 Promoter activity of Longistylin C isolated from *Cajanus cajan*

12.1. Plant Description

Cajanus cajan belongs to the family Fabaceae. It is reported to have antioxidant and antiinflammatory,¹ antiplasmodial,² and neuroprotective³ properties. Some of the isolated compounds reported from this plant are cajanol, longistylin A and longistylin C.² In this study, the leaves were used and the sample was collected from Bangladesh. During the screening activity, the MeOH extract of *C. cajan* enhanced Ngn2 promoter activity by 200% at 100 µg/mL. After removal of the chlorophyll content by Diaion HP20, fraction 1A was observed to have similar induction activity and was subjected to further isolation.

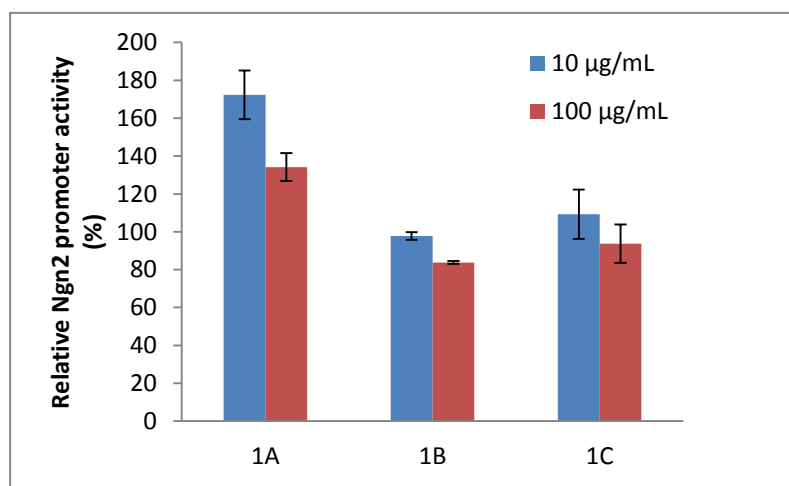


Figure 12.1. Ngn2 promoter activity of the 1 series.

12.2. Isolation of the constituents

Figure 12.2 shows the isolation scheme of *C. cajan*. The dried leaves of *C. cajan* (145 g) were extracted in MeOH and yielded 7.6 g of crude MeOH extract. The chlorophyll content was removed using Diaion HP20 column chromatography (φ50 x 270 mm) using MeOH:Acetone (1:0-0:1) to give fractions 1A-1C. Fraction 1A (6.7 g) eluted using 100% MeOH was re-suspended in 10% MeOH (300 mL) and partitioned between *n*-hexane, EtOAc, and *n*-BuOH (300 mL x 3) to afford the hexane extract (1.9 g), EtOAc extract (0.6 g), BuOH extract (2.0 g) and the water-soluble extract (2.3 g). The combined fractions of the hexane and EtOAc layers were subjected to silica column chromatography (φ50 x 240 mm) using CHCl₃:MeOH (1:0-0:0.1% TFA in MeOH) to give eleven fractions (2A-2K). Fraction 2D was then further purified by HPLC [Cosmosil 5C18-AR-II; φ10 x 250 mm; 80% MeOH] to afford fractions 3A-3D in which 3B was identified as **30** (*t*_R=35.4 min 3.1 mg). Fraction 3A was again subjected to HPLC [Phenomenex Luna 5u Phenyl-Hexyl; φ10 x 250 mm; 80% MeOH] and give **31** (*t*_R=31 min 7.6 mg).

12.3. Characterization of the isolated compounds

Activity-guided multistep separation using chromatographic techniques (silica, ODS and HPLC) led to the isolation of two known compounds (**31-32**). Their structures were identified by comparing their spectral values with those in literatures.

Longistylin C (**31**)²

¹H and ¹³C NMR see Table 12.1; ESI-MS: *m/z* 293 [M-H]⁻

Pinostrobin (**32**)⁴

¹H and ¹³C NMR see Table 12.2; ESI-MS: *m/z* 269 [M-H]⁻

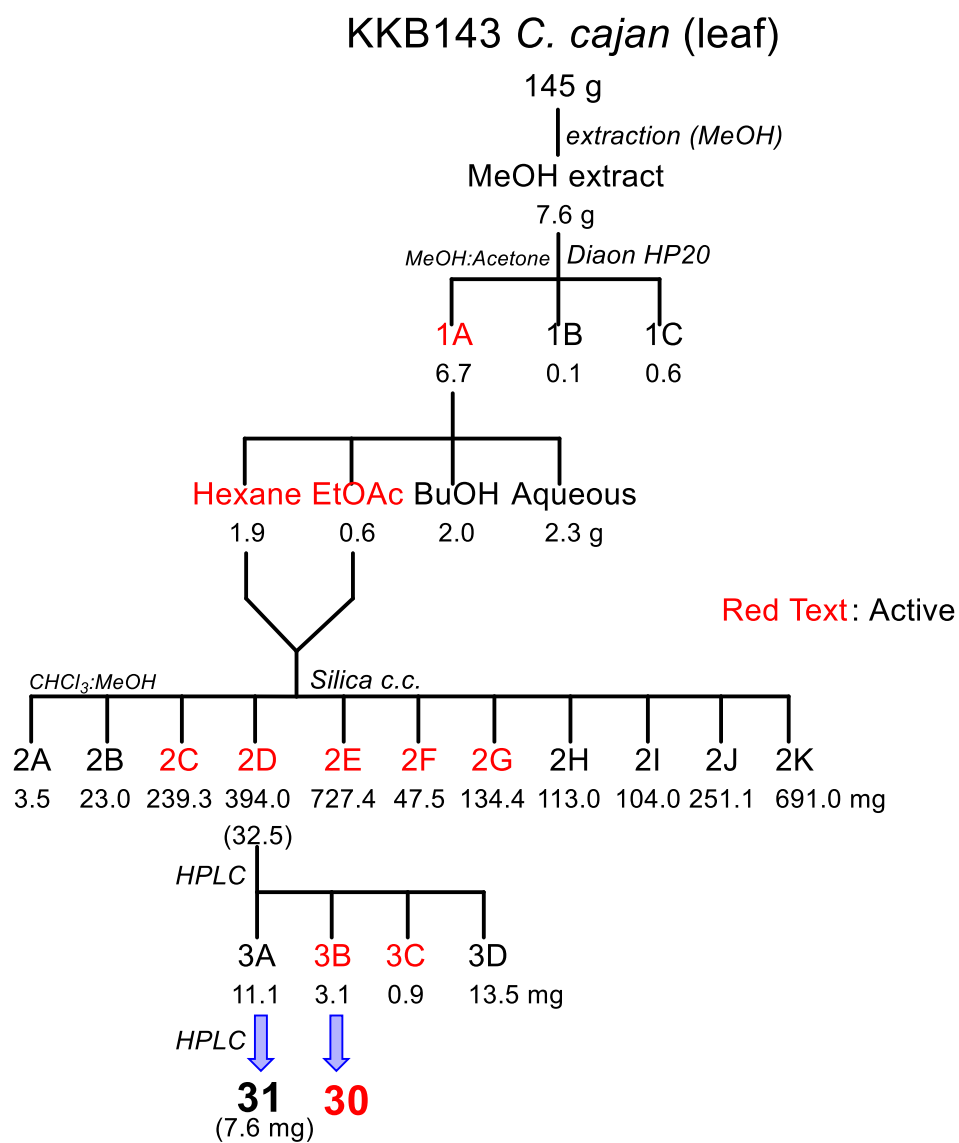


Figure 12.2. Isolation scheme of *C. cajan*.

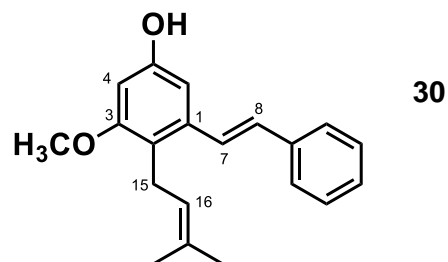


Table 12.1. NMR spectroscopic data of compound **30** (in CDCl₃).

Position	30	
	¹ H (δ, ppm; <i>J</i> , Hz) (400 MHz)	¹³ C (δ, ppm) (150 MHz)
1		137.3
2		115.0
3		158.1
4	6.62 (1H, d, 1.6)	101.6
5		155.5
6	6.64 (1H, d, 1.6)	107.0
7	6.98 (1H, d, 16)	128.4
8	7.03 (1H, d, 16)	128.4
9		136.6
10	7.48 (1H, m)	126.5
11	7.33 (1H, m)	128.7
12	7.33 (1H, m)	127.6
13	7.33 (1H, m)	128.7
14	7.48 (1H, m)	126.5
15	3.39 (2H, d, 4.4)	22.4
16	5.22 (1H, t, 7.2)	121.8
17		134.5
18	1.80 (3H, s)	17.9
19	1.72 (3H, s)	25.8
3-OCH ₃	3.87 (3H, s)	55.8

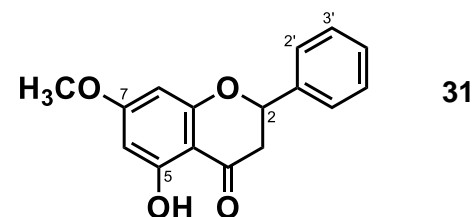


Table 12.1. NMR spectroscopic data of compound **31** (in CDCl₃).

Position	31	
	¹ H (δ, ppm; <i>J</i> , Hz) (400 MHz)	¹³ C (δ, ppm) (150 MHz)
1		
2	5.41 (1H, dd, 12, 2.8)	79.2
3	3.07 (1H, dd, 17.2, 12.8) 2.81 (1H, dd, 17, 3)	43.4
4		195.8
5		162.8
6	6.06 (1H, d, 3.2)	95.1
7		168.0
8	6.06 (1H, d, 3.2)	94.2
9		164.1
10		103.1
1'		138.4
2'	7.40 (1H, m)	126.1
3'	7.40 (1H, m)	126.1
4'	7.40 (1H, m)	128.9
5'	7.40 (1H, m)	126.1
6'	7.40 (1H, m)	126.1
5-OH	12.00 (1H, brs)	
7-OCH ₃	3.80 (3H, s)	55.7

12.4. Ngn2 promoter activity of longistylin C (30)

Figure 12.2 shows the Ngn2 promoter activity of longistylin C (**30**). It is observed that it enhanced the Ngn2 promoter activity in a dose-dependent manner. However, it was also shown that at 10 μM , it started to reach its highest activity (180%), and its activity became almost unchanged. The result suggested that longistylin C may be a potent compound that can enhance neuronal differentiation. On the other hand, pinostrobin (**31**) was inactive.

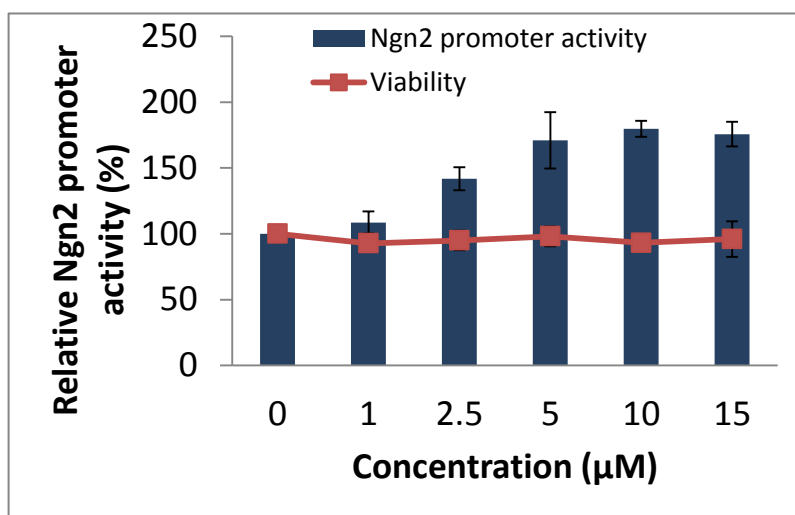


Figure 12.3. Dose-dependent Ngn2 promoter activity of **30**.

References

1. Lai, Y.-S.; Hsu, W.-H.; Huang, J.-J.; Wu, S.-C., Antioxidant and anti-inflammatory effects of pigeon pea (*Cajanus cajan* L.) extracts on hydrogen peroxide- and lipopolysaccharide-treated RAW264.7 macrophages. *Food Func.* **2012**, 3, 1294-1301.
2. Duker-Eshun, G.; Jaroszewski, J. W.; Asomaning, W. A.; Oppong-Boachie, F.; Brøgger Christensen, S., Antiplasmodial constituents of *Cajanus cajan*. *Phytother. Res.* **2004**, 18, 128-30.
3. Ruan, C. J.; Si, J. Y.; Zhang, L.; Chen, D. H.; Du, G. H.; Su, L., Protective effect of stilbenes containing extract-fraction from *Cajanus cajan* L. on Abeta(25-35)-induced cognitive deficits in mice. *Neurosci. Lett.* **2009**, 467, 159-63.
4. Ching, A. Y. L.; Wah, T. S.; Sukari, M. A.; Lian, G. E. C.; Rahmani, M.; Khalid, K., Characterization of flavonoid derivatives from *Boesenbergia rotunda* (L.) *The Malaysian Journal of Analytical Sciences* **2007**, 11, 154-159.

CHAPTER 13

Summary and Conclusion

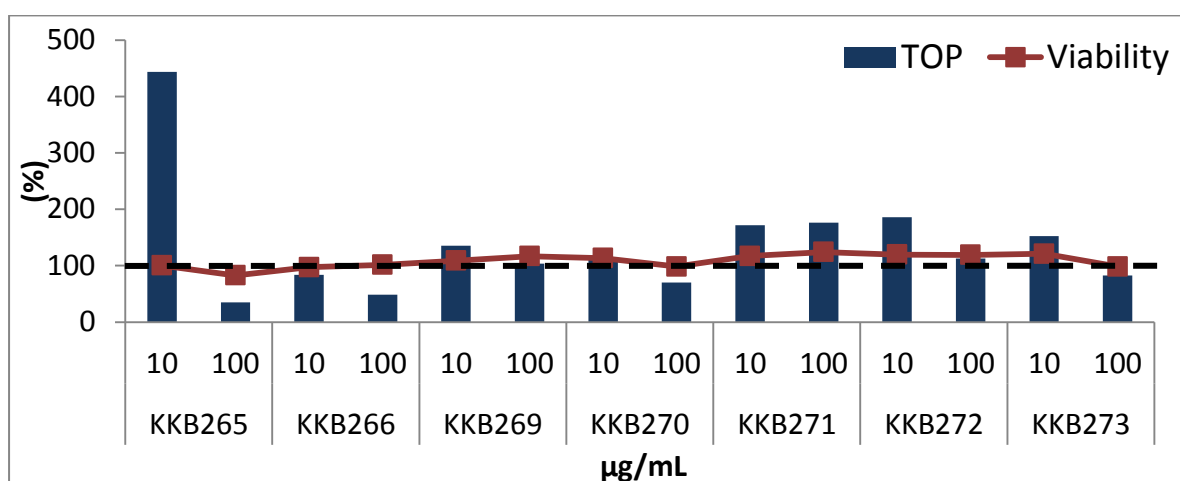
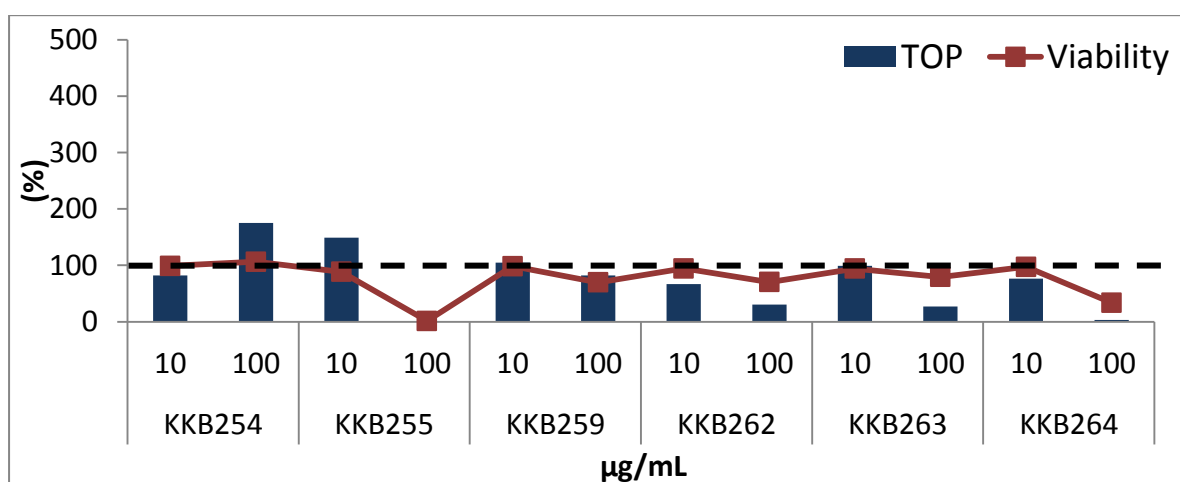
Differentiation of neural stem cells (NSCs) is controlled by many basic helix-loop-helix (bHLH) factors. Ngn2, a bHLH activator promotes the differentiation of NSCs to neurons. However, in undifferentiated cells its expression is inhibited by the repressor type of bHLH such as Hes1. Neuronal differentiation occurs when the level of proneural gene Ngn2 is sustained. In this study, we aim to discover natural compounds that would enhance neuronal differentiation of NSCs by enhancing the activity of Ngn2.

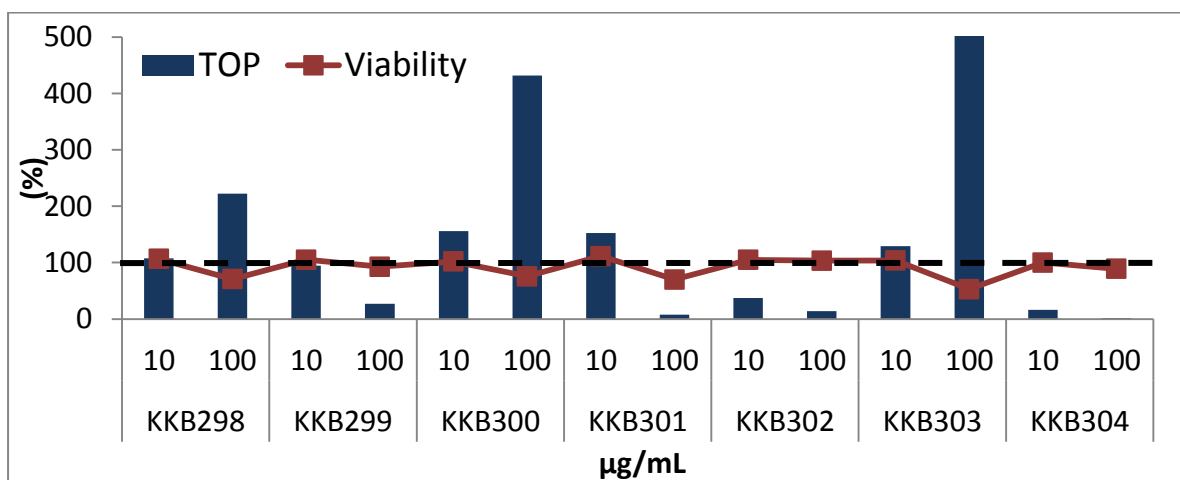
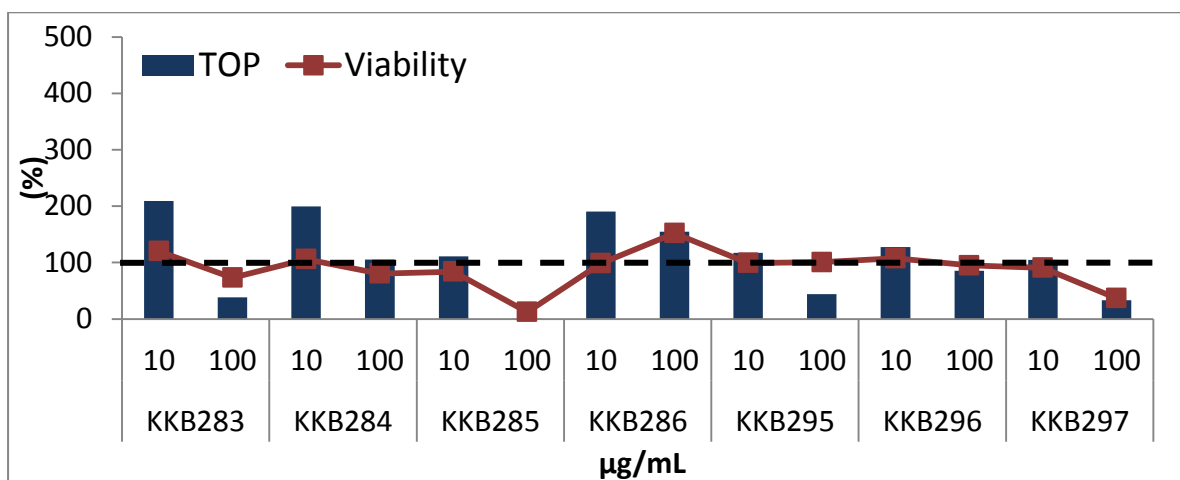
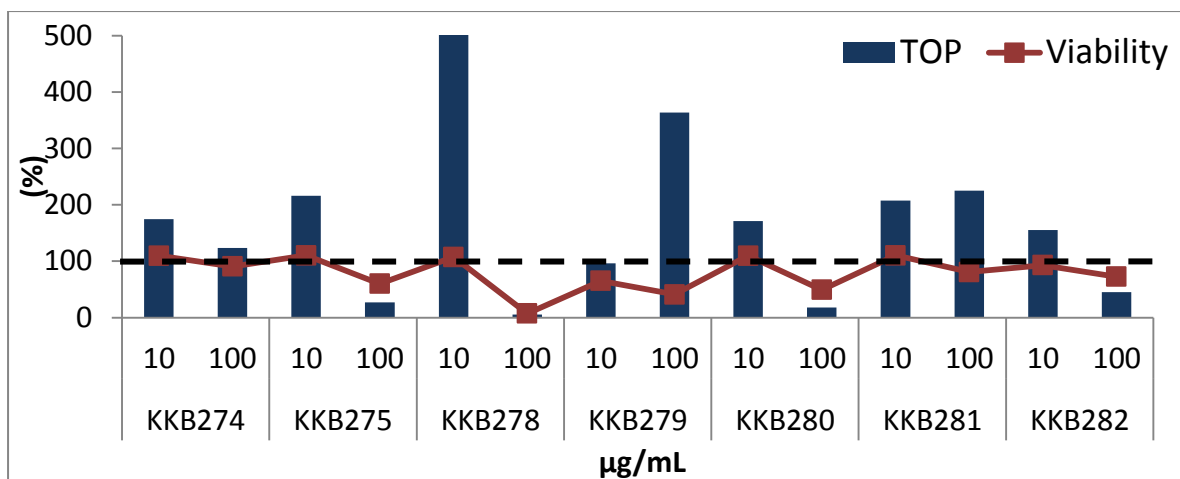
The Ngn2 promoter activity was evaluated using a cell-based luciferase assay system in which C3H10T1//2 were stably transfected with a plasmid containing an Ngn2 promoter. Using this assay, we identified KKB085 *Oroxylum indicum* and KKB143 *Cajanus cajan* to induce Ngn2 promoter activity. Activity-guided multistep separation using chromatographic techniques led to the isolation of seven known flavonoids (**23-28**), and one phenyl ethyl glycoside (**29**) from *O. indicum*; and a stilbene (**30**) and one flavonoid (**31**) from *C. cajan*. Compounds **23-26** and **31** showed the highest Ngn2 promoter activity. As compared with control, compound **23** increased the number of neurons with longer neurite using MEB5 cells. The results suggested that **23** could induce neuronal differentiation by increasing the Ngn2 promoter activity.

APPENDICES

APPENDIX I

Screening of the KKB Plant Extracts (TOP Assay)





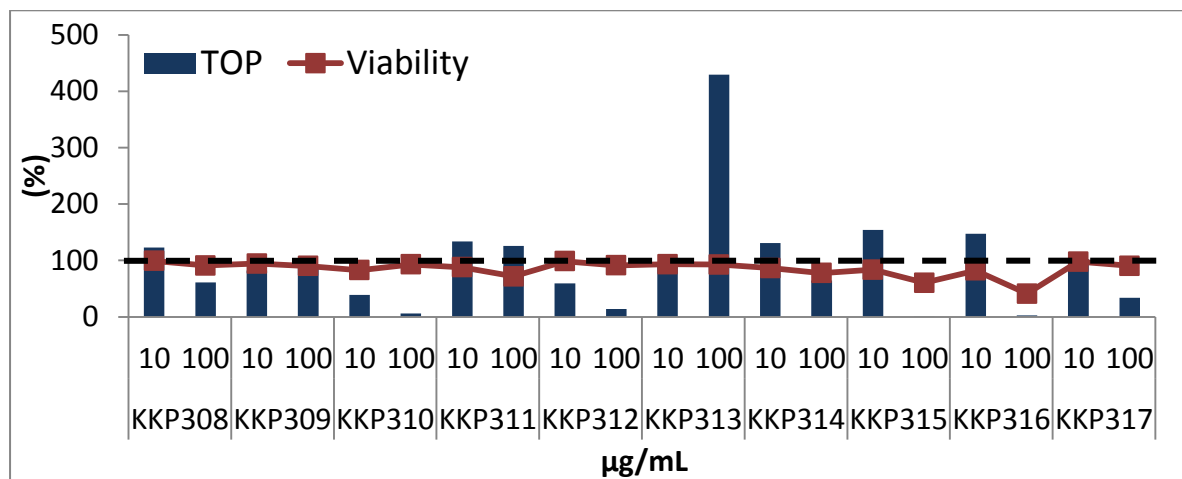
APPENDIX II

List of Screened KKB Plant Extracts (TOP Assay)

KKB NO.	SCIENTIFIC NAME	FAMILY	PLANT PART USED
KKB0254	<i>Xanthium strumarium</i>	Asteraceae	Stem
KKB0255	<i>Xanthium strumarium</i>	Asteraceae	Leaves
KKB0259	<i>Madhuca longifolia</i>	Sapotaceae	Leaves
KKB0262	<i>Solanum surattense</i>	Solanaceae	Fruit
KKB0263	<i>Solanum surattense</i>	Solanaceae	Leaves
KKB0264	<i>Phyllanthus reticulatus</i>	Phyllanthaceae	Stem
KKB0265	<i>Odina wodier</i> Roxb.	Anacardiaceae	Bark
KKB0266	<i>Sansevieria</i> sp.	Ruscaceae	Whole plant
KKB0269	<i>Acacia mangium</i>	Fabaceae	Leaves
KKB0270	<i>Tabernaemontana divaricata</i>	Apocynaceae	Aerial parts
KKB0271	<i>Jasminum</i> spp.	Oleaceae	Aerial parts
KKB0272	<i>Randia</i> spp.	Rubiaceae	Aerial parts
KKB0273	<i>Flacourtia</i> spp.	Flacourtiaceae	Aerial parts
KKB0274	<i>Syzygium cumini</i>	Myrtaceae	Leaves
KKB0275	<i>Suregada multiflora</i>	Euphorbiaceae	Aerial parts
KKB0278	<i>Croton</i> spp.	Euphorbiaceae	Leaves
KKB0279	<i>Semecarpus anacardium</i>	Anacardiaceae	Leaves
KKB0280	<i>Syzygium fruticosum</i>	Myrtaceae	Leaves
KKB0281	<i>Hollarhena</i> spp.	Apocynaceae	Leaves
KKB0282	<i>Mucuna</i> spp.	Fabaceae	Leaves
KKB0283	<i>Bridelia</i> spp.	Euphorbiaceae	Leaves
KKB0284	<i>Microcos paniculata</i>	Malvaceae	Aerial parts
KKB0285	<i>Terminalia bellirica</i>	Combretaceae	Leaves
KKB0286	<i>Dalbergia</i> spp.	Fabaceae	Aerial parts
KKB0295	<i>Evolvulus nummularias</i>	Convolvulaceae	Aerial parts
KKB0296	<i>Leea indica</i>	Leeaceae	Aerial parts
KKB0297	<i>Phyla nudiflora</i>	Verbanaceae	Aerial parts
KKB0298	<i>Hibiscus sabdariffa</i>	Malvaceae	Aerial parts
KKB0299	<i>Ecbolium linneanum</i> <i>Justicia ecbolia</i>	Acanthaceae	Aerial parts

APPENDIX III

Screening of the KKP Plant Extracts (TOP Assay)



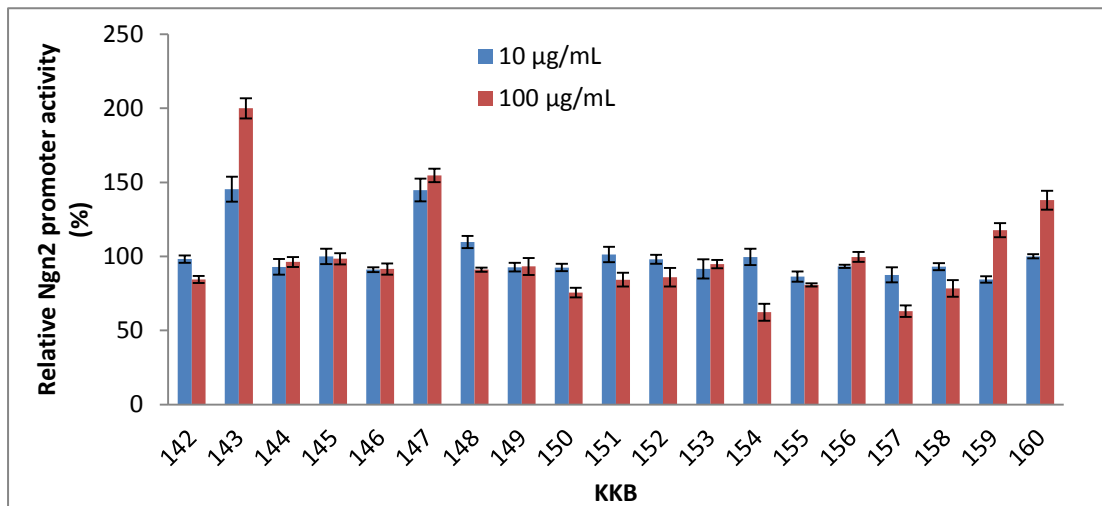
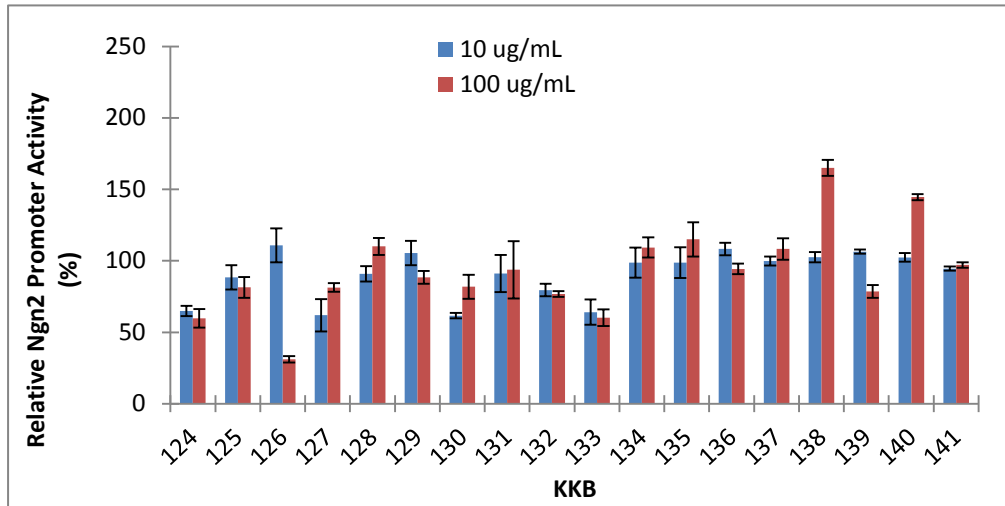
APPENDIX IV

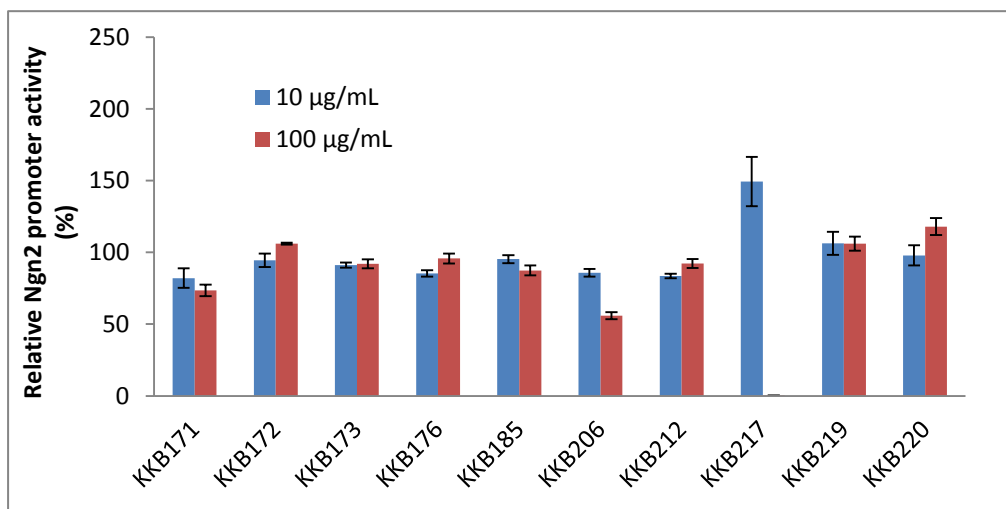
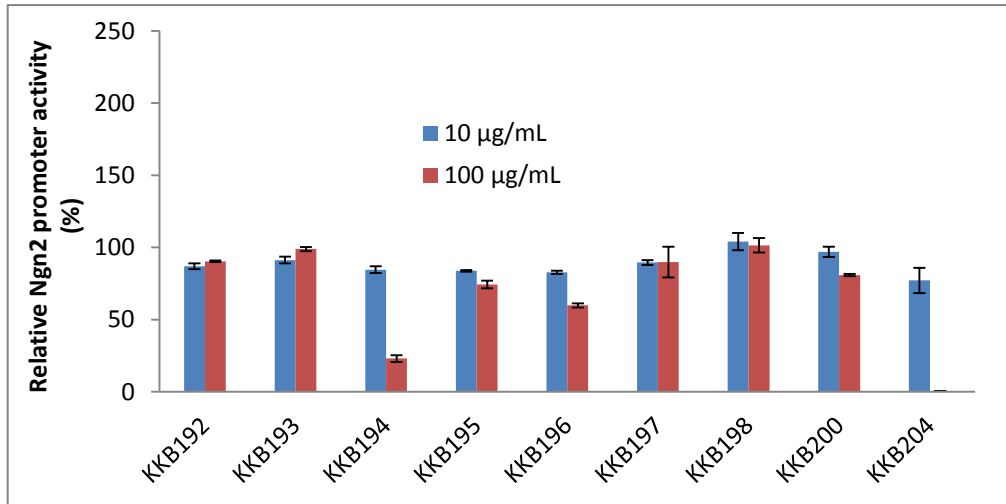
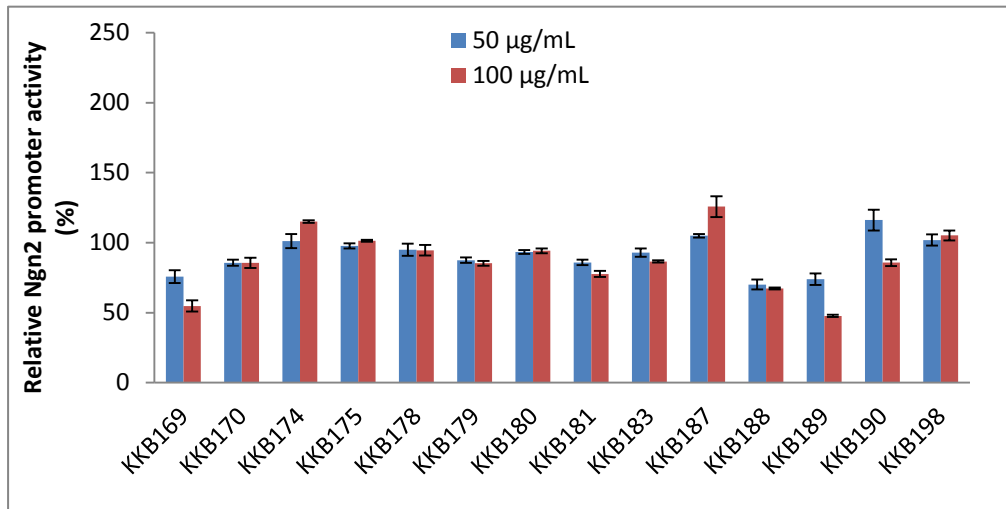
List of Screened KKP Plant Extracts (TOP Assay)

KKB NO.	SCIENTIFIC NAME	FAMILY	PLANT PART USED
KKP308	<i>Aegle marmelos</i>	Rutaceae	leaf
KKP309	<i>Citrus maxima</i>	Rutaceae	peel
KKP310	<i>Clausena lansium</i>	Rutaceae	leaf
KKP311	<i>Clausena harmandiana</i>	Rutaceae	leaf
KKP312	<i>Murraya paniculata</i>	Rutaceae	leaf
KKP313	<i>Toddalia aculeata</i>	Rutaceae	leaf
KKP314	<i>Picrasma javanica</i>	Simaroubaceae	leaf
KKP315	<i>Eurycoma longifolia</i>	Simaroubaceae	root
KKP316	<i>Canarium album</i>	Burseraceae	leaf
KKP317	<i>Canarium album</i>	Burseraceae	fruit
KKP318	<i>Alpinia oxymitra</i>	Zingiberaceae	rhizome

APPENDIX V

Screening of the KKB Plant Extracts (Ngn2 Promoter Activity)





APPENDIX VI

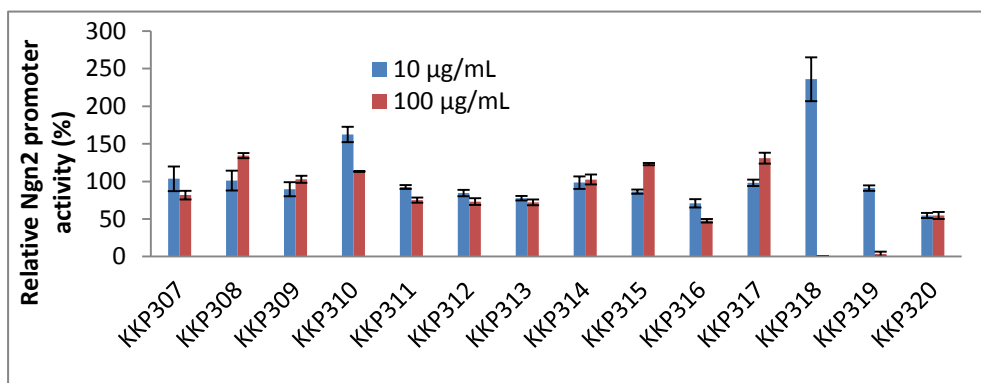
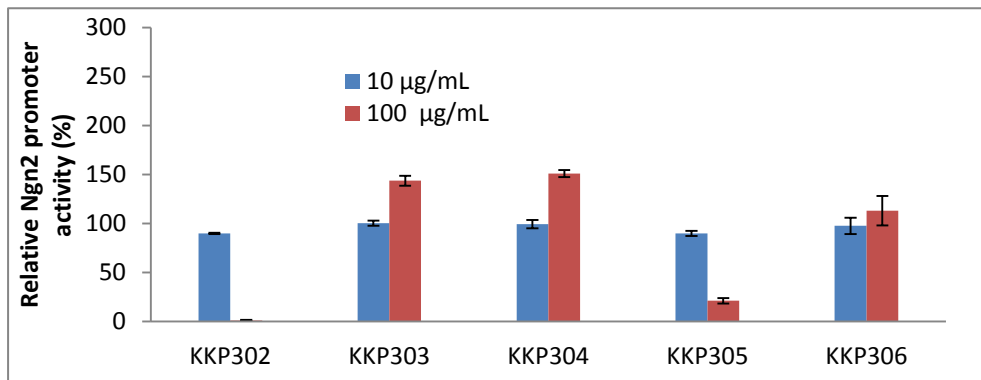
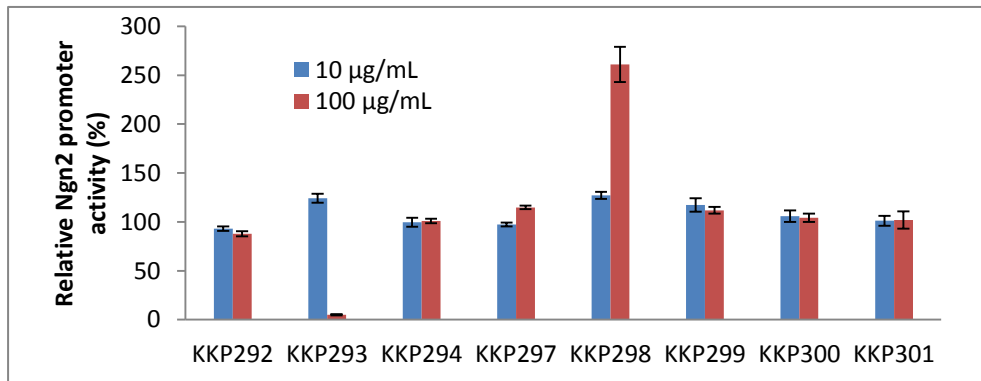
List of Screened KKB Plant Extracts (Ngn2 Promoter) Activity

KKB NO.	SCIENTIFIC NAME	FAMILY	PLANT PART USED
KKB0124	<i>Ipomoea sp.</i>	Convolvulaceae	Aerial
KKB0125	<i>Wikstroemia indica</i> Meisson.	Thymelaeaceae	Aerial
KKB0126	<i>Sida acuta</i> Burm.	Malvaceae	Aerial
KKB0127	<i>Synedrella nodifloea</i> Gaertn.	Compositae	Aerial
KKB0128	<i>Lygodium flexuosum</i> Sw.	Schizaeaceae	Aerial
KKB0129	<i>Desmodium triquetrum</i> Dc.	Papilionaceae	Aerial
KKB0130	<i>Croton lobatus</i> Linn.	Euphorbiaceae	Aerial
KKB0131	<i>Elephantopus scaber</i> L.	Compositae	Aerial
KKB0132	<i>Urena lobata</i> Linn.	Malvaceae	Aerial
KKB0133	<i>Melastoma malabathricum</i> L.	Melastomaceae	Aerial
KKB0134	<i>Ziziphus oenoplea</i> (L.) Mill.	Rhamnaceae	Aerial
KKB0135	<i>Thysanolaena maxima</i> (Rox) O. Kulze.	Poaceae	Aerial
KKB0136	<i>Solanum indicum</i>	Malvaceae	Aerial
KKB0137	<i>Spilanthes acmella</i>	Compositae	Aerial
KKB0138	<i>Eupatorium odoratum</i>	Compositae	Aerial
KKB0139	<i>Microcos paniculata</i>	Tiliaceae	Aerial
KKB0140	<i>Lantana camara</i>	Verbenaceae	Aerial
KKB0141	<i>Achyranthes aspera</i> Linn.	Amaranthaceae	Aerial
KKB0142	<i>Ocimum sanctum</i>	Labiatae	Aerial
KKB0143	<i>Cajanus cajan</i> Linn.	Fabaceae	Leaves
KKB0144	<i>Allamanda spp.</i>	Apocynaceae	Aerial
KKB0145	<i>Anisomeles indica</i>	Lamiaceae	Aerial
KKB0146	<i>Hibiscus surattensis</i> L.	Malvaceae	Aerial
KKB0147	<i>Ipomea pes-capra</i> R. Br	Convolvulaceae	Aerial
KKB0148	<i>Tecoma stans</i> (L.) Juss	Bignoniaceae	Aerial
KKB0149	<i>Clinogyne dichotoma</i> Salisb	Marantaceae	Leaves with small branches
KKB0150	<i>Flemingia congesta</i>	Papilionaceae	Leaves
KKB0151	<i>Ardisia humilis</i>	Myrsinaceae	Leaves
KKB0152	<i>Ecbolium linnaeum</i>	Acanthaceae	Leaves
KKB0153	<i>Polygonum lanatum</i>	Polygonaceae	Leaves
KKB0154	<i>Costus speciosus</i>	Costaceae	Leaves
KKB0155	<i>Sonneratia apetala</i>	Sonneratiaceae	Fruit stalk
KKB0156	<i>Gendarussa vulgaris</i>	Acanthaceae	Leaves
KKB0157	<i>Nymphaea nouchali</i>	Nymphaeaceae	Roots
KKB0158	<i>Sida rhombifolia</i> Linn.	Malvaceae	Aerial
KKB0159	<i>Bacopa monnieri</i>	Scrophulariaceae	Whole plants

KKB0160	<i>Rumex maritimus</i>	Polygonaceae	Aerial
KKB0169	<i>Azadirachta indica</i>	Meliaceae	Leaves
KKB0170	<i>Aphanamixis polystachya</i>	Meliaceae	Stem
KKB0171	<i>Aphanamixis polystachya</i>	Meliaceae	Leaves
KKB0172	<i>Tagetes erecta</i>	Compositae	Stem
KKB0173	<i>Tagetes erecta</i>	Compositae	Leaves
KKB0174	<i>Ipomoea mauritiana</i>	Convolvulaceae	Stem
KKB0175	<i>Ipomoea mauritiana</i>	Convolvulaceae	Fruit
KKB0176	<i>Argemone mexicana</i>	Papaveraceae	Stem
KKB0178	<i>Manihot esculenta</i>	Euphorbiaceae	Stem
KKB0179	<i>Manihot esculenta</i>	Euphorbiaceae	Leaves
KKB0180	<i>Coccinea cordifolia</i>	Cucurbitaceae	Stem
KKB0181	<i>Hibiscus feculneus</i>	Malvaceae	Stem
KKB0183	<i>Ficus benghalensis</i>	Moraceae	Root bulb
KKB0185	<i>Datura stramonium</i>	solanaceae	Fruit
KKB0187	<i>Cyperus rotundus</i>	Cyperaceae	Leaves
KKB0188	<i>Terminalia arjuna</i>	Combretaceae	Fruit
KKB0189	<i>Terminalia arjuna</i>	Combretaceae	Bark
KKB0190	<i>Sida cordifolia</i>	Malvaceae	Leaves
KKB0192	<i>Achyranthes aspera</i>	Amaranthaceae	Leaves
KKB0193	<i>Achyranthes aspera</i>	Amaranthaceae	Stem
KKB0194	<i>Datura metel</i>	Solanaceae	Leaves
KKB0195	<i>Datura metel</i>	Solanaceae	Stem
KKB0196	<i>Datura metel</i>	Solanaceae	Roots
KKB0197	<i>Acalypha indica</i>	Euphorbiaceae	Stem
KKB0198	<i>Ficus religiosa</i>	Moraceae	Leaves
KKB0200	<i>Ficus religiosa</i>	Moraceae	Bark
KKB0204	<i>Solanum nigrum</i>	Solanaceae	Leaves
KKB0206	<i>Eugenia jambolana</i>	Myrtaceae	Seed
KKB0212	<i>Smilax zeylanica</i>	Liliaceae	Stem
KKB0217	<i>Withania somnifera</i>	Solanaceae	Leaves
KKB0219	<i>Leucas aspera</i>	Lamiaceae	Stem
KKB0220	<i>Adhatoda vasica</i>	Acanthaceae	Stem

APPENDIX VII

Screening of the KKP Plant Extracts (Ngn2 Promoter Activity)



APPENDIX VIII

List of Screened KKP Plant Extracts (Ngn2 Promoter Activity)

KKP NO.	SCIENTIFIC NAME	FAMILY	PLANT PART USED
KKP292	<i>Bryophyllum pinnatum</i>	Crassulaceae	leaf
KKP293	<i>Artocarpus integra</i>	Moraceae	root
KKP294	<i>Streblus asper</i>	Moraceae	leaf
KKP297	<i>Millingtonia hortensis</i>	Bignoniaceae	branch
KKP298	<i>Millingtonia hortensis</i>	Bignoniaceae	leaf
KKP299	<i>Bidens pilosa</i>	Asteraceae	whole
KKP300	<i>Celastrus paniculata</i>	Celastraceae	leaf
KKP301	<i>Lophopetalum wallichii</i>	Celastraceae	leaf
KKP302	<i>Rheo discolor</i>	Commelinaceae	whole
KKP303	<i>Murdannia loriformis</i>	Commelinaceae	whole
KKP304	<i>Merremia umbellata</i>	Convolvulaceae	leaf
KKP305	<i>Santalum album</i>	Santalaceae	wood
KKP306	<i>Vitis vinifera</i>	Vitaceae	leaf
KKP307	<i>Acrornychia laurifolia</i>	Rutaceae	leaf
KKP308	<i>Aegle marmelos</i>	Rutaceae	leaf
KKP309	<i>Citrus maxima</i>	Rutaceae	peel
KKP310	<i>Clausena lansium</i>	Rutaceae	leaf
KKP311	<i>Clausena harmandiana</i>	Rutaceae	leaf
KKP312	<i>Murraya paniculata</i>	Rutaceae	leaf
KKP313	<i>Toddalia aculeata</i>	Rutaceae	leaf
KKP314	<i>Picrasma javanica</i>	Simaroubaceae	leaf
KKP315	<i>Eurycoma longifolia</i>	Simaroubaceae	root
KKP316	<i>Canarium album</i>	Burseraceae	leaf
KKP317	<i>Canarium album</i>	Burseraceae	fruit
KKP318	<i>Alpinia oxymitra</i>	Zingiberaceae	rhizome
KKP319	<i>Amomum villosum</i>	Zingiberaceae	rhizome
KKP320	<i>Aglaia odorata</i>	Meliaceae	leaf

APPENDIX IX

Characteristics of the New Compounds

Compound 1. Colorless solid; $[\alpha]_D^{26}$ -9.9 (c 0.5 MeOH); positive HRESIMS $[M+Na]^+$ m/z 381.1634 (calcd. for $C_{21}H_{26}O_5Na$ 381.1678, Δ -4.4 mmu); UV λ_{max} (MeOH) nm (log ϵ) 278 (3.6) and 223 (4.2) IR ν_{max} 3354, 2924, 1706, 1514, and 1242; 1H NMR (CD_3OD , 600 MHz) and ^{13}C NMR (CD_3OD , 150 MHz), see Table 3.1.

Compound 2. Colorless solid; positive HRESIMS $[M+Na]^+$ m/z 399.1762 (calcd. for $C_{21}H_{28}O_6Na$ 399.1784, Δ -2.1 mmu); 1H NMR ($CDCl_3$, 600 MHz) and ^{13}C NMR ($CDCl_3$, 150 MHz), see Table 3.1.

Compound 15. Colorless amorphous solid. $[\alpha]_D^{20}$ -165 (c 0.10 MeOH); HR-ESI-MS $[M+Na]^+$ m/z 667.2742 (calcd. for $C_{34}H_{44}O_{12}Na$ 667.2730, Δ +1.2 mmu); UV λ_{max} (MeOH) nm (log ϵ) 336.5 (1.9), 342.0 (1.7), 275.5 (3.1), and 203.5 (3.9); IR (ATR) ν_{max} 3489, 2961, and 1743 cm^{-1} ; 1H and ^{13}C NMR see Table 5.1.

PUBLICATION

Fuentes, R. G.; Toume, K.; Arai, M. A.; Koyano, T.; Kowithayakorn, T.; Ishibashi, M. *Heterocycles* **2014**, 88, 1501-1509.